Full-Waveform Airborne Laser Scanning for Landscape Ecological Mapping: Methods and Applications

Dissertation

submitted in partial fulfillment of the requirements for the degree of

Doktor der technischen Wissenschaften (Dr.techn.)

by

Dipl.-Ing. Werner Mücke

Registration Number 0125771

supervised by

Univ.-Prof. Dipl.-Ing. Dr.techn. Norbert Pfeifer

Research Groups Photogrammetry and Remote Sensing

Department of Geodesy and Geoinformation, Vienna University of Technology

This dissertation has been reviewed by:

....
Univ.-Prof. Dr. Norbert Pfeifer

....
Univ.-Prof. Dr. Elmar Csaplovics
(TU Dresden)

....
Dipl.-Ing. Werner Mücke

Full-Waveform Airborne Laser Scanning for Landscape Ecological Mapping: Methods and Applications

Dissertation

zur Erlangung des akademischen Grades eines

Doktors der technischen Wissenschaften (Dr.techn.)

eingereicht von

Dipl.-Ing. Werner Mücke

Matrikelnummer 0125771

betreut von

Univ.-Prof. Dipl.-Ing. Dr.techn. Norbert Pfeifer

Forschungsgruppen Photogrammetrie und Fernerkundung

Department für Geodäsie und Geoinformation, Technische Universität Wien

Diese Dissertation haben begutachtet:

....

Univ.-Prof. Dr. Norbert Pfeifer

....

Univ.-Prof. Dr. Elmar Csaplovics
(TU Dresden)

....

Dipl.-Ing. Werner Mücke

Erklärung zur Verfassung der Arbeit
Author's Statement

Hiermit erkläre ich, dass ich diese Arbeit selbstständig verfasst habe, dass ich die verwendeten Quellen und Hilfsmittel vollständig angegeben habe und dass ich die Stellen der Arbeit - einschließlich Tabellen, Karten und Abbildungen -, die anderen Werken oder dem Internet im Wortlaut oder dem Sinn nach entnommen sind, auf jeden Fall unter Angabe der Quelle als Entlehnung kenntlich gemacht habe.

I hereby declare, that I independently drafted this manuscript, that all sources and references used are correctly cited and that the respective parts of this manuscript - including tables, maps and figures - which were included from other manuscripts or the internet, either semantically or syntactically, are made clearly evident in the text and all respective sources are correctly cited.

Dipl.-Ing. Werner Mücke
Traunaustraße 20
4600 Wels

....

Contents

Danksagung

Aller Anfang ist schwer. Aber nicht, weil alle Anfänge prinzipiell schwer sind, sondern weil man sich als Anfänger davor scheut, eventuell in die falsche Richtung zu gehen. Umso wichtiger ist es dann, dass man sich auf die Unterstützung von Kollegen, Freunden und Familie verlassen kann, die einem helfen, den richtigen Weg zu finden, einzuschlagen und konsequent weiterzugehen.

In diesem Sinne gilt mein besonderer Dank ...

...meinen Kollegen in der Forschungsgruppe, allen voran Norbert Pfeifer, Markus Hollaus, Christian Briese und Camillo Ressl für die vielen inspirierenden Unterhaltungen, die oft die zündende Idee zur Folge hatten.

...Andreas Roncat für seine Matlab- und Latex-Kenntnisse, die mir mehr als einmal zur Problemlösung beigetragen haben.

...den Mitarbeitern der Projekte TransEcoNet und ChangeHabitats2, insbesondere Balázs Deák, Anke Schroiff, András Zlinszky, Agnés Vari, Hermann Heilmeier, Michael Kuttner, Anna Schneidergruber und Thomas Wrbka für ihre Erläuterungen zum Thema Landschaftsökologie für einen Laien und außerdem für ihren beinahe unermüdlichen Einsatz in der Aufnahme der Geländedaten, die mir für diese Arbeit zur Verfügung standen.

...meinen Gutachtern Norbert Pfeifer und Elmar Csaplovics, dass sie sich die Zeit dafür genommen haben.

...und als letzte, aber nicht zuletzt, meiner Familie, insbesondere meiner Frau Marlene, die mich während der ganzen Zeit fortwährend unterstützt und motiviert hat. Danke!

Diese Arbeit wurde zum Teil durch die Projekte TransEcoNet (Central Europe Program und EFRE), ChangeHabitats2 (Marie Curie - FP7-PEOPLE-2009- IAPP) und NEWFOR (European Territorial Cooperation "Alpine Space") finanziert.
Weiterer Dank gebührt dem Amt der Burgenländischen Landesregierung, Stabsstelle Raumordnung, Referat GIS-Koordination, und der Firma RIEGL Laser Messsysteme GmbH für das zur Verfügungstellen der ALS - Daten, die ich in dieser Arbeit verwendet habe.

Kurzfassung

Der kontinuierliche Verlust der bioligischen Vielfalt (i.e. Biodiversität) in den natürlichen Lebensräumen der Europäischen Staaten kann als Tatsache betrachtet werden. Angesichts dieser Situation hat die Europäische Union (EU) das Rationalisieren des Erfassungsprozesses von Biodiversitätsindikatoren als eine ihrer obersten Prioritäten definiert, um einem weiteren Verlust entsprechend entgegenwirken zu können. In der Europäischen Kommission hat man sich auf zwei Konventionen geeinigt, die zum Ziel haben, vom Aussterben bedrohte Pflanzen- und Tierarten angemessen zu schützen: dies sind die Vogelschutzrichtlinie und die Fauna-Flora-Habitat-Richtlinie (kurz FFH-Richtlinie). Beide Richtlinien werden naturschutzrechtlich durch Natura 2000 (N 2000) implementiert, welches ein grenzübergreifendes Netzwerk von geschützten Lebensräumen in den Mitgliedsstaaten der EU definiert. Die Reglementierung besagt unter anderem, dass N 2000 - Gebiete in einem regulären Intervall von sechs Jahren wieder besucht und deren Biodiversität anhand von bestimmten festgelegten Indikatoren erhoben werden sollen.

Bis heute stehen mehr als 13% der EU-Landfläche unter dem Schutz von N 2000. Die rechtlich verbindliche Zustandserfassung der entsprechenden Flächen, welche konventionellerweise manuell im Feld erfolgt, bedeutet einen enormen Arbeitsaufwand der kaum innerhalb der sechs-Jahres-Zyklen zu schaffen ist. Daher gibt es dringenden Bedarf an modernen, zeitsparenden und vergleichsweise kostengünstigen Methoden um einzelne Schritte in dem größtenteils manuellen Prozess zu unterstützen und, wenn möglich, sogar zu ersetzen.

Fernerkundung (FE) ist eine effiziente Erfassungsmethode, die sehr gut dazu geeignet ist, um Daten über große Flächen in hoher zeitlicher, spektraler und räumlicher Auflösung zu erheben. Airborne laser scanning (ALS), eine relativ junge FE-Technologie, ist bekannt dafür, sehr genaue und detailierte Aufnahmen natürlicher Lebensräume zu ermöglichen. Es besitzt die Eigenschaft, Vegetation durch kleine Lücken in der Belaubung zu durchdringen und so deren vertikale Anordnung und Struktur, sowie die darunter liegende Topographie in 3D zu erfassen. Dies sind zwei wichtige Vorraussetzungen für die Ableitung von biodiversitätsrelevanter Information.

Diese Dissertation beschäftigt sich mit der Analyse von ALS-Punktwolken hinsichtlich verschiedener Aspekte der landschaftsökologischen Datenerfassung. Sie gibt eine kurze Einleitung zum Raumkonzept und der Wichtigkeit von Struktur in der Landschaftsökologie. Weiters beschreibt sie überblicksartig den Ablauf der N 2000 - konformen Erfassung von Landschaften innerhalb der EU. Vor dem Hintergrund zweier aktueller Forschungsprojekte, welche ebenfalls kurz erläutert und deren Ziele dargelegt werden, werden drei Anwendungen von ALS - Daten und darauf basierende Methoden präsentiert. Jede einzelne davon konzentriert sich auf die Ableitung von Vegetationsstrukturparametern, um entweder direkt oder indirekt als Biodiversitätsindikator zu fungieren.

Zuerst wird ein Ansatz zur Bestimmung der Vegetationsschichtung im Wald vorgestellt. Die ALS-Punktwolke wird auf ihre Eignung hin untersucht, die vertikale Stratifizierung von Vegetation entsprechend darzustellen. Weiters wird eine Methode implementiert, die es ermöglicht, die Anzahl der vorhandenen Vegetationsschichten auf der Basis der Menge und Anordnung an ALS-Punkten zu berechnen.
Zweitens wird die ALS-Punktwolke verwendet, um darin abgebildetes Totholz, entweder stehend oder liegend, zu finden. Es wird eine Methode entwickelt, welche liegende oder stehende tote Bäume in der Punktwolke lokalisiert und, sofern möglich, zusätzliche spektrale oder geometrische Parameter aus der Punktwolke ableitet, um die Bäume weiter hinsichtlich ihres Zustandes (z.Bsp. Zersetzungsgrad) zu beschreiben.
Drittens wird die ALS-Punktwolke herangezogen, um digitale Höhenmodelle in Feuchtgebieten (i.e. ufernahe Übergangszonen zwischen Wasser und Land) abzuleiten. Basierend auf investigativer Punktwolkenanalyse wird ein Konzept zur Identifikation von Echos niedrig- und kompakt-wachsender Pflanzen vorgestellt. Dieses wird anschließend verwendet, um die Punktwolke in Boden- und Nicht-Boden-Echos zu teilen und dann aus den klassifizierten Bodenechos ein digitales Geländemodell zu erstellen. Weiters werden gängige Vorgehensweisen zur Ableitung digitaler Oberflächenmodelle getestet und deren Ergebnisse verglichen, um ihre Eignung für Feuchtgebiete abschätzen zu können.
Wo immer es möglich ist, werden zusätzliche spektrale und geometrische Informationen (abgesehen von den reinen Punktpositionen) aus den vorhandenen full-waveform ALS-Daten abgeleitet und in vorkommenden Klassifizierungsschritten eingesetzt.

Alle präsentierten Ansätze sind automatisiert einsetzbar und eignen sich daher gut, um das Ziel einer Rationalisierung des Biodiversitätserfassungsprozesses zu erreichen.

Abstract

The consistent loss of biodiversity in the natural areas of the European countries is considered a fact. Therefore the European Union (EU) has made great efforts to address this situation. The streamlining of biodiversity assessment was declared to one of the top priorities in order to be able to act against further deterioration. For this purpose, the European Commission (EC) agreed on two conventions, with the aim to conserve and protect endangered animal and plant species: the Birds Directive and the Habitats Directive. Both are implemented through Natura 2000 (N 2000), which constitutes a cross-border network of protected sites to be regularly monitored in cycles of six years.

To this day, more than 13% of the EU's land mass are under the protection of N 2000. The obligatory assessment of the respective sites, which is conventionally achieved through in-situ manual field work, is an enormous effort, hardly manageable within the prescribed six year periods. Thus, there is an urgent need for novel, cost- and time-effective methods to support or, if possible, replace certain steps in the mostly manual process.

Remote sensing (RS) provides efficient means for area-wide data collection at high temporal, spectral and spatial resolution. Airborne laser scanning (ALS), as one rather novel discipline of RS, is able to provide highly accurate and detailed maps of the natural environment. Its ability to penetrate through small gaps in the foliage makes it an ideal measurement method for the stratification of vegetation and the depiction of topography in 3D, two important requirements for the derivation of biodiversity relevant information.

This doctoral thesis is oriented towards the analysis of ALS point clouds to support various aspects of landscape ecological data assessment with respect to certain declared biodiversity indicators. It gives an introduction on the concept of space and the importance of structure in landscape ecology, and how the assessment of landscapes is accomplished within the EU.
On the background of two recent research projects, which are briefly introduced, three applications are presented, each of which is focused on the estimation of vegetation structure to act either directly or indirectly as an indicator for biodiversity.
First, an approach for the derivation of forest layer structure is proposed. The capability of ALS is investigated to assess the vertical stratification of vegetation and a method is implemented to derive vegetation layers from the point cloud based on the abundance of ALS echoes.
Second, it is examined whether ALS point clouds are a suitable data basis for the identification of dead trees in forests, either standing or fallen. A method is developed to find the locations of snags and downed trees and, additionally if possible, derive spectral and geometric parameters from the point cloud describing them.
Third, a method for the derivation of accurate digital height models (DHM) in wetlands is proposed.

Based on investigative point cloud analysis, a concept for identification of echoes from low and compact growing plants is presented. It is subsequently used to classify terrain and off-terrain echoes and create a digital terrain model (DTM) in a wetland area. Furthermore, the results of different standard methods for digital surface model (DSM) computation are examined and compared against each other.
Wherever possible, additional information gathered from full-waveform parameters is included in involved classification tasks.

All of the proposed approaches are automated and therefore highly suitable for a rationalization of the biodiversity assessment process.

1 Introduction

Earth observation (EO) is the art and science of gathering information about states and processes of the Earth's systems. This includes, among others, acquisition, analysis, and presentation of geographic data. Photogrammetry, as one major discipline of EO, confines this concept to retrieve information from area-wise imaging the Earth, traditionally in the visible and, more recently, also in the near infra-red domain of the electromagnetic spectrum [Kraus 2007]. The extraction of topographic information for map production has a long tradition in photogrammetry, considering especially man-made features in large scales (1:5000 and higher resolutions). Compared to these artificial parts of the environment, the mapping of more natural ones (i.e. vegetated areas) has for a long time stood in the background, because the traditional passive photogrammetric methods, meaning those that cannot be operated without the utilization of sunlight, were not able to penetrate plant foliage and adequately describe the vegetation in its entirety.

With the emergence of active measurement techniques, a wide range of new applications was opened, as these techniques are capable of providing information about the stratification of vegetation. The work in this thesis is based on data from the (comparably) modern active measurement method airborne laser scanning (ALS) and it is oriented towards a more detailed analysis of vegetation as part of the natural environment. It concentrates on the application of ALS to support various aspects of landscape ecological data assessment with respect to the stratification of vegetation.

In this chapter, an introduction to landscape ecology and relevant terminology is given (see Sec. 1.1). Furthermore, it gives a basic overview on the legal background in connection with landscape mapping within the European Union (see Sec. 1.2), and, on the examples of two recent research projects, an insight on how the integration of EO in landscape ecological assessment tasks can be achieved (see Sec. 1.3). Although these sections represent a technical (ecologically unprofessional) point of view, they are meant to foster an essential understanding of the concept of space in landscape ecology, as well as of the importance of the composition of vegetation, both in horizontal and vertical direction.

1.1 An Outline of the Concept of Space in Landscape Ecology

In the 1930s a broader conception of the landscape and the therein contained ecosystems began to form within the classical views of ecology. At that time, a novel concept of spatial heterogeneity, combined with larger spatial extents than in traditional ecology, and the integration of the human role in creating and influencing landscapes, was introduced [McGarigal 2013; Turner et al. 2001]. Ecosystems, defined as communities of living organisms (animals, plants, microbes) and non-living components (air, soil, water, etc.), are not static. On the contrary, they are characterized by high variability, both in time and in space. Furthermore, a landscape is neither homogeneous nor isolated, but rather it is influenced by constant exchange and interaction between adjacent landscape elements or ecosystems [Odum and Barrett 1971]. The landscape elements feature spatial relationships among each other and are subject to continuous flows of energy, materials and nutrients [Grillmayer 2002]. Promoted by a growing awareness of these landscape dynamics, the German geographer Karl Troll coined the term *Landscape Ecology* [Troll 1939] as a cross-discipline of ecology and geography.

Landscape ecology observes and analyses the spatial heterogeneity of landscapes and the processes happening therein, from local and regional ecosystems to continents. A landscape is not necessarily limited by size or extent, it is more precisely defined by the composition of its elements, which possibly consists of many different ecosystems. Starting with the island bio-geography model developed by MacArthur [1967] in the 1960s, Forman [1995] and later Turner et al. [2001] introduced a terminology and fundamental concept of modern landscape ecology: the so-called *patch-corridor-matrix* approach. A *patch* is thereby defined as a habitat area that differs from its surroundings. It is also the smallest ecological unit in landscape mapping and classification. *Habitats*, in turn, are the characteristic living environments of certain animal or plant species or whole communities. A habitat is therefore more defined by the inhabitant, than by geographic features. It may include multiple patches, range across regions and serve various different needs (e.g. food, shelter, nesting, travel, etc.).
Corridors are narrow and usually elongated patches, acting as links or barriers between patches. Their conception thus depends on the perspective, as they can either have a positive (enhancing) or negative (blocking) effect on the dispersal of plants and animals in landscapes. For example, a corridor can be a stepping stone for a species to travel, but it can also be a way for diseases to spread (e.g. invasive species, bark-beetle attacks, etc.) [Kimberly 2002].
Finally, the *matrix* is defined as the landscape surrounding the patch, while not including the respective patch itself. It is the ecological system in the background and through its configuration it is strongly related to the connectivity or spatial continuity of the patch.

The relative portion of different habitat types within a landscape (e.g. how many grasslands, forests, wetlands, etc.) defines the *landscape composition*, while the term *landscape configuration* relates to the specific pattern formed by patches, corridors and the matrix. It describes the arrangement of elements and, thus, the degree of spatial heterogeneity, and it also refers to characteristics of single patches (e.g. size, shape, area-perimeter-ratio, etc.) [Clark 2010]. The configuration of a landscape is also referred to as *mosaic*. Composition and configuration together define the *landscape structure*, which is affected by *ecological processes* (e.g. land transformation, loss of habitat quality, fragmentation, soil moisture changes, freeze-thaw-cycles, etc.). The study of the relations of these patterns and ecological processes is, among others, one key topic of landscape ecology.

With the emergence and advance in information technology, like remote sensing (RS), geographic information systems (GIS), statistical methods and computer hard- and software, large area data sets became accessible. Improvements in assessment, processing and analysis techniques enabled experts in landscape ecology to characterize patterns and processes across various scales, which was not possible before. Moreover, the continuous availability and repetitive assessment cycles of these data sets help to incorporate the temporal scale, which is of high significance because many processes or patterns can only be identified if they are investigated over periods of time [e.g. Bissonette and Storch 2007; Turner 1990]. However, there is no universally applicable scale in landscape ecology, as the relevance of some phenomenon or relationship varies with degree of detail (c.f. a mouse and a moose habitat) [Turner et al. 2001]. Broad (or small) scales look at interactions across countries or even continents, whereas fine (or large) scales study interactions down to single patches or habitats. Put in more casual terms, it can be said that in landscape ecology different problems require different scales, and most problems require multiple scales. It is thus another of this discipline's key topics to identify the respective scale that is best for characterization of a certain relationship.

Patterns and processes of landscapes remain difficult to embrace empirically or to summarize quantitatively due to spatial extent, heterogeneity and temporal variation [Clark 2010]. One approach in related research focuses on the assessment of landscape structure as a determinant for biological diversity (also referred to in short as biodiversity) [e.g. Lapin and Barnes 1995; Nichols et al. 1998; Tews et al. 2004]. Biodiversity is defined as the variability among organisms of terrestrial or aquatic origin, and the ecosystems they belong to [United Nations 1992]. A positive correlation between the complexity of a landscape or its structure and biodiversity was proven by various studies [e.g. Moser et al. 2002; Schindler et al. 2008b]. This implies that a quantification of biodiversity always relates to a certain area. Retrieving structural information on that area therefore seems a promising approach to evaluate its biodiversity.

As a consequence, mathematical descriptions of landscape characteristics related to structure were developed and initially they were only planimetric (i.e. 2D) [e.g. McGarigal et al. 2002; Ricotta et al. 2003; Schindler et al. 2008a]. Commonly, the calculations for these metrics base on a combination of airborne or spaceborne EO data, land use and cover maps, soil maps, and other additional thematic input data. The crucial point is that considering only the 2D composition of landscape elements is in fact a simplification of reality, which can hardly suffice for every application [e.g. Hoechstetter 2009]. It is not only the 2D structure that is of relevance for biodiversity, but also the third dimension (e.g. composition of the vegetation, the foliage, etc.) must be taken into account [e.g. Blaschke et al. 2004; Jenness 2004; Kati et al. 2009; MacArthur and MacArthur 1961]. This requires measurement methods able to provide data that allow for a description of the 3D composition of landscape elements, a key feature of ALS.

In the next sections, first the legal background of landscape and habitat mapping in Europe is briefly illustrated, followed by an introduction of two recent research projects dealing with the integration of 3D information in landscape character and habitat assessment for the retrieval of biodiversity relevant parameters: TransEcoNet and ChangeHabitats 2.

1.2 The Assessment of Landscapes in Europe

The European Commission (EC) agreed on two mutual conventions to conserve and protect wildlife in the European Union (EU). These two agreements are known as the Birds Directive, established in 1979 [European Commission 1979], and the Habitats Directive, established in 1992 [European Commission 1992a]. The directive's main objective is the conservation of animal and plant species, as well as their typical habitats. Thereby the Habitats Directive pursues the approach of preservation of a *favourable conservation status*, implying a definition of the habitat type and the characteristic species composition in question. The status of a habitat should be assessed, evaluated and retained if found favourable. If the opposite is the case, then steps should be taken in order to restore it. In general, it is assumed that all species are of equal worth, are endangered, and thus deserve protection.

Both directives are combined and practically implemented through the so-called Natura 2000 (N 2000) network. This is a coherent European cross-border network of sites of community interest: *Special Areas of Conservation* (SAC) designated by the Habitats Directive, and Special Protection Areas (SPA) designated by the Birds Directive [European Commission 1992b]. Coherent in this context refers to the selection of habitats of adequate and comparable number, size and quality throughout the EU. After this selection, the EU member states are obliged to initially assess the status of the selected sites. Subsequently, regular monitoring cycles of six years are prescribed, in which each member state is required to report on the actual conservation status of the species, habitats and the measures taken under the directive. N 2000's highly ambitious overall goal is to assure the maintenance of biodiversity in Europe.

The conventional approach followed for the reporting is in-situ field work executed by biologists, ecologists or other experts in landscape character and functionality assessment. Passive remote sensing techniques, referring to those that utilize available sunlight (e.g. true-color or infra-red images, imaging spectroscopy (IS) data from airborne or spaceborne platforms), are commonly used to support the monitoring and mapping efforts, but the data acquisition is still predominantly manual and terrestrial. As the extents of the (terrestrial) N 2000 sites currently cover approximately 13.4% of the EU's total area (583 888 km^2), this obligatory regular monitoring is an enormous challenge, which is hardly accomplishable in six year periods. Realizing the magnitude of the task and the limited capacities (i.e. man-power), there is an urgent need for novel, effective methods for N 2000 habitat monitoring. This is where the requirements of N 2000 meet the objectives of the TransEcoNet and ChangeHabitats 2 project.

1.3 TransEcoNet and ChangeHabitats2

The abbreviation TransEcoNet (TEN) stands for *transnational ecological networks*. It is an EU project financed by the INTERREG initiative and implemented through the Central Europe programme [Central Europe 2013] co-financed by the European regional development fund (ERDF) [ERDF 2013]. The focus of TEN lies on the assessment and analysis of protected and unprotected landscapes along and across the borders of neighbouring European states. Wildlife corridors connecting these areas can be more or less degraded, in the worst case leaving the respective sites isolated.

The ecological value of corridors consists in the dispersion of animal and plant species along these natural pathways, therefore increasing migration and reproduction of animal and plant species and decreasing the risk of extinction [MacArthur 1967].

Corridors and protected regions, meaning also but not exclusively N 2000 areas (e.g. national parks, biosphere reserves, etc.), sometimes extend across regional or national borders. In order to meet this challenge, TEN involves 15 partner institutions based in Slovenia, Hungary, Slovakia, Czech Republic, Poland, Germany and Austria. These are universities, research institutes, administrative organizations of protected areas, regional development agencies and nature protection NGOs, working in the fields of remote sensing, geoinformatics, nature protection, landscape ecology, history of architecture and arts, as well as environmental sciences. Their goal in the project is to assess and analyse four selected regions within central Europe regarding their ecological connectivity, history, and natural as well as cultural resources that deserve preservation [TransEcoNet 2013].

One of five work packages in the project deals with the assessment of landscape functionality and ecosystem (or landscape) services in a number of study sites of the project region. The chosen approach for landscape assessment follows the concept as proposed by Forman and Godron [1986], which describes a distinction of three different attributes per patch: structure, function and changes. Structure refers to spatial relations between landscape elements, the distribution of energy among them, as well as the availability of resources and species in relation to patch size, shape, number and type [Hermann et al. 2010]. Function means the interaction between adjacent landscape elements, like flows of materials and energy, as well as the exchange of species between ecosystems [Bianchin et al. 2012]. Changes of structure and function of the mosaic over time are estimated through comparison of multi-temporal data sets. The term structure in this case does however not only include natural, but also artificial elements, thus reflecting the history and influence of human disturbance. Landscape services can be understood as the benefits of human society through tasks performed by the natural environment or gained through its usage (e.g. provision of drinking or irrigation water, waste water treatment, air purification, etc.).

In practice, landscape functionality and landscape services cannot be assessed directly. They are derived based on the presence or absence of certain relevant features, so-called proxies (e.g. species, structures, disturbances, fragmentation, etc.). Within TEN, landscape functionality is derived through the evaluation of corridor connectivity [Hermann et al. 2010]. After a corridor was identified as such, it is investigated with respect to several relevant features: e.g. is it connecting or dissecting, does it lead through valuable or disturbed matrix, is the matrix artificial or natural. Ecological research has shown that different species place different requirements on corridors, deciding whether the movement along the corridor is accommodated or not [e.g. Fleury and Brown 1997]. This indicates the necessity for a description of not only where such natural pathways are located, but also how they are composed in terms of e.g. vegetation structure, concealing cover, topography, light conditions, etc. All of which are features that are very laborious to assess in the field or are impossible to measure with airborne passive imagery. Therefore, metrics derived from ALS data are employed in order to directly measure the relevant features, and if this is not possible, to provide a substitute measure (i.e. proxy) based on which the existence of another feature is indicated. Vertical stratification or foliage composition of vegetation is one of these measures or proxies. It relates to the type of animal that is likely to use a certain patch as a corridor or habitat (e.g. for nesting and breeding), but it also indicates the level of forest development (e.g. regeneration).

Furthermore, the presence of certain plants or plant types is considered a landscape service. This is strongly connected to an area's capability for supporting animals, e.g. the grazing of deer or cattle, which are dependent on these plants to feed on. The ability of ALS to identify low and compact growing plants is investigated, and if possible to discriminate certain plant types which have the ability to suppress the usual food plants consumed by domestic live stock.

A methodological framework was developed within TEN to assess and map landscape services based on parameters acquired in the field and spatial parameters extracted from airborne imagery. For the combination of these parameters to finally derive landscape services, an even deeper knowledge and understanding of the action and interaction of landscape elements is needed, which will most probably always involve a human interpreter. However, again certain measures and proxies can be provided by remote sensing to support this decision making process.

The ChangeHabitats 2 (CH2) project is more formally called *Network for habitat monitoring by airborne-supported field work - An innovative and effective process in implementation of the Habitat Directive*. It is realized and funded in the framework of the Industry-Academia-Partnership-Pathways (IAPP) program of the EU's Marie Curie Actions [European Commission 2013b]. Hence, it is dedicated to the coordination of interdisciplinary research activities of three universities and five small-and-medium-enterprises (SMEs) from Germany, Poland, Hungary and Austria. This is partly achieved through a transfer of knowledge from industry to academic facilities and vice versa by an exchange of personnel (i.e. secondments) for certain periods of time. The involved partners cover a broad spectrum of expertise in N 2000 and Habitats Directive regulations and implementation policies, terrestrial ecological habitat assessment, airborne IS and laser scanning data acquisition and analysis, water resources management, as well as software development.

CH2 aims to develop operable methods for monitoring habitats according to the regulations of N 2000. The overall goal is to establish an evaluation procedure for habitat quality (HQ) through field work supported by remote sensing. HQ can be understood as the suitability of a certain patch as a living environment for a certain species. According to the Habitats Directive, three main attributes define HQ: structure, range and long-term sustainability. The concept of CH2 provides for a translation of these three attributes to ones that can be mapped in the field: presence of typical species, presence of typical vegetation structures and degree of human influence [ChangeHabitats2 2013; Mücke et al. 2012b].

Taking into account the extents of N 2000 areas in Europe, a special focus in CH2 lies on the design of time and cost-efficient procedures, which should be automated to a large extent. This demands for the application of innovative airborne data assessment techniques that allow for an economically viable assessment of relevant features over large areas. Field mapping often concentrates on species or structures which are supposed to be indicators for certain ecological processes (e.g. tree diameter distribution as an indicator for age structure, herbaceous species as an indicator for wetness or dryness, etc.). These indicators are specially chosen because they are relatively easy to map in the field, they may however not be by remote sensing. Thus, in CH2 existing terrestrial mapping

methodologies are extended to, on the one hand, fulfil the requirements of the Habitats Directive, but on the other hand, serve as a reference for aerial data analysis. Correlations between field mapped and remotely sensed indicators are then investigated in order to evaluate the potential of remote sensing data for automated extraction of relevant habitat parameters.
Wherever possible, CH2 strives to make use of existing methods for feature extraction through remote sensing. In these cases their usefulness for N 2000 HQ mapping is tested and if necessary, knowledge or methodological gaps are filled with the invention of new algorithms. The field mapping schemes shall be supported as far as possible, or, if applicable, replaced through the usage of these methods.

The novelty of the approaches of TEN and CH2 is the application of high resolution vegetation mapping with full-waveform ALS for the description of vegetation composition and structure in landscape ecological research questions. Remote sensing, if applied in the conventional ecological assessment strategies, is usually based on passive acquisition techniques. Used for visual interpretation, they are a highly valuable source for preparations of field mapping campaigns and if printed or copied to digital mapping devices (e.g. hand-held and tablet PCs) they can also be used for orientation during the field work. Furthermore, these images are also often used as the basis for supervised or unsupervised classification for a number of biodiversity relevant tasks. Making use of image processing and segmentation techniques, as well as object based image analysis (OBIA), information like land cover, connectivity of vegetation patches, but also on species can be extracted (see Chap. 3).

However, information from this kind of data is generally limited to the depiction of two-dimensional features (e.g. horizontal distribution of vegetation). With passive remote sensing (e.g. conventional photogrammetric methods) there is no penetration of the plant foliage. The height distributions of a plant's components cannot be measured. Because of the dependency on sunlight, even the analysis of gaps in the vegetation with high resolution aerial photographs (e.g. ground sampling distance (GSD) $<$ 25 cm) is constrained due to object shadows. Additionally, the sunlight may also vary during data acquisition, which sometimes creates the need for extensive post-editing and calibration of single images.

ALS, as an active measurement technique, offers direct 3D measurements of vegetation components down to the Earth's surface. It's ability to penetrate through small gaps in the foliage eliminates this disadvantage of passive imagery and thus makes it a highly valuable data basis for vegetation analysis in TEN and CH2. As the application of ALS for landscape ecological assessment is comparably new, especially on large areas, an extensive set of ALS-derived parameters and novel methods are investigated in both, TEN and CH2. Three of these methods and applications were chosen for presentation in this thesis, all of which are used for the description of vegetation structure and composition: (1) the assessment of vegetation stratification through analysis of the vertical distribution of neighbouring ALS echoes, (2) the direct and geometry-based identification of dead wood based on the ALS point cloud and (3) the investigation of ALS observations for identification of vegetation and ground echoes, as well as the discrimination of low growing plant types in wetlands.

2

Thesis overview and aims

2.1 Objectives

As outlined in chapter 1, the common practice of vegetation structure assessment with respect to landscape ecological questions and problems is currently and conventionally 2D. However, numerous applications exist that require a more thorough investigation of the vegetation composition in 3D, which cannot be achieved through the acquisition of passive EO data. TEN and CH2 investigate the usage of ALS data for the derivation of biodiversity relevant parameters.

This thesis presents three selected analyses and applications, which were developed within TEN and CH2 to either (1) directly estimate factors of landscape functionality or habitat quality, (2) act as proxies for the same purpose, or (3) support the overall evaluation process as additional information. All of the presented methods are related to vegetation stratification and composition, thereby covering various aspects of biodiversity evaluation. It is further the aim of this work to investigate the benefits of full-waveform ALS data if applicable to the respective application.

In the following, the three topics are introduced, research goals are formulated and novelties of the methodologies with respect to existing approaches (see Chap. 3) are outlined:

1. **Derivation of the forest layer structure:**

   (a) Investigate the possibility of ALS to derive vertical vegetation stratification within forests.

   (b) Develop a method to automatically derive the number of existing vegetation layers from the ALS point cloud solely based on occurrence of vegetation components in certain heights.

   Novelty of the approach: Development of a robust method for vegetation layer extraction with respect to applicable ecological layer definitions in forests and for area-wide application.

2. **Identification of dead trees:**

(a) Investigate whether an ALS point cloud contains the necessary information about standing dead trees and downed stems to detect them.

(b) Develop a method to find the locations of standing dead and downed tree stems.

(c) As a result, the analyses and methods shall additionally derive parameters of dead trees.

Novelty of the approach: Direct identification of dead wood, either standing or fallen, based on the full-waveform ALS point cloud and the derivation of geometric features in connection with dead trees.

3. **Point cloud classification and digital height models (DHM) in wetlands:**

(a) Investigate the capability of ALS to penetrate the ”canopy” of usually dense, low and compact growing wetland plants and provide accurate measurements of the ground surface below.

(b) Analyse whether full-waveform ALS data gives an additional benefit for the discrimination of vegetation and non-vegetation echoes, as well as for the discrimination of occurring plant types.

(c) Derive accurate digital surface models (DSMs) and digital terrain models (DTMs) in wetlands, which will provide area-wide estimates of the vegetation height.

Novelty of the approach: Benefit of using full-waveform data for DTM generation in wetlands covered by low and compact vegetation. Investigation of the representation of selected wetland plant types in full-waveform ALS data and whether full-waveform observations are able to discriminate among them.

2.2 Structure

The following chapter 3 gives a summary of related work on each of the three afore mentioned topics with respect to the application of ALS.

Chapter 4 introduces the study areas for the presented work. As it was conducted in two different research projects pursuing a number of objectives, different areas where chosen for different applications according to (1) presence of relevant vegetation structure, (2) highest possible diversity of this structure, in order to create robust methods that can be applied with as few limitations as possible, and (3) availability of suitable reference data.

Chapters 5 to 7 describe the developed methods in detail, as they were outlined in section 2.1. Each method and application is discussed in a dedicated chapter, with sections on the methods themselves, the results, evaluations and discussions, as well as conclusions.

In chapter 8 a summary is given and an outlook on possible further research is formulated.

2.3 Publications

This thesis is based on or has partly been published in research papers, book chapters and conference contributions. In the following, the relevant publications are listed in chronological order and their thematical connection to the respective sections of this thesis is given in brackets. Publications listing Werner Mücke as the first author are those where the therein described methods are his own development, as well as he has initiated and conducted the writing process. To all other listed publications, Werner Mücke has contributed significantly to the writing process. If several methods are described, only those are contained in this manuscript, which were developed by himself.

2.3.1 Publications in scientific journals

1. Mücke, W., Zlinszky, A., Rieger, P., Hollaus, M., and Pfeifer, N. [2012b]. "Towards operative habitat mapping using airborne laser scanning - Applications in the ChangeHabitats2 project". In: *European Journal of Remote Sensing*. (Manuscript in preparation) (Chaps. 5 and 6).
2. Mücke, W., Deák, B., Schroiff, A., Hollaus, M., and Pfeifer, N. [2013a]. "Detection of fallen trees in forested areas using small footprint airborne laser scanning data". In: *Canadian Journal of Remote Sensing* 39(s1), pp. 32–40. DOI: `10.5589/m13-013` (Chap. 6).
3. Mücke, W. and Hermann, A. [2010]. "Estimation of biodiversity relevant quantities from airborne laser scanning data". In: *Österreichische Zeitschrift für Vermessung und Geoinformation (VGI)* 4, pp. 201–210. URL: `http://www.ovg.at/index.php?id=2042` [visited on 02/12/2014] (Chap. 5).
4. Hollaus, M., Mücke, W., and Eysn, L. [2012]. "Forest structure and stem volume assessment based on airborne laser scanning". In: *Ambiência* 8, pp. 471–482. DOI: `10.5777/ambiencia.2012.04.03` (Chap. 5).
5. Zlinszky, A., Mücke, W., Lehner, H., Briese, C., and Pfeifer, N. [June 2012]. "Categorizing wetland vegetation by airborne laser scanning on Lake Balaton and Kis-Balaton, Hungary". en. In: *Remote Sensing* 4 [6], pp. 1617–1650. DOI: `10.3390/rs4061617` (Chap. 7).

2.3.2 Contributions to books

1. Mücke, W., Hollaus, M., and Briese, C. [2011]. "Applications and analysis of airborne laser scanning data on reed beds". In: *International Symposium on Advanced Methods of Monitoring Reed Habitats in Europe*. Fernerkundung und angewandte Geoinformatik. Rhombos-Verlag, pp. 109–121. ISBN: 978-3941216785 (Chap. 7).
2. Hollaus, M., Mücke, W., Roncat, A., Pfeifer, N., and Briese, C. [2014]. "Full-waveform recording systems and their possibilities in forest applications". In: *Forestry applications of airborne laser scanning – Concepts and Case Studies*. Ed. by M. Maltamo, E. Næsset, and J. Vauhkonen. Managing Forest Ecosystems. Heidelberg London New York: Springer Science+Business Media B.V.. Chap. 3. ISBN: 978-94-017-8662-1. DOI: `10.1007/978-94-017-8663-8__3` (Chaps. 5 and 6).

2.3.3 Contributions to national and international conferences

1. Mücke, W., Hollaus, M., Pfeifer, N., Schroiff, A., and Deák, B. [2013b]. "Comparison of discrete and full-waveform ALS for dead wood detection". In: *ISPRS Annals of the Photogrammetry, Remote Sensing and Spatial Information Sciences*. Vol. II-5/W2. talk: ISPRS Workshop Laser Scanning 2013, Antalya, Turkey; 2013-11-11 – 2013-11-13, pp. 199–204. DOI: 10.5194/isprsannals-II-5-W2-199-2013 (Chap. 6).
2. Mücke, W. and Hollaus, M. [2012]. "Estimation of forest layer structure and canopy density using airborne laser scanning data". In: *Proceedings SilviLaser 2012 - The 12th International Conference on LiDAR Applications for Assessing Forest Ecosystems*. Ed. by N. C. Coops and M. Wulder. Vancouver, British Columbia, Canada (Chap. 5).
3. Mücke, W., Hollaus, M., and Pfeifer, N. [2012a]. "Identification of dead trees using small footprint full-waveform airborne laser scanning data". In: *Proceedings SilviLaser 2012 - The 12th International Conference on LiDAR Applications for Assessing Forest Ecosystems*. Ed. by N. C. Coops and M. Wulder. Vancouver, British Columbia, Canada (Chap. 6).
4. Mücke, W., Zlinszky, A., Hollaus, M., and Pfeifer, N. [2012c]. "Towards operative habitat mapping using airborne laser scanning - The ChangeHabitats2 project". In: *Proceedings ForestSat 2012 - Promoting science based application of remote sensing and other spatial data in forested systems*. Ed. by W. B. Cohen, M. V. Duane, and M. G. Wing. Corvallis, Oregon, USA (Chaps. 5 and 6).
5. Mücke, W, Hollaus, M., and Prinz, M. [2010a]. "Derivation of 3D landscape metrics from airborne laser scanning data". In: *Proceedings SilviLaser 2010 - The 10th International Conference on LiDAR Applications for Assessing Forest Ecosystems*. Ed. by B. Koch, G. Kändler, and C. Teguem. Freiburg im Breisgau, Germany (Chap. 5).
6. Mücke, W., Hollaus, M., and Briese, C. [2010b]. "Reed structure mapping in airborne laser scanning data". In: *Proceedings ForestSat 2010 - Operational tools in forestry remote sensing techniques*. Ed. by D. Miranda, J. Suárez, and R. Crescente. Lugo, Spain (Chap. 7).
7. Mücke, W., Briese, C., and Hollaus, M. [2010c]. "Terrain Echo Probability Assignment Based On Full-Waveform Airborne Laser Scanning Observables". In: *ISPRS Technical Commission VII Symposium 2010: 100 Years ISPRS - Advancing Remote Sensing Science, Vol. 38 (Part 7A)*. ed. by W. Wagner and B. Szekely. Vienna, Austria. URL: http://www.isprs.org/proceedings/XXXVIII/part7/a/pdf/157_XXXVIII-part7A.pdf (Chaps. 5 and 6).

Other related publications

1. Leiterer, R., Morsdorf, F., Schaepman, M., Mücke, W., Pfeifer, N., and Hollaus, M. [2012]. "3D Vegetationskartierung: flugzeuggestütztes Laserscanning für ein operationelles Waldstrukturmonitoring". In: *Proceedings AK Fernerkundung 2012 Bochum*. Ed. by AK Fernerkundung. Bochum, Germany. URL: http://publik.tuwien.ac.at/files/PubDat_211134.pdf (Chap. 6).

2. Heilmeier, H., Burai, P., Lénárt, C., Mücke, W., and Schroiff, A. [2011]. "ChangeHabitats2 - Habitat monitoring by airborne laser scanning and hyperspectral imaging supported field work". In: *Abstract Book 12th European Ecological Federation Congress "Responding to Rapid Environmental Change"*. Ed. by EEF. Avila, Spain: Asociación Española de Ecologia Terrestre, p. 69. URL: http://publik.tuwien.ac.at/files/PubDat_204939.pdf (Chaps. 5 and 6).

3. Hollaus, M., Eysn, L., Mücke, W., Pfeifer, N., and Mandlburger, G. [2011a]. "Forest Delineation and Structure Assessment Based on Airborne Laserscanning Data". In: *Proceedings European LiDAR Mapping Forum (ELMF) 2011 Conference*. Ed. by ELMF. Salzburg, Austria. URL: http://publik.tuwien.ac.at/files/PubDat_204692.pdf (Chap. 5).

3
Background and Related Work

3.1 Estimation of the Forest Layer Structure

One of the key-research topics in landscape ecology is the analysis and characterization of landscape pattern and structure (c.f. Sec. 1.1). Diversity of structure leads to diversity of species because different ecological niches are created, which can be used as habitats [e.g. Paillet et al. 2010; Tews et al. 2004]. Not only structural diversity on the surface, but particularly in the third dimension leads to further diversification of habitats, which benefits especially birds and insects [Burel 1992]. The term structure in this context refers to the *organization in space and time, including the position, extent, quantity, type, and connectivity, of the above- ground components of vegetation* [Parker et al. 1995]. It is of critical importance, as forest dwelling animals may have special demands for possible nesting and breeding areas, whereas others may just be dependent on sheltering pathways to travel or foraging [e.g. Goetz et al. 2010; Hill et al. 2004; Sallabanks et al. 2001; Tews et al. 2004].

In view of the close relationship of species and structure, it became common practice to derive information on vegetation stratification in order to predict possible habitats for certain animals. Manual ground assessment, carried out by foresters, biologists and ecologists, is still the common practice in this context. However, especially in forests, it suffers from certain limitations. It is a time-consuming process, as the areas to be mapped are often remote, and it quickly becomes a tedious task with increasing vegetation density and complexity. Furthermore, it is hardly accomplishable for areas with large geographical coverage. As many individual field workers are needed to succeed within reasonable time frames, the assessment results are prone to inter-operator errors, which in the worst case make the data incomparable or even unusable [e.g. Foody 2010; Strand et al. 2002].

ALS provides efficient and consistent methods for area-wide assessment of vegetation stratification. In several studies it was shown that ALS data can accurately depict the 3D forest structure, including sub-canopy elements (i.e. sub-dominant trees, shrubs, etc.) and the forest terrain [Hyyppä et al. 2004; Næsset et al. 2004; Wagner et al. 2008; Wulder et al. 2012]. It has however been observed that

ALS has a tendency to underestimate the height of tree tops or vegetation canopies [e.g. Gaveau and Hill 2003; Næsset et al. 2004] . This is either because of penetration, when the laser enters the canopy for a short path before it is reflected by parts of the foliage, which is likely to happen in deciduous vegetation. Or because of insufficient sampling density, when the true tree tops are missed and only flanks of the trees are mapped, which is more likely in coniferous forests. It was further discovered that the laser pulse energy (often referred to as intensity) is subject to attenuation as it travels through the foliage and portions get so strongly intercepted or absorbed that they are lost and can no longer be detected [e.g. Korpela et al. 2012; Wagner et al. 2008].
For forest layer structure estimation this indicates that caution should be exercised when deriving layer height ranges, or when using intensity information for classification tasks in sub-canopy environments, as the respective measures might be biased. But presuming adequate penetration, which can easily be examined, an estimation of general presence or absence of vegetation components simply based on the abundance of ALS echoes in a certain height interval is not assumed to be affected by these drawbacks and therefore considered feasible.

Various techniques can be found in the literature and while all have to same goal, namely deriving estimates of vegetation stratification, they differ in their approaches. Lefsky et al. [1999] derived 3D forest structure from SLICER waveforms [NASA 2014], treating the canopy as a matrix of voxels. The voxels were defined as containing canopy or not, based on the return energy of the corresponding waveform in that location. Using stepwise multiple regression they predicted and compared, among other parameters, estimates of total biomass and basal area, achieving correlations of $R^2 = 0.91$ and 0.87, respectively. Another approach using ALS waveforms as direct input was proposed by Lindberg et al. [2012]. They analysed waveform data and discrete ALS data for their suitability of vegetation volume prediction. Through normalization of the waveforms with an algorithm based on the Beer-Lambert law for light absorption, they were able to compensate shadowing effects of overgrowing vegetation, producing an RMSE of 27.6%, compared to 31.9% when using not normalized waveforms and 36.5% when using discrete data.

Coming from waveform analysis to the actual 3D point cloud, methods were developed that estimate the amount of vegetation layers based on the distribution of echoes in space. Miura and Jones [2010] used laser pulse return types (i.e. single, first of many, intermediate, last of many) to stratify vegetation into four different layer classes. They pre-defined height levels to sort ALS echoes into canopy strata and classified them afterwards based on their return type by calculating ratios of echoes of different types. The so derived measures were found to be good predictors for field recorded variables (e.g. presence of low vegetation, $R^2 = 0.82$). Maltamo et al. [2005] also used echo height distributions and computed proportions of echoes above different height quantiles. A thresholding approach was proposed to afterwards separate tree storeys from the histograms holding the proportions for the various quantiles. They observed that the achievable accuracy is very much dependent on the density of the dominant tree layer. Martinuzzi et al. [2009] employed random forest classification on numerous ALS derivatives, such as minimum and maximum height, mean height, different quantiles, slope, aspect and curvatures, to name but a few, mapping the existence of understory shrub species and snags. They stated that the percent of vegetation echoes in the lower canopy strata, as well as measures of vertical heterogeneity were suitable indicators. The achieved overall accuracies of 83% for the classification of shrubs, and 86 to 88% for different snag diameter classes. The results were used to refine habitat prediction maps for birds. The work presented by Jaskierniak et al. [2011] compared 44 distribution functions to determine suitable ones representing ALS height density estimates. Contrary to other approaches, which used uni-modal distribution models (such as Weibull) [e.g. Coops et al. 2007; Gobakken and Næsset 2005; Thomas et al. 2008], Jaskierniak et al. [2011] focused only on bi-modal functions, which they found to be better candidates for the purpose. Overstorey stand volumes, as well as overstorey and understorey basal area were predicted with correlations ranging from $R^2 = 0.67$ to 0.88% for stand volume, and $R^2 = 0.61$ to 0.89% for basal area.

Furthermore, segmentation-based methods were proposed, effectively analysing and grouping the ALS point cloud into more or less homogeneous clusters representing individual vegetation parts, such as single shrubs or tree crowns. In Ferraz et al. [2012] a statistical approach based on the mean shift clustering algorithm was tested for that purpose. The produced segments were then assigned to forest vegetation layers. They detected 98.6% of the existing dominant trees, but sometimes (probably depending on the complexity of the scene) only 12.8% of suppressed trees. Morsdorf et al. [2010] employed Gaussian mixture models in a clustering approach for classification of the point cloud into individual canopy elements. A two-dimensional feature space, consisting of ALS echo height and intensity, was used to obtain a quantitative vertical stratification of vegetation. They found good agreement with field data, achieving correlations ranging from $R^2 = 0.73$ to 0.96% for three-layered to one-layered structures. Their method worked best for one-layered plots and dominant layers on multi-layered plots. It was comparably less successful for sub-dominant layers in more complex situations.

In Blaschke et al. [2004] single trees were segmented based on a canopy height model and subsequently statistics were computed for each segment (e.g. number of echoes, mean height, percent coefficient of variation, etc.). The goal was to derive proxy indicators from ALS metrics to contribute to ecological forest biodiversity monitoring. In Hill et al. [2004] and Gaveau and Hill [2003] the authors found relations of nestling masses for different bird species to canopy height and complexity, for which they extracted corresponding metrics from ALS data.

The majority of the above reviewed methods deal with vegetation structure in forestry-related applications. In this context, estimates of vertical vegetation composition are often used in operational forest monitoring in order to derive stand attributes like biomass or growing stock [c.f. Hyyppä et al. 2004; Næsset et al. 2004]. Some of the techniques are also applicable for habitat suitability analysis like in Martinuzzi et al. [2009], or for the pure derivation of sub-canopy vegetation layers (including height ranges and / or horizontal extent), as they directly produce results of that kind [e.g. Ferraz et al. 2012; Jaskierniak et al. 2011; Maltamo et al. 2005; Morsdorf et al. 2010]. But those methods that are based on statistical regression analysis may require extensive data for tuning of the algorithm and variable estimation, and those that are using segmentation and clustering approaches may be computationally demanding. Both features may turn out as drawbacks in large area applications.

3.2 Identification of Deadwood

Deadwood plays a crucial structural and functional role in forest ecosystems in many ways [Esseen et al. 1992; Ohlson et al. 1997]. It is a key component of biodiversity in European forests, since several groups of animals, fungi and plants are dependent on dead woody material [Paillet et al. 2010]. It is living and foraging substrate for saproxylic invertebrates [Lassauce et al. 2011; Riffell et al. 2011], which are important prey for several bird species [Lohr et al. 2002]. Many bird and mammal species rely on woody debris, as it offers nesting habitats, shelter, travel corridors and food supply [Butts and McComb 2000; Christensen et al. 2005; Sallabanks et al. 2001] and it provides a favourable micro climate, moisture and nutrients for fungi, lichens, mosses and several vascular plant species [Juutilainen et al. 2011]. Deadwood was identified as an important indicator for the nature conservation status of forest habitats [Christensen et al. 2005] as it positively correlates with resource availability, species richness and naturalness. Therefore, the survey of dead trees is part of nature conservation and monitoring, and it is important for sustainable forestry management [European Commission 2013a; Verkerk et al. 2011]. However, the manual quantification of deadwood is extremely time-consuming and costly to carry out through conventional field survey, especially in extended or rather inaccessible forested areas. Amounts and dimensions need to be estimated or measured by field workers, an assessment method which is influenced by personal experience and judgement, and thus prone to introduce inter-operator errors. Furthermore, the detection of downed and standing dead trees that are partly or completely overgrown by surrounding vegetation should be focused on. It is often the case that competitive trees around the dead ones close canopy gaps and make snags and fallen trees disappear below the vital foliage. Detection with passive remote sensing techniques would be difficult if not impossible, as they are only able to depict the top-most parts of the canopy.

ALS data, however, provide an excellent basis for the estimation of live and dead biomass in forests. For example, Vehmas et al. [2011] used an ALS-based CHM for the detection of canopy gaps in a boreal forest. They investigated ALS-based distribution and height metrics for a differentiation between types of canopy gaps featuring differing compositions of vegetation and amounts of coarse woody debris (CWD) inside the detected gaps. Their study showed promising results for the automated delineation of canopy gaps, also for large areas. Further, it suggests that canopy gap types featuring dense low vegetation can be robustly identified by the ALS height metrics. Bater et al. [2009] employed a set of various ALS predictor variables (e.g. height density metrics, mean, maximum, standard deviation and coefficients of variation of vegetation echo heights, etc.) in a statistical regression-based approach in order to predict the cumulative amount of standing dead trees on a plot level. The coefficient of variation of ALS echo heights was identified as the best variable for prediction of dead tree proportion (RMSE = 16.8%). Kim et al. [2009] investigated the capability of ALS for the mapping and discrimination of live and dead standing tree biomass. They found the echo intensity and computed canopy volume to be the most critical measure for accurate estimation of live biomass (RMSE = 26%). Their results indicate that the prediction of dead biomass was more challenging using the echo intensity alone as the most significant parameter (RMSE = 63%). They were also able to correlate the resulting biomass maps with maps of recent wild fires. Pesonen et al. [2008] also derived ALS height and intensity metrics , and they also used regression models for the prediction of standing and downed dead wood volumes. They investigated several combinations of dependent and independent variables in order to select the parametrization of the regression model and identified the natural logarithm as best suited. Plot-level estimates of downed trees was achieved with adequate accuracy (RMSE 51.6%), whereas the estimates for the standing dead trees were less significant (RMSE = 78.8%). The authors stated that these results would probably be better if the calculations were based on the stand level, and not the plot level. The found that all the computed ALS metrics turned out to be significant in the regression analysis, the standard deviation of the normalized echo heights being the most significant predicator in the CWD models.

All of the afore mentioned studies have in common that they rely on statistical modelling and most often regression analysis for the identification of relevant ALS parameters, correlation analysis and prediction of dead wood volume. This also requires significant amounts of field data, in order to train and calibrate the models. To the author's best knowledge, four studies exists that investigate the capability of ALS for direct mapping of CWD, or discrimination between live and dead standing trees on the object level (where the single tree is the object). First, in Blanchard et al. [2011] methods of object-based image analysis are used for the mapping of downed logs. Their study focused on the detection of downed logs based on gridded (i.e. rasterised) ALS data using rule-based OBIA and classification algorithms. A study site was selected which recently suffered a severe storm and wind throw. Thus, this is now a rather open forest site, with only a few live trees left, so the detection process is not influenced by vegetation overgrowing the downed stems. They documented automated classification accuracies of 73% based on the ALS raster data and when compared to manually digitized downed logs as a reference data. Second, Yao et al. [2012] used the single tree segmentation method proposed by Reitberger et al. [2009] and subsequently derived geometric and reflection features for each segment. These features at the single tree level included amongst others the volume and diameter of the tree crown, mean intensity and the gap fraction. A support vector machine classification was employed in order to discriminate standing dead trees from live ones based on the afore mentioned features. For their high density ALS data set (> 25 echoes per m^2) they achieved accuracies up to 73% for leaf-on and 71% for leaf-off situations when validated with ground truth data. In Nyström et al. [2014] the difference between two terrain models created from high density ALS data (> 65 echoes per m^2) was used as a basis for detection of wind-thrown trees under the canopy. The two DTMs differed in their level of detail, being created only from single and last returns using the active surface algorithm as described by Elmqvist et al. [2001]. The DTM computation was tuned in a way that it allowed for the stem objects to be still included in the final surface. Afterwards template matching was applied to the difference image to automatically extract the tree stems. They achieved an overall detection rate of 38%, being significantly better for tree stems longer than 27m. When aggregated to 40 x 40 m^2 grid cells to identify the cells where at least one stem was located, the detection success was improved to 77% of the cells that actually contained at least one field-measured tree stem. Lindberg et al. [2013] worked on the same area as Nyström et al. [2014], but applied a line template matching algorithm directly to the ALS point cloud, with the hypothesis that downed stems would be depicted as a line-like feature. They detected and linked 41% of the automatically detected stems to the field-measured stems.

3.3 Mapping of Wetlands

Wetlands are ecotones located in the transition area between water and land habitats. They are characterized by continuous or periodic flooding through standing or slowly flowing saline or fresh water, which creates specific spatial and temporal patterns of their hydrologic budget [Solomon et al. 2011]. Wetlands or marshes, if only referred to biotopes which are dominated by herbaceous plants, are of unique ecological importance. They serve as shelter, habitat and rich food source for different kinds of invertebrates, mammals and birds [Keddy 2010].

Common reed (*Phragmites australis*) is one of the most widely occurring wetland plants in Europe. It is very dominant and aggressively growing, sometimes spreading quickly over large areas, while completely occupying the place and replacing the original and natural plant communities. Its typically dense growing structure often leads to undesired aggradation effects, which can alter shoreline habitats significantly within a period of only a few years [e.g. Zlinszky et al. 2012]. Ecological research has also found correlations of reed stand structure, edge distribution and fragmentation, and the abundance and spatial distribution of animals living in the reed beds, e.g. various breeding birds or mammals [Benassi et al. 2009; Ostendorp 1993; Trnka and Prokop 2006]. All the animal and plant communities have to be highly adopted to the recurring changes in the water level, which on its part influences plant growth and soil conditions. Provided the water level is high enough, organic plant matter will decay beneath it and wetlands act as sink of carbon dioxide (CO_2). Otherwise, they become a source of CO_2 and of relevance as an indicator and influence for climate change [Joosten et al. 2009; Lenart 2009].

Constant monitoring is required to assess a wetland's current state and possible changes it might undergo, in order to be able to preserve and protect these important areas. The conventional approach of mapping wetland areas is through manual field work. However, wetlands are most often difficult to access, especially if the vegetation has grown very dense or the water is muddy. Entering these areas is always connected with disturbance for the residing animal and plant communities, which are sometimes highly sensitive to this kind of influence, especially during breeding seasons [Baldi and Kisbedenek 1999]. Thus, field work and manual data acquisition can be very laborious, time consuming and hard to accomplish. Area-wide analyses are nearly impossible to carry out while still being economically efficient.

To overcome the limitations introduced by passive remote sensing techniques (i.e. sensitivity to shadows, no penetration of the foliage), approaches including active (ALS) and passive (e.g. optical, IS) data together were investigated, aiming to combine the strengths of both methods while compensating for their individual drawbacks. The spectral resolution of modern IS sensors is generally superior to ALS, which is usually single wavelength, apart from a few innovative (and / or experimental) systems featuring dual- or multi-wavelength recording [e.g. Hancock et al. 2012; Morsdorf et al. 2009; Wang et al. 2014; Wei et al. 2012; Woodhouse et al. 2011]. The majority of commercial ALS systems operate in the near-infra-red part of the spectrum (i.e. wavelengths from 700 nm to 1.4 μm), which is one of the three regions of absorption of electromagnetic radiation of water. As a result, echoes from open water surfaces are highly unlikely and drop-out rates (i.e. the proportion of received compared to emitted pulses) are usually high [e.g. Höfle et al. 2009]. But on the other hand, ALS can deliver 3D information about wetland vegetation and non-inundated topography. Consequently, they are often used for the derivation of basic digital height models (either DSMs or DTMs) to complement the IS data with geometric information [e.g. Arroyo et al. 2010; Straatsma and Baptist 2008] and create combined data sets with a strong potential for species mapping [e.g. Chust et al. 2008; Gilvear et al. 2004; Jenkins and Frazier 2010; Morris et al. 2005].

ALS as ”stand-alone” tool was successfully used for the delineation of depressional wetlands based on a DTM calculated from pre-classified terrain echoes and subsequently derived contour lines [Ellis et al. 2012]. It served as input for the determination of surface roughness relevant for hydrological applications based on ALS-derived vegetation height models [Cobby et al. 2003] or maps comprising indices for vegetation density and laser beam penetration [Vetter et al. 2011]. Zlinszky et al. [2012] derived a set of ALS-based features related to vegetation and terrain properties of a large and shallow lake, creating various independent input data sets for a multivariate classification of wetland plants. ALS-based canopy height models and penetration measures were also used for the mapping and description of riparian zones and associated vegetation [e.g. Hutton and Brazier 2012; Johansen et al. 2010].

The accurate discrimination of the laser point cloud into vegetation and non-vegetation echoes (a step also called ”filtering”) is crucial with respect to the quality of the DTM. Echoes from low vegetation, which feature only small height differences to their surrounding echoes, should be eliminated from the point cloud before interpolation, otherwise they are likely to cause small but non-natural surface discontinuities and the resulting DTM will be too high. Filtering algorithms described in the literature rely on different geometric criteria for the identification and exclusion of such non-terrain echoes. These involve distances to prior computed surfaces of different scales or levels of detail [Axelsson 2000; Kraus and Pfeifer 1998], relations of planimetric distance and height difference [Vosselman 2000] or orientation of normal vectors as homogeneity criterion in segmentation based approaches [Tóvari and Pfeifer 2005]. As explained in the introduction (see Chap. 1), it is especially dense low vegetation causing problems for filtering strategies solely relying on geometric constraints. Wetlands are often predominantly occupied by such plants, so special emphasis must be put on the method of ground echo selection, DTM generation and quality. Hopkinson et al. [2005] evaluated the use of ALS data (approx. 3 echoes / m^2) for the mapping of short vegetation (less than 5 m high) in a boreal wetland in Canada. The main purpose of their study was the evaluation of remotely sensed plant heights of four different cover types (aquatic, grasses and herbs, low shrubs, high shrubs), so they compared ALS-based DSM heights to manually measured plant heights at GNSS-measured positions and observed average differences of 0.29 m. The largest differences were found for aquatic vegetation (0.52 m) and low shrubs (0.24 m), which they assumed to result from (1) increased laser penetration into the foliage and thus underestimation of plant height, together with (2) weak laser backscatter from saturated ground or water and therefore erroneous range estimations. Due to the range resolution of the used scanner (Optech ALTM 2050, pulse length 15 ns = 2.25 m), only one canopy echo was available in areas overgrown by low and dense shrub vegetation and a DTM could not be derived. Terrain heights were compared by subtracting manually measured plant heights at GNSS-measured locations from the ALS-based DSM. Montane and Torres [2006] described a similar study in a salt marsh in South Carolina, USA, using a high density ALS data set (approx. 16 echoes / m^2). In this case the heights of ALS ground echoes were directly compared with the heights of ground control points (GCP) measured by GNSS and a mean difference of 0.096 m was observed.

They found the largest errors to originate from areas covered with higher and denser vegetation. Additionally, they investigated the influence of varying topography within the footprint of the laser beam (in their case 0.37 m) and found that it was negligible. However, they stated that the study site was rather flat.

Approaches for actually compensating accuracy diminishing effects in wetland DTM creation are described by Hladik and Alber [2012] and Wang et al. [2009]. Hladik and Alber [2012] compared the elevations of an extensive set of over 1800 GNSS-GCPs from ten vegetation cover classes with heights up to 2 m to those extracted from an ALS-based DTM. A 1 x 1 m^2 DTM was computed by a kriging method from pre-classified ground echoes (identified by TerraScan in-built software classification mechanisms) [TerraScan 2013]. They found mean residuals of 0.11 m $\pm$ 0.11 m (overall mean error), which increased significantly with plant height. Moreover, the DTM errors were found to be larger than elevation differences between some of the selection vegetation cover classes, which would prevent accurate discrimination. A correction of the DTM based on the observed residual for each class was proposed, which lead to an improvement in accuracies of 0.01 m $\pm$ 0.10 m (overall mean error). They also stated that the sensor was unable to discriminate ground from vegetation for the lowest cover classes. Wang et al. [2009] identified the size of the search window used for ground echo selection during the interpolation process as a source of possible error. Dense growing structures of plants in wetlands made penetration of vegetation unlikely and decreased the possibility for a ground echo to be found within the defined window. Based on a training data set consisting of 240 GNSS-GCPs they investigated the behaviour of different windows sizes with respect to elevation differences between an ALS-derived DTM and the GCPs. For the available ALS data set (8 echoes / m^2) they varied the window size and always selected the lowest ALS echo within the defined window. They found a DTM created from a window size of 3.5 x 3.5 m^2 to correspond to minimal residuals of -0.022 m $\pm$ 0.063 m. Both last-mentioned approaches have in common that they require field measurements in order to derive and apply the proposed corrections. Without this necessary ground truth data, both methods cannot be calibrated. Also the proposed methods assume that the penetration rate and depth remain constant throughout the whole data acquisition area, which is not necessarily the case, as they vary greatly with vegetation density and structure, even within plants of the same species.

4

Study Areas and Data

4.1 Description of study areas

4.1.1 Uckermark

The Uckermark is a geographic region in north-eastern Germany, its biggest part located in the federal state of Brandenburg, the remaining parts in Mecklenburg-Vorpommern (see Fig. 4.1). The region is highly fertile, characterized by a number of bigger lakes (the so-called Naturpark Uckermärkische Seen) and by various rivers, which are often found together with alder-dominated riparian forests. Apart from that it is dominated by beech forests, extensive pastures and wet meadows [Uckermark 2014]. The selected study site (yellow rectangle in Fig. 4.1 and enlarged detail in Fig. 4.2) is part of the FFH-area *Hardenbeck - Küstrinchen*, which is located in the centre of the ALS acquisition zone [European Environment Agency 2014c]. It is a beech stand (*Fagus sylvatica*) with only few other individual species (*Quercus robur*, *Picea abies*, *Fraxinus excelsior* and *Carpinus betulus*). The structural characteristics of the stand vary from a hall-like appearance (i.e. old trees of 30 m and larger with only few to no understory) to successional younger parts (i.e. very dense or lots of shrub vegetation). There is only little variation in its relief and a few footpaths and driveways cross the area. Its extents are approximately 1200 x 900 m^2. No forestry management is practised and the site features a high amount of dead wood.

4.1.2 Nagyerdö

The second study area is the Nagyerdö (a.k.a. the Great Forest of Debrecen) in Eastern Hungary and it is included in the *Debrecen-Hajdúböszörményi tölgyesek* N 2000 area (see Fig. 4.3). As a N 2000 area it was designated for two habitats of community interest: Euro-Siberian steppe woods and Riparian mixed forests along the great rivers. In the matrix of the natural stands there are several tree plantations with black locust (*Robinia pseudo-acacia*), red oak (*Quercus rubra*) and Scots pine (*Pinus*

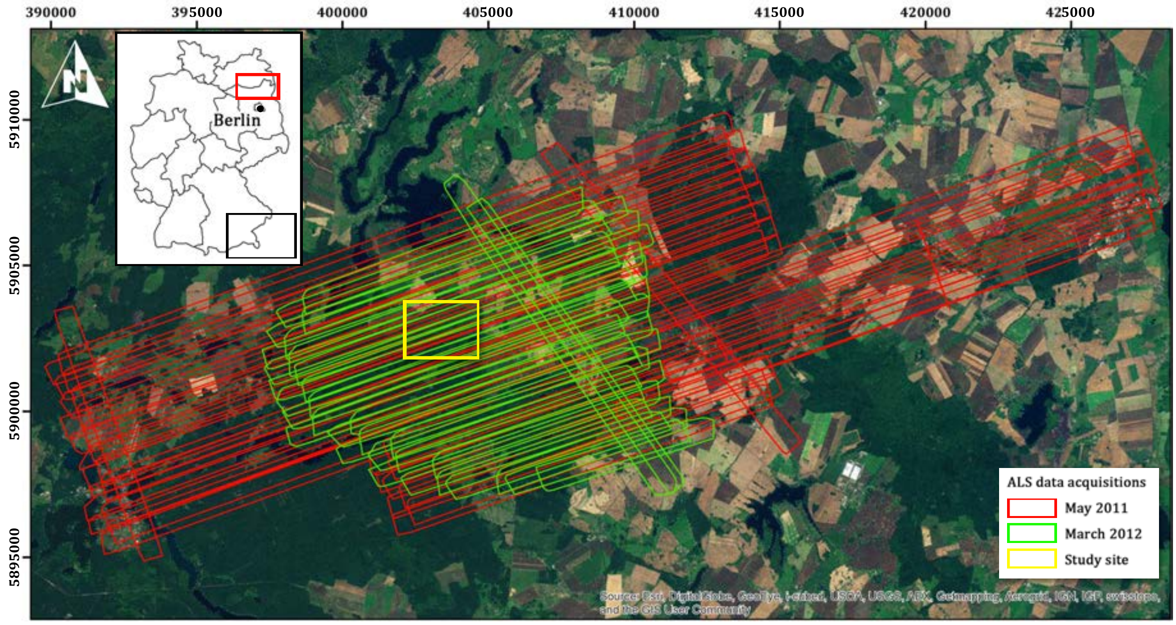

Figure 4.1: Overview of CH2 study area Uckermark with ALS flight strip layout for the data acquisition in May (red outlines) and June (green outlines).

sylvestris) [European Environment Agency 2014a; b]. The selected study site (see yellow rectangle in Fig. 4.3 and enlarged detail in Fig. 6.7) is a 120-year-old stand, formed on sandy soils with a high nature conservation value. The stand is multi-layered: it has two distinct canopy layers, a dense shrub and a species rich herb layer. The canopy layers are dominated by pedunculate oak (*Quercus robur*), field maple (*Acer campestre*), wild cherry (*Cerasus avium*) and linden species (*Tilia spp.*). There is also no forestry management practised and significant amounts of dead wood were found.

4.1.3 Seewinkel

The Austrian area east of the Neusiedler See is called Seewinkel. It is located in the Austrian province Burgenland and lies on the border to Hungary, where it connects with the Hungarian Hanság (see Fig. 4.5). The whole area is part of the cultural landscape *Fertö / Neusiedler See*, which since 2001 comprises a cross-border UNESCO world heritage [Verein Welterbe Neusiedler See 2013]. The Seewinkel consists mainly of extensively used agricultural areas, as well as vineyards, bog lands, extensive reed belts and the so-called Lacken. These are small lakes and wetlands, where surface water is being retained and no outflows to other water bodies occur. The water content of the Lacken is charged solely through rain and the water level usually is less than 1 m in depth. They periodically dry out through the summer, leaving trough-like depressions with very saline soils, which appear almost white in true-color aerial images (see Fig. 7.1). Most of the Lacken are surrounded by reed areas, which comprise a unique habitat especially for birds nesting in the reed. The so-called Zicklacke, although it did not belong to the core study sites of TEN, was chosen because of its reed growth. The Lacke is about 2 kilometres long, 1.5 kilometres wide and stretches from north-east to south-west. The north-eastern part of the lake shore is overgrown by common reed (*Phragmites australis*), which also formes a few islands in the inner parts of the lake (see Fig. 4.6a).

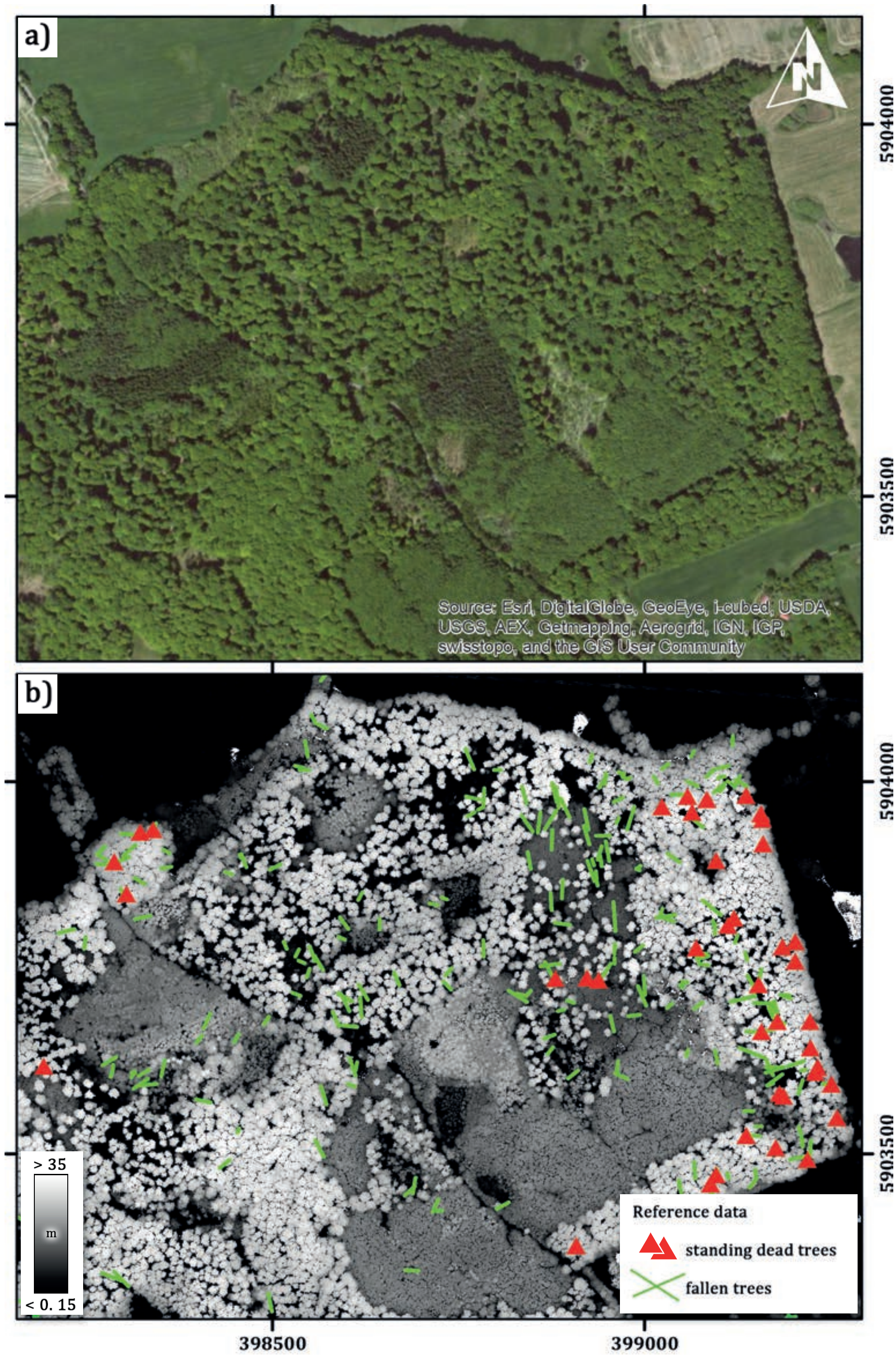

Figure 4.2: The Uckermark study site. (a) True-colour aerial image, (b) nDSM, the red triangles indicate ground truth measurements of standing dead trees, the green lines of fallen trees.

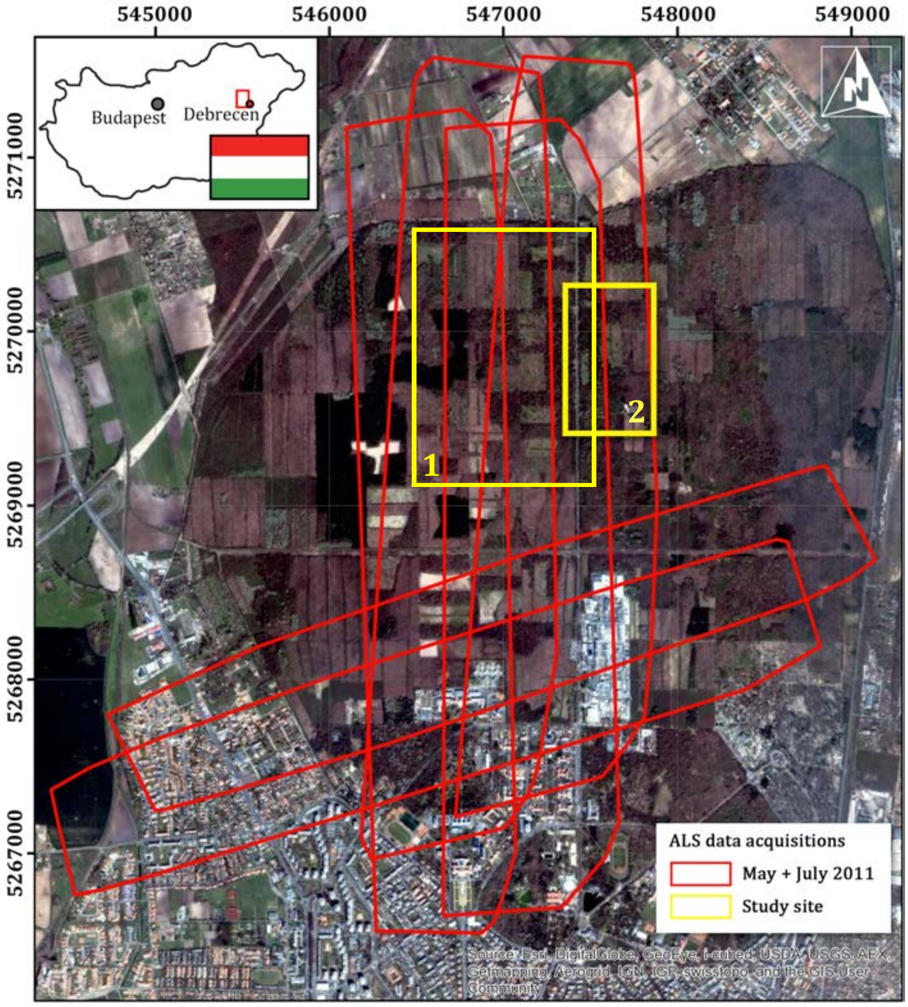

Figure 4.3: Overview of CH2 study area Nagyerdö with ALS flight strip layout for the data acquisition (red outlines). The same flight pattern was used for both acquisition times, in March and in July. The details marked in yellow outlines show the study sites for the layer structure estimation (1; Fig. 4.4) and the deadwood estimation (2; Fig. 6.7).

The second study site in the Seewinkel is a paddock for Hungarian grey cattle on the shore of the Neusiedler See and approximately 4 kilometres south of the Zicklacke (see Fig. 4.6b). The site is regularly used for grazing of the livestock. Like the rest of the Seewinkel, it is a rather flat area, which is also periodically flooded. The predominant plant species occurring in the area are sea rush (*Juncus maritimus*, see Fig. 4.7) and sawtooth sedge (*Cladium mariscus*, see Fig. 4.8), with some scattered patches of common reed (*Phragmites australis*, see Fig. 4.9). All of them are densely growing, while the first two are also short in height (to large extents less than 1 metre, as far as the study site is concerned). The three species differ significantly in their growth pattern. Sea rush forms clumps and has rigid, needle-sharp stems, a few of them always emerging out of the rest and reaching perennial heights of 1 - 1.2 m. In contrast, sawtooth sedge has larger leaves, can grow up to 2.5 m and usually covers larger areas. The edges of the leaves are, as the name suggests, hard serrated. Because of these "protective" or "defensive" features, both species are improper fodder plants for cattle. Common reed, on the other hand, can grow large shoots up to 6 m tall in one year and it usually forms extensive stands. The stems are 1 - 1.5 cm thick and the leaves can be 20 - 50 cm long, which is very similar to sawtooth sedge, although reed does not grow as dense as the sedge species [EOL 2013].

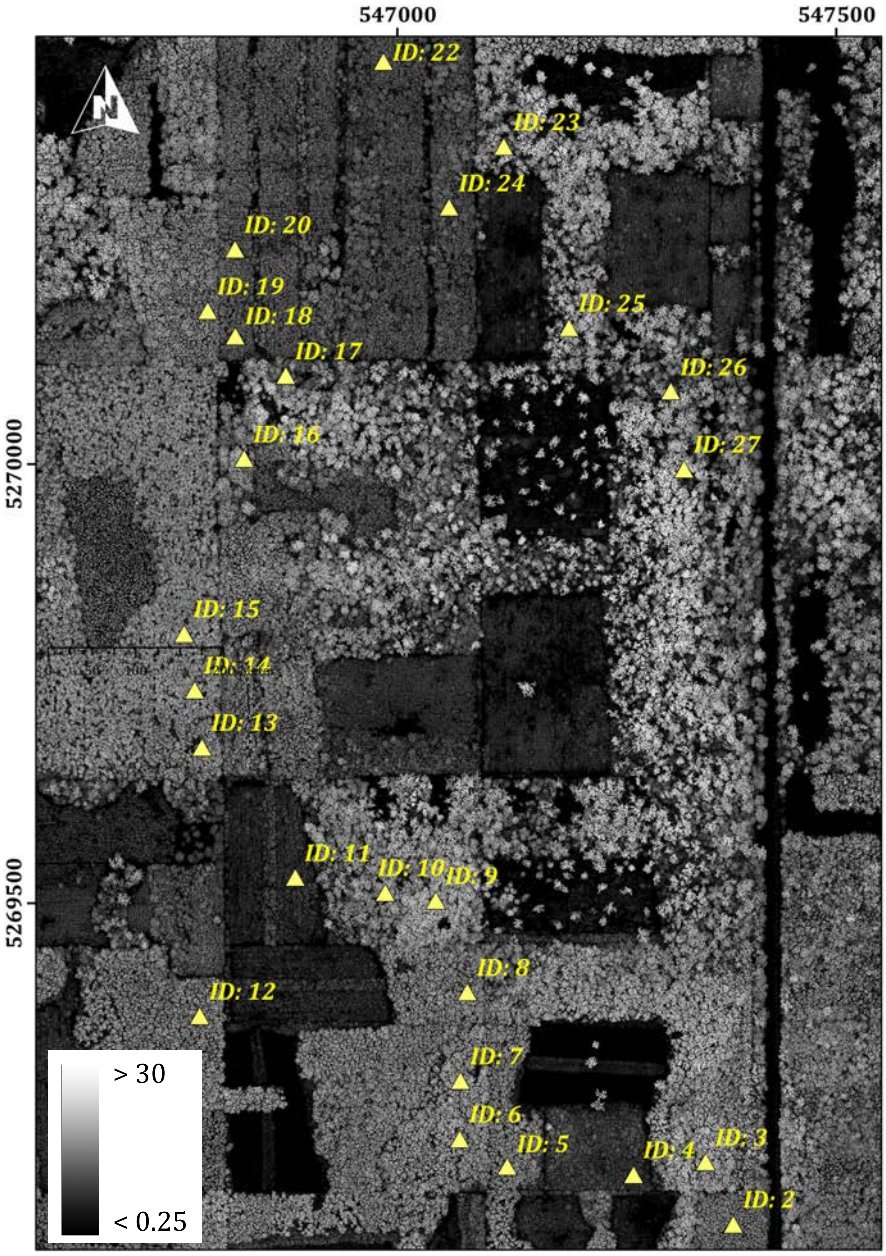

Figure 4.4: Colour-coded normalized DSM showing the study site used for forest layer structure estimation in the Nagyerdö. The sample plots (marked with the yellow triangles) were measured with dGNSPS and the vertical stratification within a radius of 15 m was estimated in the field at those locations.

4.2 Field data

4.2.1 Uckermark and Nagyerdö

Throughout the years 2011 and 2012, that means on multiple times and all seasons, field-mapping campaigns for the purpose of N 2000 mapping took place in the Uckermark and the Nagyerdö. The data collection was conducted by CH2 project partners who are experts in habitat assessment and forest ecology. An especially developed mapping methodology was carried out in order to identify all features of a certain habitat that are relevant for HQ mapping. Relevant habitat patches, species, natural and artificial landscape features were included in a checklist for each occurring habitat type and the field efforts were aimed at locating as many of these features as possible. Depending on the

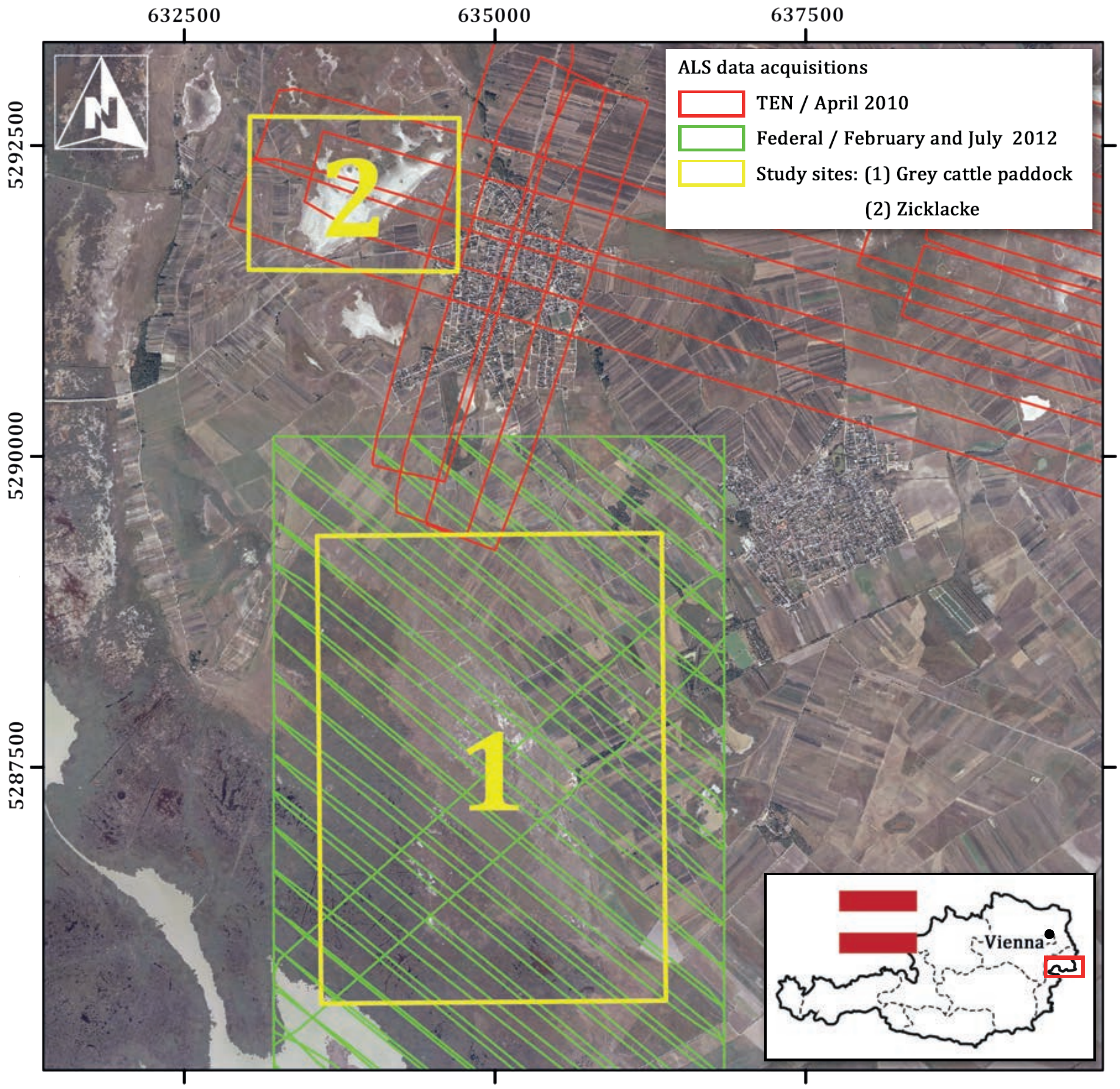

Figure 4.5: Overview of the Seewinkel with TEN and federal ALS data acquisition coverage, and locations of selected study sites (1) grey cattle paddock and (2) Zicklacke. In the case of the TEN ALS flight, the same strip pattern was used for both flights.

type of the feature, it was noted either qualitatively (e.g. presence of animal or plant species) or quantitatively (e.g. number of habitat trees, downed trees, wild boar diggings, etc.).

Each of the selected N 2000 areas consisted of a number of assessment plots, which were selected based on the chosen habitat types for investigation. The plots were as equal in size as possible and as big as they were just manageable for the field assessment crews (usually not more than a few hectares). For each assessment plot the number of vertical vegetation layers was estimated in the field. A vertical layer was counted as such, if a significant amount of foliage or biomass was present at a certain height level, and if it distinguished itself clearly from other layers (e.g. through a difference in species, age class, or a significant gap between two crown layers).
In the Nagyerdö test site, the vertical layering of the canopy was additionally estimated on a point basis. A GIS-grade global navigation satellite system (GNSS) receiver (single frequency, accuracy in open areas approx. 1-3 m) was used to map the locations of a series of 25 points, where in the circular surrounding of 15 m the number of layers was estimated. This plot-based assessment was only

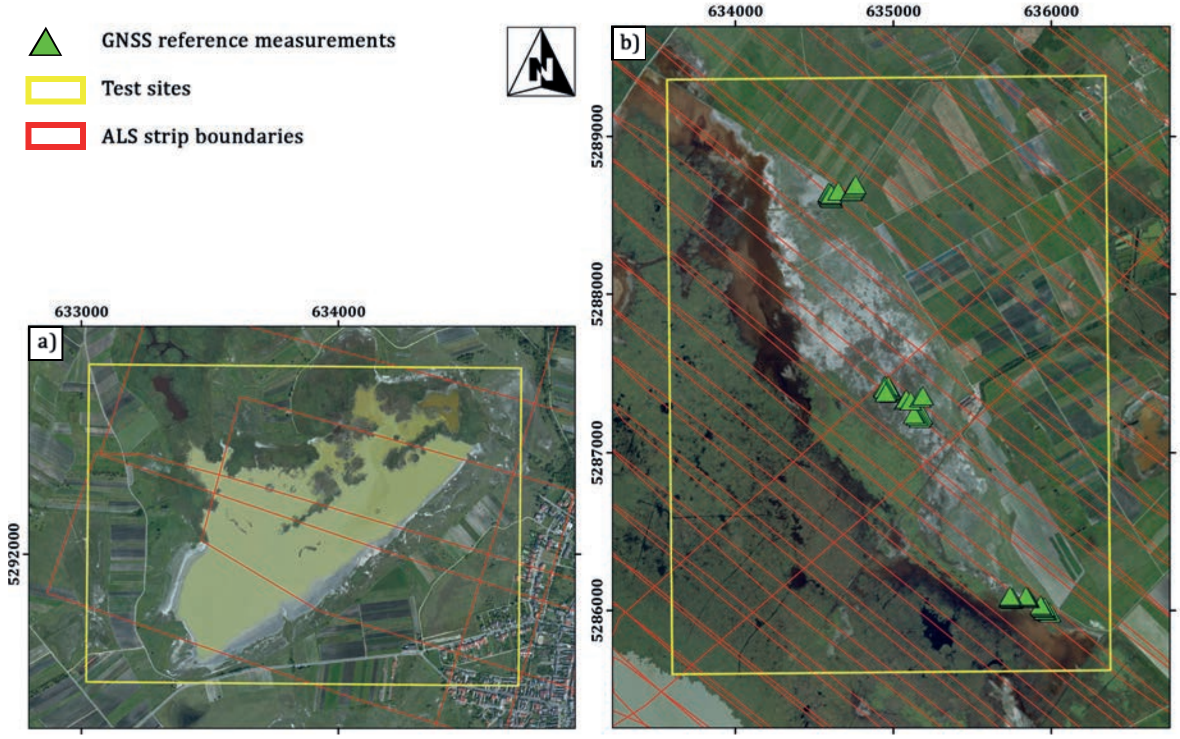

Figure 4.6: Study sites in the Austrian Seewinkel. (a) the Zicklacke and (b) the grey cattle paddock.

Figure 4.7: Examples of sea rush (Juncus maritimus) at the time of ground truth data acquisition in the grey cattle paddock. (I) shows a sparsely covered patch, (II) a medium dense distribution, and (III) shows a very dense patch of sea rush.

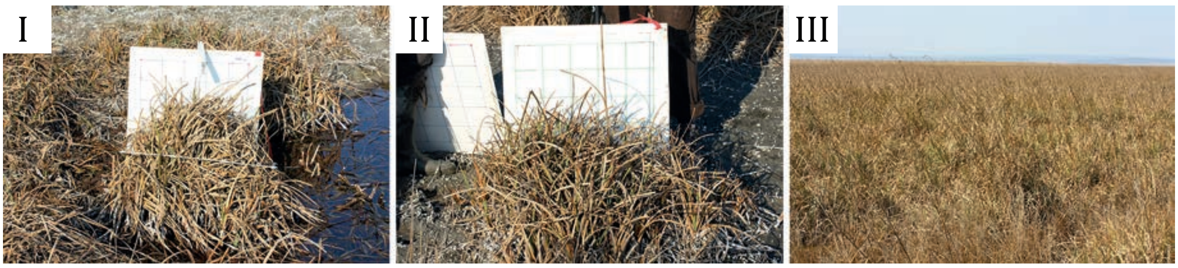

Figure 4.8: Examples of sawtooth sedge (Cladium mariscus) at the time of ground truth data acquisition in the grey cattle paddock. (I) and (II) show medium dense distributions, whereas (III) shows a very dense and extended patch of sawtooth sedge.

carried out during leaf-off conditions. Out of the 25 plots, a shrub layer was found in 24 locations, an intermediate layer in 16 plots and a top tree layer in all locations.

During the mapping significant amounts of downed and standing dead trees were encountered in both study sites. The start- and endpoints of the downed stems and large or thick branches with a diameter bigger than 30 cm were measured using a GIS-grade GNSS receiver. This type of dead wood is also referred to as coarse woody debris (CWD) [e.g. Keddy and Drummond 1996]. All

Figure 4.9: Examples of common reed (Phragmites australis) at the time of ground truth data acquisition in the grey cattle paddock. All images show very dense patches of common reed, as no other coverage type was encountered in the study site.

GNSS coordinates were measured in the global coordinate reference system WGS84 using geocentric Cartesian coordinates and were transformed to ETRS89 using the UTM projection (UTM zones 33 and 34 N). Using a stem diameter of 30 cm as the lower limit for observance is an established rule in the N 2000 assessment (e.g. in Hungary it is 30 cm, in Germany 35 cm). Additionally, the exact diameters and lengths were tape measured and noted. Tree stumps and piles of thin branches (also referred to as fine woody debris, FWD) from fallen trees were mapped with one GNSS point in their centre and photographs were taken accordingly. Furthermore, in the Nagyerdö a deadwood decay state was assigned to all encountered woody debris (fine and coarse), which is described as in Tab. 4.1.

Table 4.1: Deadwood decay states as used in the Nagyerdö study site for all encountered woody debris (fine and coarse).

Decay state	Description
State 1	Fresh downed wood; little to no decay; the bark is still on; the timber is hard.
State 2	Older downed wood; patches of starting decay; bark is loose; patches of soft timber.
State 3	Older downed wood; high level of decay; decay present in the whole stem; bark has fallen off; timber is soft, sometimes falling to pieces.

The locations of the standing dead trees with a diameter at breast height (DBH) bigger than 30 cm and higher than 3 m were also measured with GNSS, their DBH was tape measured and noted. The height of the trees were estimated with a Blume-Leiss-Altimeter. Most of the standing dead trees were broken or decayed to a degree were crown-forming branches were no longer present. Terrestrial photographs were taken of all dead trees and stored together with the cardinal direction of the image acquisition. These were very useful in exploratory data analysis and prove also valuable in the validation process of the methods. In total, in the Uckermark study site 29 downed and 40 standing dead trees were measured, and 86 downed trees or areas of accumulated woody debris (WD) were mapped in the Nagyerdö study site. Standing dead trees were not mapped in Nagyerdö. Figures 4.10 and 4.11 give an impression from the study site during the dead wood measurements in the field.

Figure 4.10: Impressions from the forest study sites during the mapping of the layer structure and dead wood. (a) shows an example of a standing dead tree (snag) in the foreground and some downed CWD in the background. The foreground also shows a hall-like forest with only one mature tree layer and a very young shrub layer. (b) shows a multi-layered forest with a snag on the left and some FWD in the centre. A downed tree (CWD) is covered by the FWD.

4.2.2 Seewinkel

Ground truth measurements in the Seewinkel study site on the grey cattle paddock was conducted in March 2012 by a team of ecologists who are experts in landscape ecological assessment and for wetland vegetation. A random sampling strategy was used to arbitrarily select patches of the three predominant species (sea rush, sawtooth sedge and common reed; see Sec. 4.1.3). The centre positions and elevations of 51 so selected patches was recorded using a geodetic-grade dGNSS receiver (dual frequency, accuracy in open areas approx. 0.1 m). To describe the growth pattern of the plants,

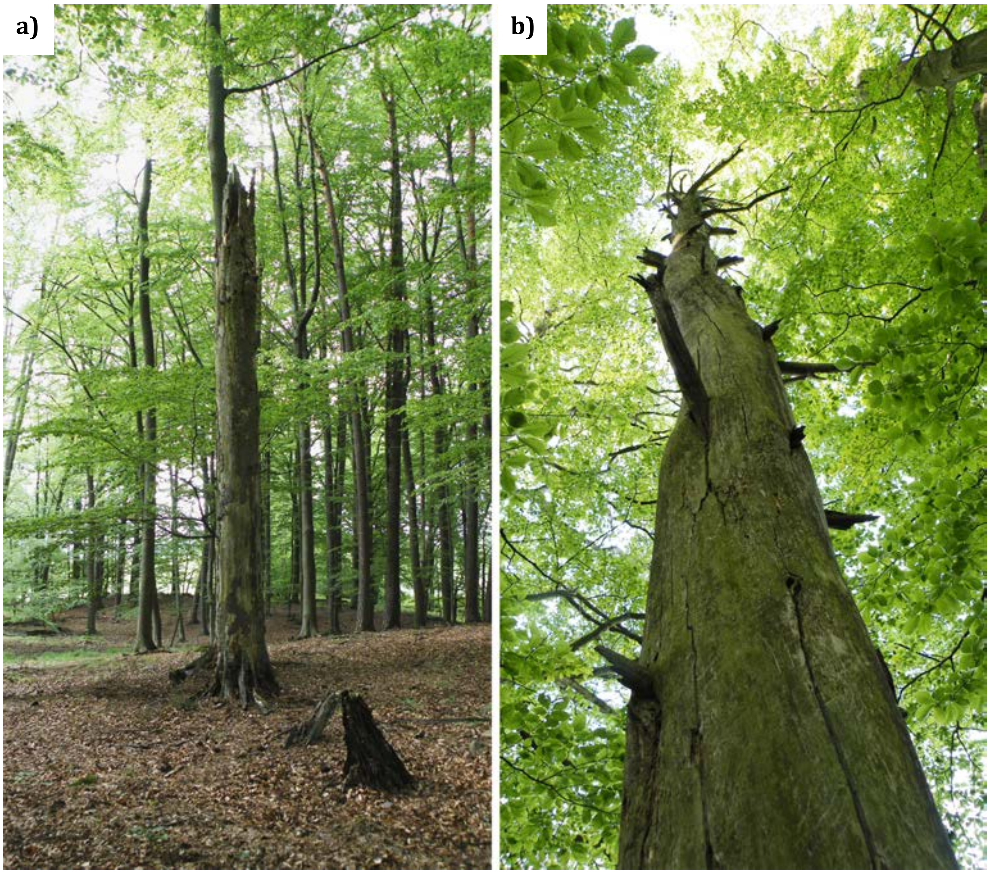

Figure 4.11: Some examples of standing dead trees in the forest study sites.

the maximum height above ground and the height densities per every 20 % step were estimated for each individual using a measurement board (see Fig. 4.12 III). Additionally, the ground coverage, as encountered in the field, was noted in five classes as presented in Tab. 4.2. For practical reasons these five classes were re-classified to three classes as shown in Tab. 4.3. A customized set of datum transformation parameters for the Helmert transformation, which was the same as for the ALS data covering the area, was used to transform the recorded geocentric Cartesian WGS84 coordinates to ETRS89 using the UTM projection (UTM zone 33 N). Due to temporal constraints and sub-optimal weather conditions, ground truth measurements could not be performed in the Zicklacke.

Table 4.2: Classification of ground coverage classes for wetland plants as used in the grey cattle paddock study site in the Seewinkel. Open means either short grass or bare earth.

Class number	Description
Class 1	50% sea rush and 50% open
Class 2	10% sea rush and 90% open
Class 3	80% sawtooth sedge and 20% open
Class 4	100% sawtooth sedge
Class 5	100% common reed

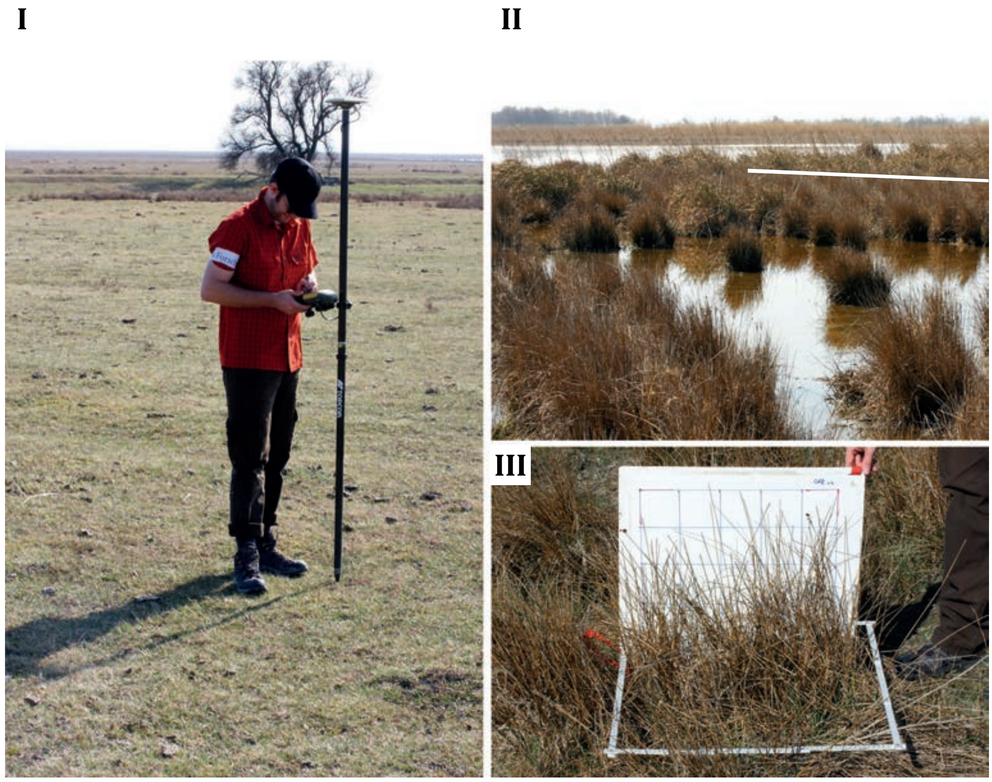

Figure 4.12: Photographs from the ground truth data acquisition in the grey cattle paddock / Seewinkel. (I) measurement of a reference height in an open short grassland area. (II) border between sea rush and sawtooth sedge in the open water of Lake Neusiedl (indicated by the white line). (III) an example of the measurement board for height density estimations of plants.

Table 4.3: Re-classification of ground coverage classes for wetland plants based on the classification used in the grey cattle paddock study site in the Seewinkel. Given class numbers refer to the classes presented in Tab. 4.2.

Class type	Description
Dense	classes 3, 4 and 5
Medium	class 1
Sparse	class 2

4.3 Specifications of airborne laser scanning data and derived height models

4.3.1 Uckermark and Nagyerdö

In the two forest study areas, the Uckermark and Nagyerdö, a RIEGL LMS-Q680i full-waveform laser scanner was used for data acquisition. For detailed specifications of the instrument the reader is referred to the manufacturer's website [RIEGL Laser Measurment Systems GmbH 2013a]. This ALS sensor is capable of emitting and detecting multiple pulses in the air simultaneously, referred to as "multiple-time-around" (MTA). Conventionally, this feature requires careful adaption to the flying height in order to assign each emitted pulse to its respective reflection and make unambiguous range measurements possible. For the flights available for this study a novel method for pulse assignment was used, which makes the data acquisition of multiple pulses in the air independent from the flying height. This is achieved through the application of a specific pulse-position-modulation scheme to the train of emitted pulses, which ensures that the emitted pulse and its respective reflection can be precisely identified regardless of the acquisition altitude [Rieger and Ullrich 2011]. Thus, the data acquisition is much more flexible, allows for higher pulse repetition frequencies compared to conventional systems and requires less tuning with respect to topography. Consequently, more echoes can be detected, which is especially valuable for vegetation analysis, as the depiction by the point cloud is much more detailed.

To study possible influences of vegetation phenology, each study area was flown twice: once in leaf-on and once in leaf-off state. Specifications and settings for the flights are given in Tab. 4.4. The extraction of the single echoes (i.e. returns) from the raw FWF data was achieved by Gaussian decomposition [Wagner et al. 2006] implemented in the software package RiPROCESS [RIEGL Laser Measurment Systems GmbH 2013b]. The 3D ALS data then existed in geocentric Cartesian WGS84 coordinates and were transformed and projected to ETRS 89 coordinates using the UTM projection (UTM zones 33 and 34 N).

Table 4.4: Specifications of the ALS data acquisitions in the Uckermark and Nagyerdö study sites.

	Uckermark		**Nagyerdö**	
Acquisition time	May 2011	March 2012	March 2012	July 2012
Phenological state	leaf-on	leaf-off	leaf-off	leaf-on
Aircraft	Helicopter		Aeroplane	
Number of strips	36	33	8	6
Lengthwise strip overlap (min.)	50%		50%	
Deflection angle (max.) [°]	± 30		± 30	
Altitude [m]	∼ 500		∼ 500	
Footprint size [m]	∼ 0.25		∼ 0.25	
Echoes / m^2	21.9	16.2	27.5	29.4

A DSM was computed based on the first echoes from the leaf-on flights using moving planes interpolation (i.e. moving least squares interpolation) [Kraus 2000]. A DTM was created from the last echoes using hierarchical robust filtering [Kraus and Pfeifer 1998] based on the leaf-off data and incorporating the full-waveform information as described by Mücke [2008]. Subsequently, this DTM was used to augment the ALS point clouds with normalized point heights (i.e. the height of the echoes above the terrain), and to generate a normalized DSM (nDSM). All described height models were created with a grid size of 0.25 x 0.25 m^2.

Using the normalized point heights, height distributions of laser echoes and penetration rates could be calculated for both study sites. The term height distribution refers to the frequency (or density) of laser echoes in a certain height interval above ground level. The penetration rate is defined as the relation of ground echoes to all echoes within a defined area. High penetration rates and, consequently, a good description of the vegetation in the point cloud are an important prerequisite for vegetation analysis with ALS data. Naturally, the more laser shots reach through the foliage (during leaf-on season) or the upper most branches (during leaf-off season) and range down to the sub-dominant vegetation layers, the better the entire vegetation structure is depicted. The denser the foliage or branch structure, the quicker the laser pulses are attenuated. Portions of the energy are lost in the canopy and ground echoes are less likely.

Figs. 4.13 and 4.14 show the distribution of the laser echoes for the vegetated areas for both test sites and acquisition times. Tab. 4.5 gives an overview on the estimated penetration rates. These statistics demonstrate that the data sets of both study areas and acquisition times show similar echo distributions, which indicates comparable penetration and depiction of the vegetation structure down to sub-dominant layers. However, from the histograms of the leaf-off data sets, which feature higher frequencies in the near-ground height levels, a better representation of the lower vegetation parts can be assumed.

The (slightly) bimodal distributions of the histograms from Nagyerdö (see Fig. 4.13 a and b)

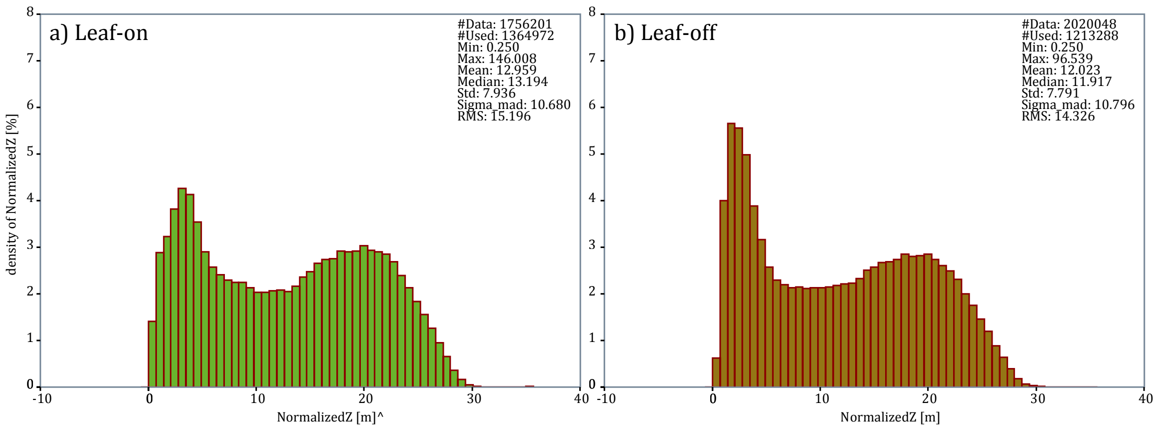

Figure 4.13: Height distribution of laser echoes in the Nagyerdö study site during (a) leaf-on and (b) leaf-off conditions. Both data sets show a similar distribution indicating comparable depiction of the vegetation structure. The leaf-off data feature better representation of the lower vegetation parts.

generally imply very evenly distributed vegetation, possibly with a clearly distinct shrub layer (i.e. vegetation usually lower than 5 m). Whereas for the Uckermark, a multi-modal distribution can be observed (see Fig. 4.14 a and b), indicating the possible existence of (1) a top layer, consisting of high trees, (2) a medium high layer, consisting of younger successional trees, and (3) a shrub layer. The

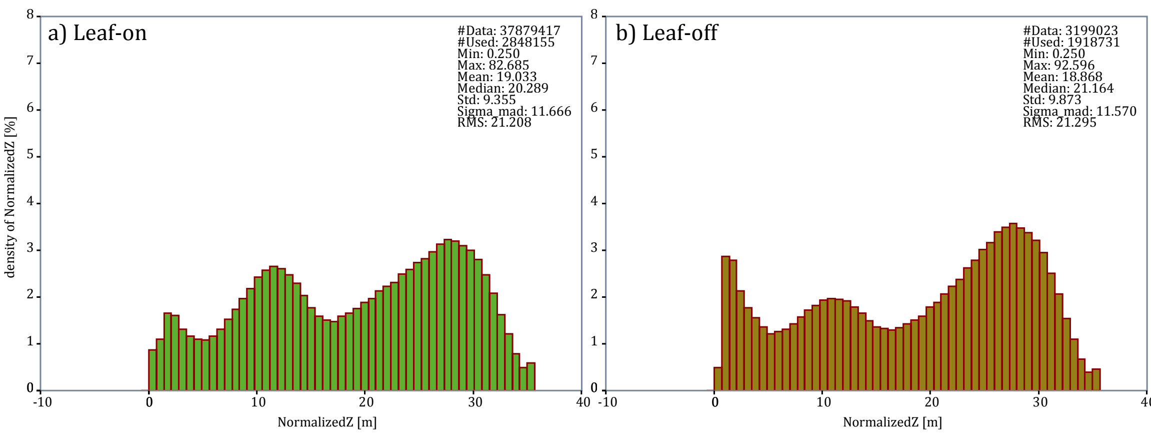

Figure 4.14: Height distribution of laser echoes in the Uckermark study site during (a) leaf-on and (b) leaf-off conditions. Both data sets also show a similar distribution indicating comparable depiction of the vegetation structure. The leaf-off data feature better representation of the lower vegetation parts. The multi-modal histogram further indicates the possible existence of multiple vegetation layers.

penetration rates show considerable differences between the leaf-on and leaf-off acquisitions, which points out that the representation of ground in (mainly deciduous) forests, comparable to the ones in the two study areas here, is generally better during leaf-off than leaf-on state.

Table 4.5: Penetration rates for study sites in the Uckermark and Nagyerdö.

	Uckermark		**Nagyerdö**	
Phenological state	leaf-on	leaf-off	leaf-on	leaf-off
Penetration rate [%]	10,6	44,0	10,3	40,0

4.3.2 Seewinkel

The ALS data of the Zicklacke study site and the grey cattle paddock in the Seewinkel were also acquired using a RIEGL LMS-Q680i. The main parameters of the flights are summarized in Tab. 4.6. Likewise as for the CH2 acquisitions, two flights were carried out covering the Zicklacke in order to study vegetation phenology. The ALS data for the grey cattle paddock were extracted from a federal data set provided by the surveying department of the province Burgenland.
FWF decomposition was also conducted in RiProcess and ETRS89 with UTM was used for projection of the data from the Zicklacke. As mentioned in section 4.2.2, a specific set of parameters was derived for the Helmert transformation and used to transform and project the data of the grey cattle paddock from WGS84 to ETRS89 with UTM. During both ALS data acquisitions the Zicklacke was covered with water (depth less than 1 m).

One of the hypotheses of this thesis is that the derivation of height models (DTMs and DSMs) in wetlands, such as the area around the Zicklacke, with very low topographic energy and high amounts of low-growing vegetation, is far from trivial. In fact it is a principal topic discussed in this study. Therefore, unlike the description of echo distributions and basic height models in the former section 4.3.1, the reader is referred to section 7, where a detailed analysis of the point cloud with respect to vegetation description and height modelling is given.

Table 4.6: Specifications of the ALS data acquisitions in the Seewinkel study sites.

	Zicklacke		**Grey cattle paddock**
Acquisition time	February 2010	July 2010	April 2010
Phenological state	leaf-on	leaf-off	leaf-off
Aircraft	Aeroplane	Aeroplane	Aeroplane
Number of strips	18	14	30
Lengthwise strip overlap (min.)	50%		50%
Deflection angle (max.) [°]	± 30		± 30
Altitude [m]	∼ 500	∼ 490	∼ 500
Footprint size [m]	∼ 0.25		∼ 0.25
Echoes / m^2	14.1	13.7	14.3

5

Estimation of the Forest Layer Structure

5.1 Aims

Knowledge about the 3D structure of the vegetation is of critical importance for N 2000-related habitat assessment (c.f. Sec. 1.1 and 3.1). Especially the presence or absence of understory (sub-dominant tree and shrub layers) can indicate that a forested area is suitable as a habitat or corridor for a certain species.

ALS is known to quite accurately depict the canopy surface, an ability that is usually exploited to derive vegetation heights and to compute a nDSM. Depending on the extent of an assessment area, a nDSM may also depict multiple vegetation layers. However, this information can only be based on the upper crown heights of the dominant plants (see Fig. 5.1, case 1). Yet, ALS is capable of entering the canopy through small gaps and thus depicting the arrangement of foliage masses below, a fact that cannot be accounted for in the nDSM (see Figs. 5.1, case 2, and 5.2).

In the following chapter, the penetration capability of ALS shall be used to derive information on the abundance of sub-dominant vegetation layers. An automatic detection method shall be implemented, which makes use of the distribution of ALS echoes in the canopy to identify clusters of echoes representing different vegetation strata. The success of the method will be evaluated using field assessment data from the Nagyerdö test site.

5.2 Methods

The underlying hypothesis is that the distribution of ALS echoes in vegetation allows to draw conclusions on its structural complexity. Given adequate penetration of the canopy, as discussed in section 4.3.1 for the ALS data at hand for this study, a lack of echoes in a certain height interval is therefore considered to be founded in the absence of vegetation to act as a reflector, rather than in

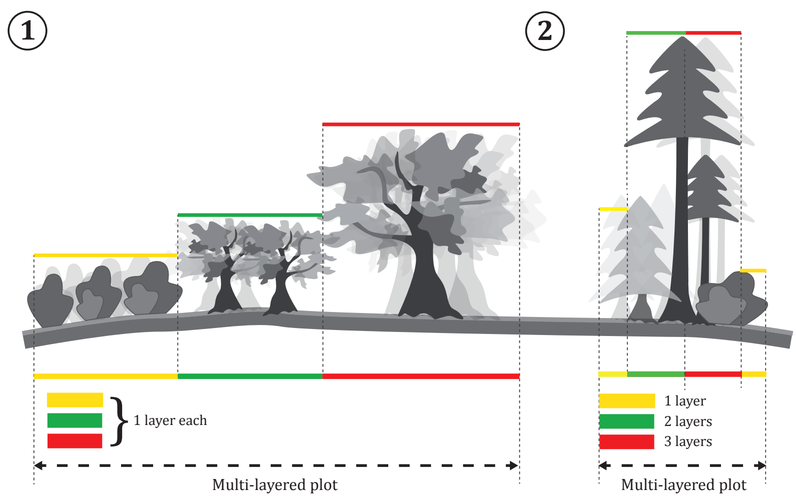

Figure 5.1: Illustrations of two different ways of how a forest layer structure can be observed. (1) shows a scene, where each part individually can be seen as one-layered. An assessment plot may include multiple one-layered structures of different height, thus becoming multi-layered. This type of structure is depicted by a nDSM. (2) shows a multi-layered scene including shrubs, sub-dominant and dominant trees of different heights overgrowing each other.

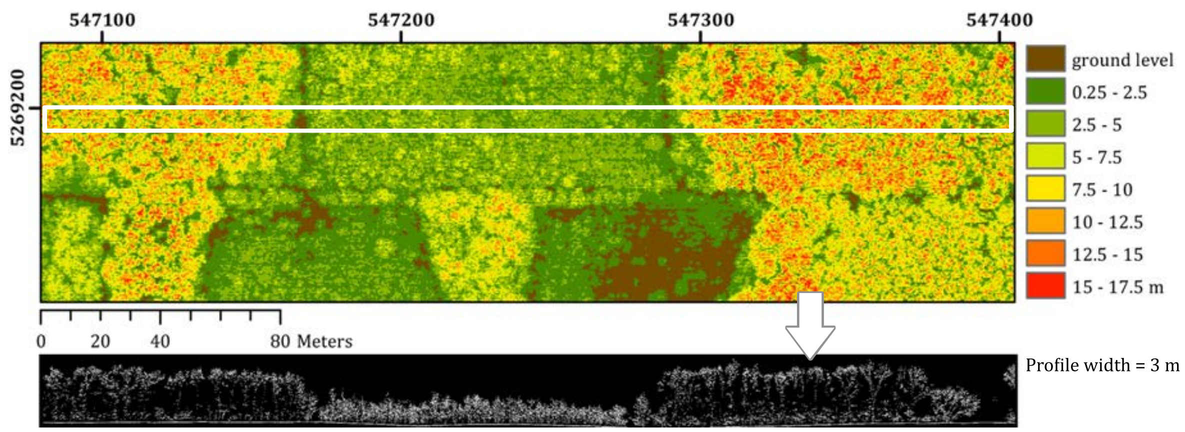

Figure 5.2: The nDSM on top represents the upper crown heights of the dominant tree layer. It depicts a multi-layered part of a forest, where the vegetation heights range from 0.25 to above 17.5 m. The ALS point cloud profile in the bottom (position marked by white rectangular in nDSM) clearly shows the additional information contained in ALS point clouds, disclosing additional sub-dominant tree and shrub layers, not visible in the nDSM (e.g. at the position of the white arrow).

the occlusion from higher parts of the canopy. The clustering of ALS echoes on the other hand is an indication for the presence of a significant amount of foliage (or canopy) mass, and is consequently considered to represent a vegetation layer.

The presented approach is based on this hypothesis. It has two parts, starting from the ALS point cloud. The full workflow for the proposed layer structure estimation is illustrated in figure 5.3. The first part deals with preliminary computations, calculating and preparing the necessary input data. In the second part, the actual layer structure estimation is carried out for each pixel (i.e. pixel level) and for a (usually) larger assessment area (i.e. plot level). Concentrating on two assessment units like this brings the benefit of exploiting the high resolution offered by ALS to detect vegetation layers also for vegetation objects or foliage masses with only little area coverage, thus estimating the layer structure with high detail. On the other hand, these fine resolution results can then be examined in the context of a larger area, in order to deal with higher variation in stratification and derive an overall estimate for area wide assessments, as they are needed for N 2000 protocols.

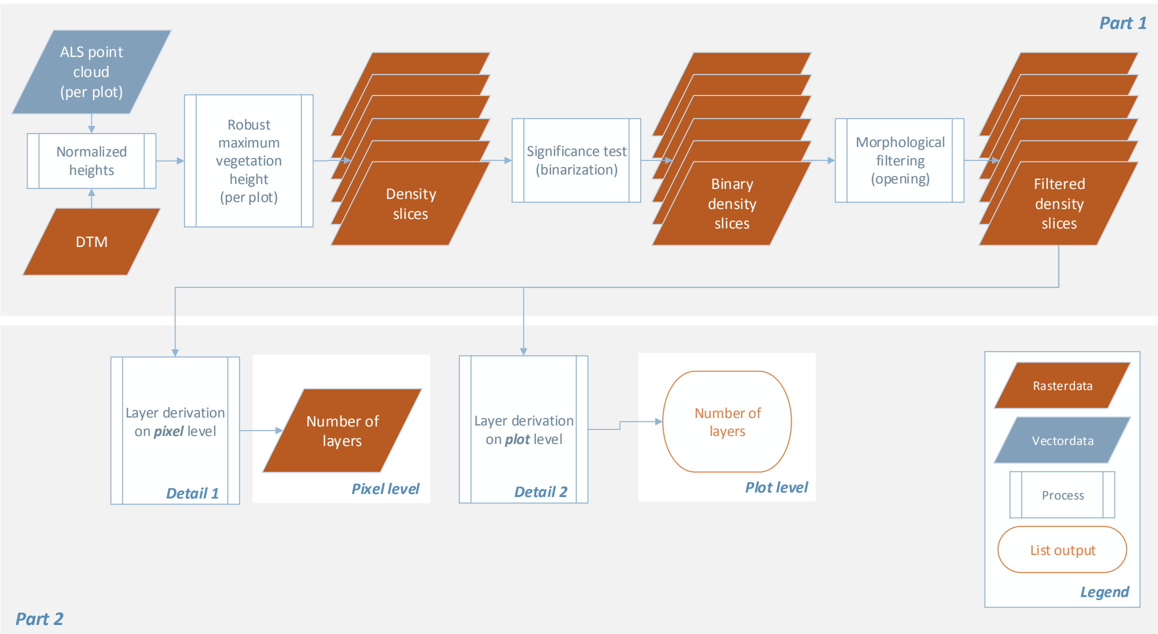

Figure 5.3: Illustration of the workflow for the automatic estimation of the forest layer structure based on the ALS point cloud. The derivation of the layers on pixel level (Detail 1) is shown in figure 5.4a, the derivation of layers on assessment plot level (Detail 2) is shown in figure 5.4b. and 5.5. The output on pixel level is a raster map containing the total number of layers per grid cell. The output for the plot level is given as text for each assessment plot.

For each grid cell (i.e. pixel) in the assessment area, the point cloud is divided into equal height intervals (i.e. levels of height above ground). These intervals are defined as a percentages of the maximum vegetation height in the assessment area. The maximum vegetation height (i.e. normalized height, nZ) is determined robustly, as described by equation 5.1, so that single high trees or occasional outliers of ALS echoes do not influence the estimation.

$$max_{nZ}^{rob} = med_{nZ} + 3 * \sigma_{nZ} \tag{5.1}$$

where $\max_{nZ}^{rob}$ is the robustly determined maximum vegetation height, med_{nZ} the median of all calculated normalized heights, and σ_{nZ} their single standard deviation.

Essentially, this partitioning of the point cloud on the basis of a pixel in the footprint and a certain height range in vertical direction creates a volumetric space which is reminiscent of a so-called volumetric pixel or voxel. However, in the case presented here, the volumetric space does not necessarily have to be exactly cubic, as a voxel usually is. Furthermore, from a programming point of view, it is not a voxel representation that is used in the presented approach, in fact all calculations are based on the pixel.
For each pixel the number of ALS echoes inside one height level divided by the total number of ALS echoes inside the pixel column is then calculated. This results in the relative point count or density for each pixel, thus they are further referred to as density pixels. All such density pixels of one height interval together are further referred to as a density slice (see Fig. 5.4a).

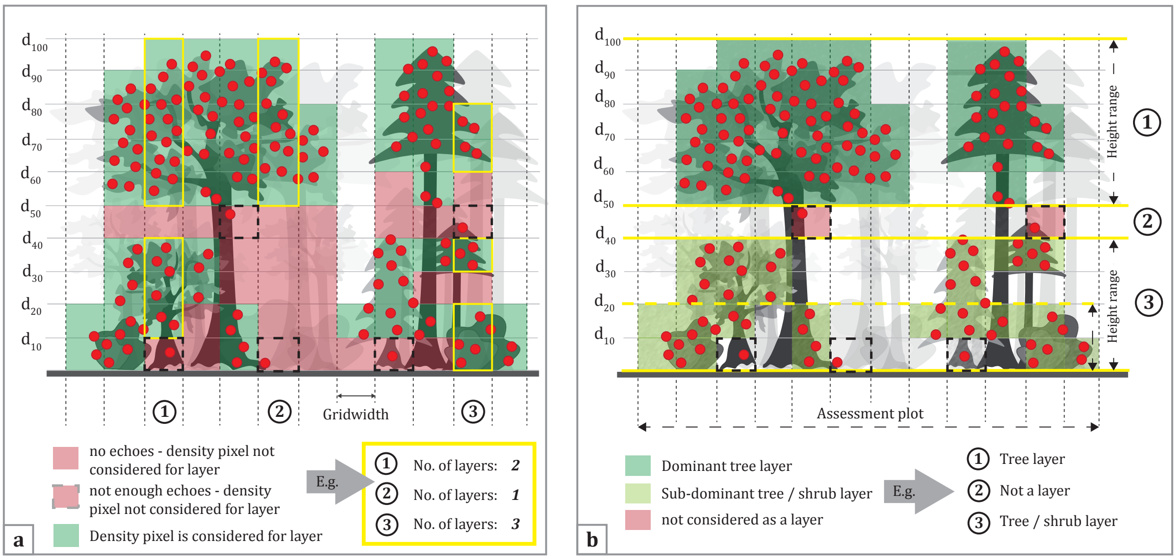

Figure 5.4: (a) Derivation of the vegetation layers for each density pixel. Example 1 shows two sequences of density slices creating two layers (sub-dominant and dominant tree layer), example 2 one sequence for a one-layered scene (dominant tree layer) and example 3 three comparably short sequences which form a three-layered scene (shrub-, sub-dominant- and dominant layer). The density pixels marked with the dashed black outline did not pass the significance test and were therefore not considered. The detected layers for the three example pixel columns are marked with a yellow outline.
(b) Derivation of the vegetation layers on assessment plot level. Examples 1 and 3 show vertically connected density slices representing two separate vegetation layers. Example 2 constitutes a gap in the vegetation structure, including the density pixels that were not considered.
The bottom four density slices at first constitute a single layer, but are in a further step separated into a shrub layer and a sub-dominant tree layer (dashed yellow line).

A density pixel is expected to contain a defined minimum number of ALS echoes in order to be included. This is called the significance test. A minimum density threshold, which is referred to as the significance level, can be set for one density pixel. This is intended to account for pixels which hold too few echoes to represent a structure that would in practice be regarded as a significant foliage mass. A similar situation is described by figure 5.4a, examples 1 and 2 (density pixels not considered are marked with a dashed blacked line). The significance test results in a binary classification of the density pixel: if the pixel passes the test, it is set to 1, otherwise it is set to 0.
Subsequently, morphological opening is applied to each binary density slice. This filtering step is meant to reduce noise which was introduced by pixels that narrowly passed the significance test, but do not have the support of their neighbourhood, in the sense that they are isolated. Although care

must be taken in this step not to eliminate too much information in the process, thus the kernel size (which defines the neighbourhood of the operation) is set to a minimum of 3 x 3 pixels.

After the calculation of the densities for each pixel and the significance test (see Fig. 5.3, part 1), the method carries on in two ways (part 2):

1. it calculates the number of possible vegetation layers per pixel.
2. it determines the number of vegetation layers for an assessment area based on the a-priori per pixel estimates.

To achieve action (1), the algorithm probes all pixel (column) positions for vertical sequences of consecutive density pixels set to 1 during the significance test. A sequence begins or ends if a 0-density pixel is encountered. The total number of sequences in one column is considered to correspond to the total number of vegetation layers in that respective pixel (see Fig. 5.4a, examples 1 to 3, yellow outlines represent one layer).

Action (2) requires a definition of an assessment area for which the layer estimation is carried out. This area then includes a number of density pixels, or more specifically columns. The area extent defines the size and the shape of the density slices.
To determine the number of layers present in the area, the algorithm proceeds in a similar way as for the pixels. It starts from the bottom density slice and moves upwards, thereby comparing each slice with its consecutive one above. The comparison is achieved through calculation of the difference in coverage of two binary density slices. The coverage is defined by the number of pixels set to 1 divided by the total number of pixels in the assessment area, whereas always the second (consecutive) slice is subtracted from the first (current) slice (see Fig. 5.5).

Based on the presence of gaps (i.e. all-0 or empty density slices), the number of layers in the area can be detected (see Fig. 5.4b, examples 1 to 3, and Fig. 5.5). If the difference between two consecutive density slices, where one is an empty slice, is negative, the beginning of a layer is found. Likewise, if a positive difference is encountered, a layer end is found. Likewise as for the density pixels, a vertical sequence of density slices depicting 1s corresponds to one vegetation layer. All detected sequences together give the total number of layers for the assessment area (see Fig. 5.4b and Fig. 5.5).

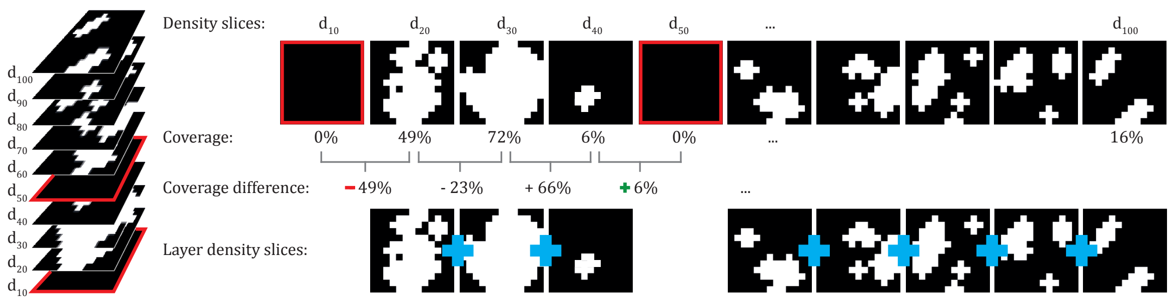

Figure 5.5: Example for the calculation of vegetation layers for an assessment plot. The top row shows ten density slices, two of which are all-0 (empty) and therefore represent a gap in the vertical structure. The accumulated density slices between the gaps represent one vegetation layer each.

The detection is obviously limited by the fact that if two consecutive layers do not distinguish each other through a gap in between them, the method cannot recognize them as two distinct layers

and they will be combined into one continuous canopy. A threshold-based decision strategy was included in order to account for this fact. After the layers were initially detected, they are inspected following a specific rule-set and, when indicated, they are separated or recombined. The rules for this step were derived from the manual ground assessment method and aim to imitate it:
(1) The shrub layer, here the lowest while still counted vegetation layer, is only considered as such if it is actually lower than a certain height. This definition depends on N 2000 assessment instructions of the country where the assessment takes places, but in the case of this study (Hungary) it is 5 m. Above this threshold, any vegetation would not be seen as a shrub, but more likely as a small tree.
(2) To be counted as distinct entities, two layers have to show a certain height difference between their canopies, either for the crown starting- or end-points. Following the applied practical approach during field vegetation surveys within CH2, this height difference was defined as 30% for the kind of forest in the study area. Methodically, it is used as a threshold and it is implemented as such that first a potential shrub layer is searched (as described by (1)), and afterwards the next occurring layer start or end above the shrub layer is tested. If it is by more than the given percentage higher than the upper end of the shrub layer, the respective layer will be treated as distinct. Otherwise it will be connected with the shrub layer. This test is carried out for all consecutive layers, proceeding in the same manner. It prevents that only one layer is identified for continuously detected canopies, ranging from ground level to e.g. 25 m, which would be unrealistic.

It is to be expected that the results of the estimation method will exhibit dependencies from certain parameters, which is a fact that requires inspection. These parameters are (1) the *grid size*, (2) the definition of the height intervals, so-called *stepsize* and (3) the threshold used as a minimum percentage of ALS echoes per density pixel for the significance test, so-called *significance level*.
The other two involved parameters (i.e. the maximum height of the shrub level and the height difference between canopies) may of course also be varied. However, they are defined and derived from incorporated ground assessment protocols and forest types, and are thus assumed constant for the assessment areas in this study.

In order to determine adequate parameter settings, the three parameters are varied in meaningful ranges and permuted. The parameter ranges are given in table 5.1.

Table 5.1: Different parameters used for the layer structure derivation in the Nagyerdö forest plots.

Stepsize [%]	Grid width [m]	Significance level [%]
5	1	5
10	2.5	10
20	5	15
25	10	20
	25	25
	50	

For every possible combination of parameters the presented method is applied on the 25 sample plots collected in the Nagyerdö forest site. Through comparison of the presence or absence of a certain layer to the corresponding information from the ground assessments, the detection success of the method is evaluated. A layer which is detected by the above described approach and is also noted in the field assessment protocols is called a true positive (TP), one which is not in the ALS-based result, but was noted in the field is called a false negative (FN), and finally a layer that is detected in the automated estimation but is not present in the field notes is a false positive (FP). The numbers of TPs, FNs and FPs are then used for calculating the detection completeness and correctness for every parameter combination (see qg. 5.2) [Heipke et al. 1997].

$$Completeness = \frac{||TP||}{||TP|| + ||FN||} \qquad Correctness = \frac{||TP||}{||TP|| + ||FP||} \tag{5.2}$$

In this way, the dependency and robustness of each parameter can be investigated and also the most accurate settings can be identified by selecting the combination with the best success, defined by the highest numbers in completeness and correctness.

The field assessment for the estimation of the forest layer structure took place in the Nagyerdö forest site during leaf-off conditions. However, all involved computations for this study were carried out for the leaf-off and leaf-on data sets likewise, in order to investigate possible influences caused by phenological phenomena. Furthermore, the field assessment accounts for three possible strata: shrub layer, intermediate (or sub-dominant) and top (or dominant) tree layer. However, in theory, the presented approach is capable of detecting more than three layers. The evaluation was thus carried out so that it accounted for the same definition of structure for both, the manual and the ALS-based assessment. If an intermediate layer was found in the field and more than one intermediate layers were found automatically, which actually means that more than three layers in total were detected, than the detection of the intermediate layer was counted as successful.

The method, including the evaluation as described above, was programmed in Matlab [Mathworks 2013], whereas for some raster-data-based operations OPALS [OPALS 2013] was used. The employed DTM was calculated with SCOP++ [SCOP++ 2008], and the visualisations were achieved with FugroViewer [FugroViewer 2014] and ArcMap [ESRI 2013].

5.3 Results and discussion

5.3.1 Layer detection on pixel level

The proposed layer detection method produces two separate outputs: the number of layers on pixel and on plot level. First the results on pixel level shall be examined. The respective output is a raster map, which shows at every pixel location the sum of the layers found on the basis of vertically connected density pixels in every pixel column. The maps were produced for all 25 locations in the Nagyerdö forest, which were surveyed during the field assessment. Automated evaluation of the results on pixel level was not possible due to the differing mapping areas. The field assessments were carried out for circular plots of 15 m radius, thus also the notes on the assessed structure referred to this area. The pixel-based automatic result however features much higher resolution and thus more detail. Therefore the results were visually examined, the focus being primarily on the correspondence of the output and the abundance of vegetation layers in the ALS point cloud, represented by clusters of echoes.

Figure 5.6a - d shows examples for four of the 25 plots in Nagyerdö, including colour-coded layer maps created with different parameter settings, as well as two profiles through the ALS point cloud for each location. To investigate the robustness of the method for various parameter combinations, the colour-coded maps always represent different results for the same plot. The ALS point cloud profile width is in all cases equal to the grid width of the raster map.
These four locations were selected because they assemble a diverse range in terms of vertical vegetation structure. All plots have a shrub or intermediate (sub-dominant) tree layer, as well as a dominant tree layer overgrowing the plot. However, figures 5.6a and c show a part of the forest which has a homogeneous canopy, meaning the top most surface features only small height undulations, and both plots are clearly two layered. On the contrary, figures 5.6b and d have very diverse canopies and are multi-layered, featuring complex vertical stratification.

For easier visual comparison, the above described profiles were not only extracted from the ALS point cloud, but also from their corresponding areas in the colour-coded layer maps. In figure 5.6 they were plotted below each corresponding ALS profile. The raster maps on the left always represent the higher (finer) resolution.

It can be seen that the layer map created with smaller grid widths in general represents the visual impression from the point cloud profile very well. Where a distinct shrub layer and a top layer are present, the method detected two layers correctly. In some cases, as in figures 5.6b and d, also intermediate layers were correctly indicated. This is especially noteworthy, as these two plots have a very complex vertical vegetation structure. For figures 5.6a and d, also the larger grid widths (25 and 5 m, respectively) provide a good estimate of the present foliage clusters. In figures 5.6b and c, which were created with larger grid widths and significance levels than the others, the adequacy is varying. Sometimes the profile views give the impression as if more layers were mapped by the laser scanner than actually indicated by the layer map. A possible reason is that in these cases the significance level was not passed, because there were after all not enough echoes in the corresponding density pixel to make it count. Especially figure 5.6c gives that impression for the larger grid width. Only a one-layered plot is depicted by the raster map, whereas the profile clearly shows understory.

The layer maps shown in figures 5.6a, b and d indicate three layers, with only b and d holding more than one such three-layered pixel. Closer investigation of the point clouds from the corresponding plots revealed that for figures 5.6b and d the result is true, as can also be seen in figure 5.6d, which shows a profile through the three-layered part (on the locations of the dark green pixels).
In figure 5.6a the stepsize was set to 5% and the gridwidth to 2.5 m, which created a very fine resolution. The single three-layered pixel was actually caused by a stem of a large tree, which was along the stem probably not evenly sampled by the laser scanner. Consequently, the significance test was only passed for some of the density pixels. This obviously created three short sequences of connected density pixels, which resulted in the detection of an additional layer that was actually not present in the field, or was not seen as such by the field worker.

This points out a general dependency for the settings of the detection method. The two parameters defining the extents of a density pixel are the gridwidth and the stepsize, the latter being responsible for the respective selection height. If the space limited by one density pixel is much smaller than the vertical extent of the usual foliage mass that would be considered for a layer, then an effect similar

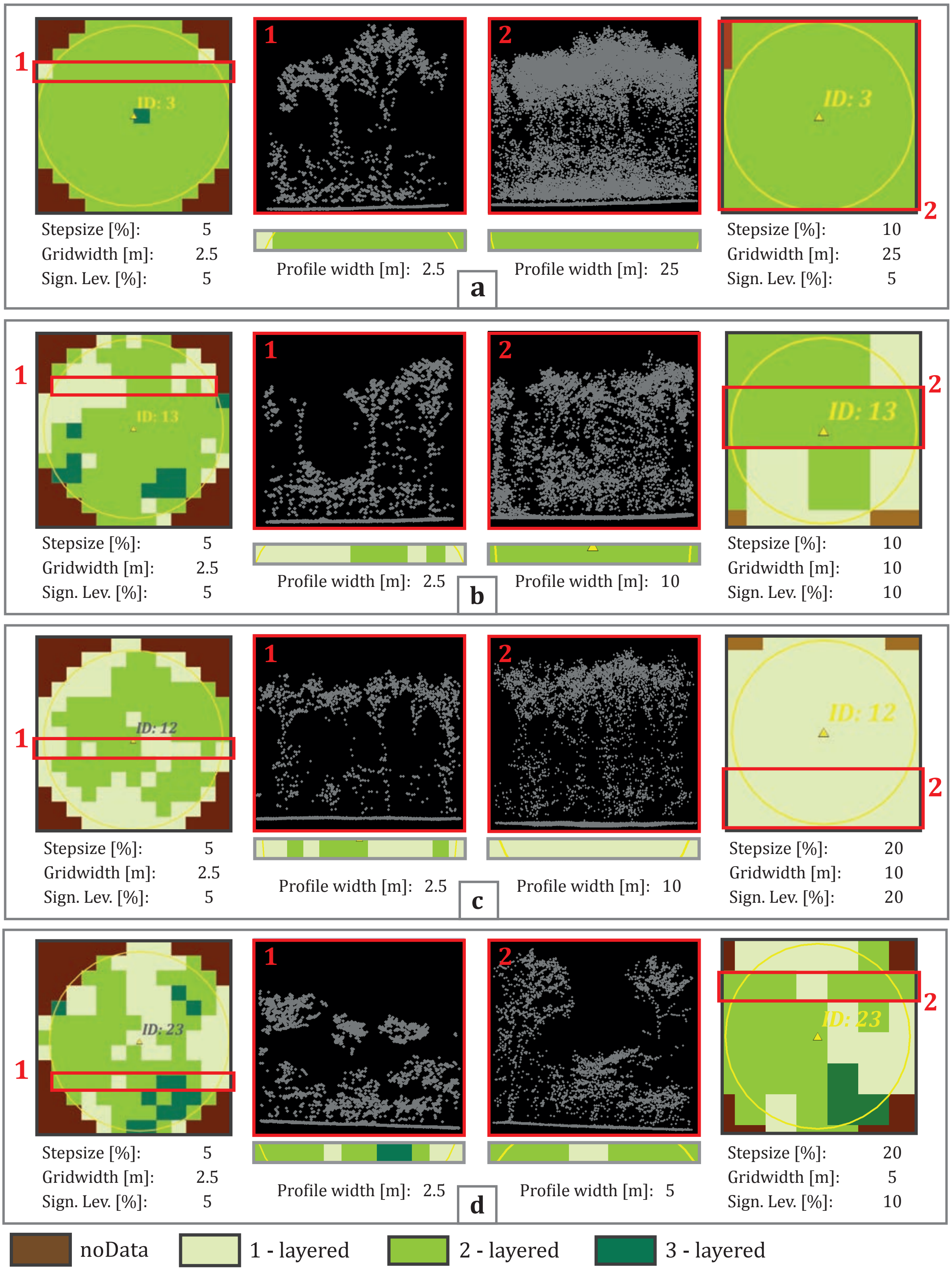

Figure 5.6: Examples of the layer structure estimation on pixel level given for five different plots (a - e) measured in the Nagyerdö. The colour coded maps on the left an right show the total number of layers per pixel. Next to the raster maps, two profiles through the respective ALS point clouds are given. Profile 1 belongs to the left raster map, profile 2 to the right. The profile widths are for all examples equal to the gridwidth of the corresponding raster map and their locations are indicated with red polygons. Below the profile a clipping of the respective part of the raster map is shown to simplify comparison.

to oversampling can occur. In the case of a point cloud including some scattered clusters of echoes probably representing many single branches, it will lead to the detection of more layers than actually present.
To give a definition for the extents of foliage mass to qualify in that sense is however not easily possible. One way would be to examine the ground assessment data to find out about the smallest vegetation object that was actually mapped and use this as a guideline.

With this in mind, it can be reasoned that before application of the method, the vegetation heights of the assessment area should be examined (e.g. by basic statistics or visually in a 3D point cloud viewer) and the stepsize should be adapted. It should create meaningful height intervals, big enough to cover an occasional gap between foliage masses which are not expected to form distinct layers, e.g. a few large branches. This adaption may require a-priori knowledge of the type of forest in question. Such information could be if it is deciduous or coniferous, or what the approximate age or development stage is. These are parameters that can indicate a typical growing structure. However, it shall be pointed out that in the case of N 2000 assessments, where the biggest problem are the repetitive assessment cycles and not the initial ground survey, this type of information is usually at hand.
An assumption based on such a-priori knowledge is in fact already included in the detection method, as well. As described in section 5.2, the 5 m shrub layer threshold, as well as the 30% height difference between two consecutive layers to form two distinct canopies, are based on effective assessment strategies, which always relate to a certain habitat or biotope type. Both thresholds may be defined differently for other types of forest.

Examination of the results on pixel level and comparison with the ground assessment data revealed that it never occurred a top tree layer was present and was not detected. Every field plot used for evaluation included a dominant tree layer and it was detected in every case with any parameter setting. Thereby it was regardless if the top tree stratum was a single layer, or a combination of shrub and multiple (sub-dominant and dominant) tree layers.
Due to the nature of ALS, which measures vegetation from the top downwards, the dominant layer is always depicted in the point cloud to a certain extent, depending on penetration depth. The way the presented layer detection method works, even if the dominant tree layer has very little crown extents, it would in any case be identified. Also, if the method would only detect one layer, represented by a continuous foliage mass from ground to a certain height, then this single layer would be additionally examined for its height range. If it exceeded the shrub level (here 5 m), it would be regarded as two layers, a shrub and a tree layer. And furthermore, if there were only two layers, the second (higher) one would be classified as a dominant tree layer.

As expected, the results from the pixel-based visual evaluation give an indication that also dependencies between the method's parameters exist, which is investigated in the next section.

5.3.2 Layer detection on plot level

For the plot-based results the evaluation could be carried out automatically through a comparison of layer presence or absence in the field data and the ALS-based results. For all parameter combinations (see Tab. 5.1) the success of the detection was determined by computing completeness and correctness for each version. Figures 5.7 and 5.9 show the results for the leaf-off data, figures 5.8 and 5.10 the results for the leaf-on data. The figures are further grouped by shrub and intermediate layers, respectively. All charts show pairs of completeness and correctness for every computed parameter combination, whereas each chart represents the variations of gridsize and significance level at consistent values for the stepsize.

As stated in section 5.3.1, due to the measurement principle of ALS and the design of the detection method, the dominant tree layer is always detected. Therefore a detailed evaluation of presence or absence of the dominant tree layer on plot level is unnecessary and the evaluation results are only given for the detection success of the intermediate (or sub-dominant) tree layer and the shrub layer.

In the following, the results are compared by layer type (first shrub, then intermediate) and they are grouped by leaf-off and leaf-on data.

Evaluation of the shrub layer detection

The charts demonstrate that the shrub layer is very reliably detected. The automatic method delivers high correctness (> 80% to 100%) for most combinations of stepsize and gridwidth, whereas the completeness features larger variations (> 40% to 100%). The best results (100% completeness and 97% correctness) were achieved for smaller gridwidths (i.e. 1 and 2.5 m). A general slight downward trend for both, completeness and correctness, can be observed with increasing gridwidths, being more pronounced for completeness than for correctness. This strengthens the impression gained from the pixel-based evaluation (see Sec. 5.3.1), where it was stated that the size of the density pixels should be set appropriately for the minimum mappable vegetation object that would contribute to or be considered as a layer. With increasing size of the density pixel, which is defined by stepsize and gridwidth, and constant significance level, the chance for smaller foliage masses to remain unrecognised increases, as well. The effect is strongest for the largest selected gridwidth of 50 m.

Additionally it can be observed that the completeness tends to decrease with increasing significance level, the effect becoming stronger the larger the gridwidth becomes. Gridwidth, stepsize and significance level are obviously correlated, as the bigger a density pixel gets, the lower the significance level has to be in order to still have enough echoes inside the pixel to make it count for a layer. This is supported by the fact that the effect is weaker for larger stepsizes, which again makes the density pixel bigger (by increasing the selection height). Sometimes the significance levels are too high for the smaller gridwidths and stepsizes to even detect a single layer, then completeness and correctness are reduced to 0%.

For larger stepsizes the method is more robust. It can be seen that both, completeness and correctness, become less dependent from the choice of the other two parameters.

The results from the leaf-on and leaf-off ALS data show similar behaviour. It can be stated that for small gridwidths ($\leq 2.5 \times 2.5\ m^2$) and low significance levels (< 10%), the presented method achieves comparable quality for the shrub layer detection during both acquisition times and regardless of stepsize. This assuming penetration rates better than or equal to 10% (which is the minimum encountered for the ALS data used in this study), whereas the results might degrade for lesser point densities. This was however not investigated in this study and remains speculation.

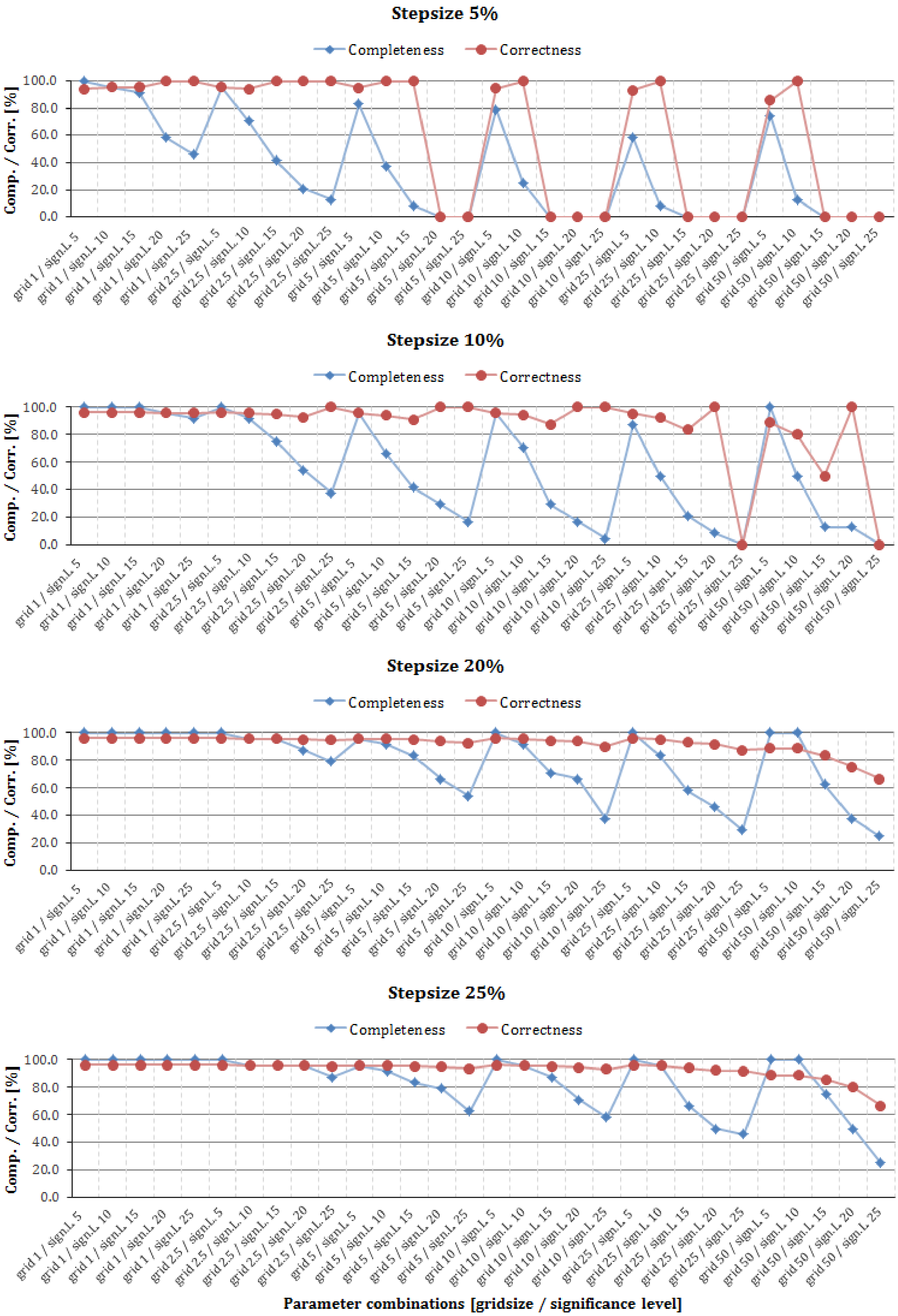

*Figure 5.7: Pairs of completeness and correctness as results of the evaluation of the **shrub layer** detection based on the **leaf-off** ALS data. Each chart shows the variation of gridsize and significance level at consistent stepsizes.*

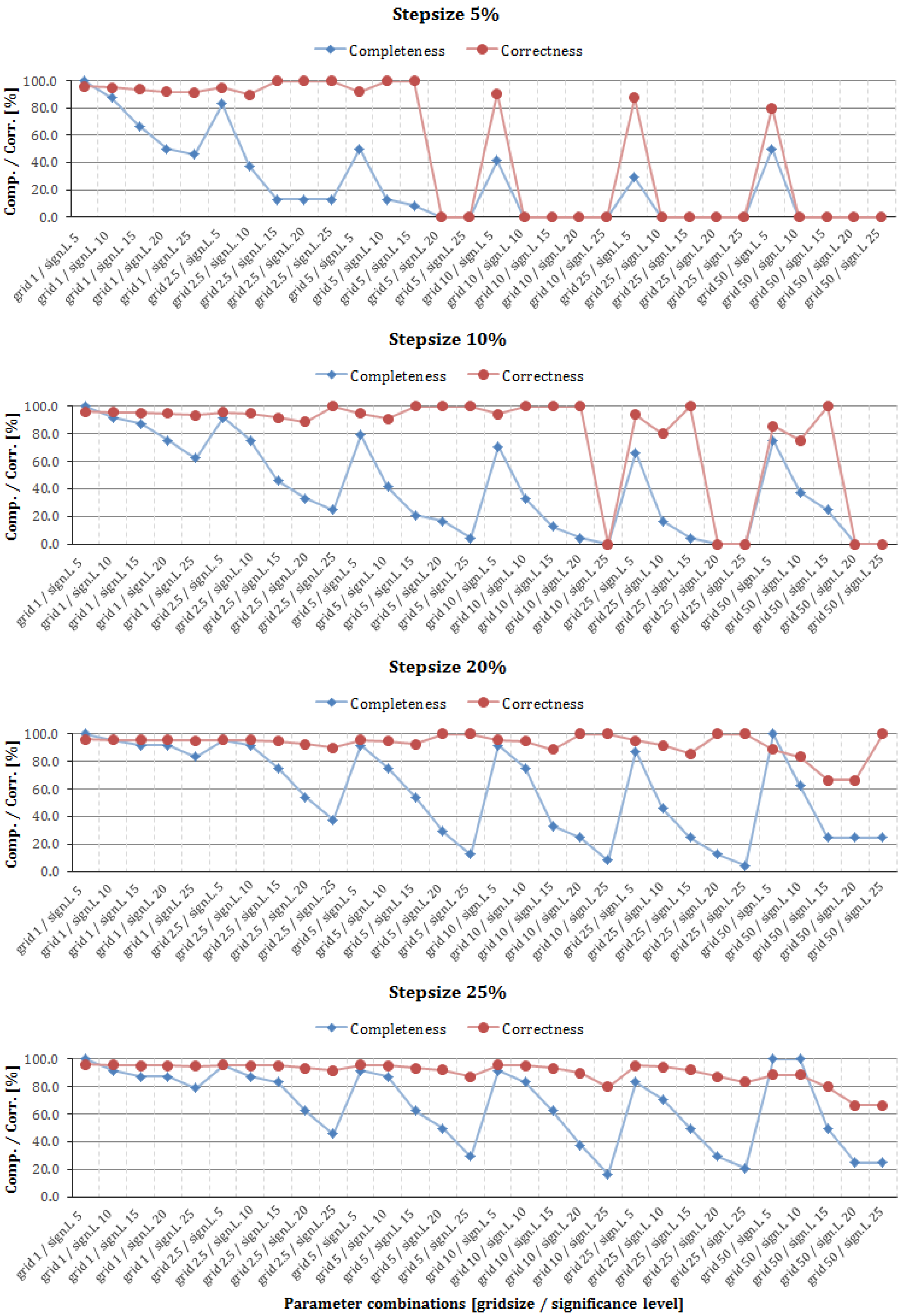

Figure 5.8: Pairs of completeness and correctness as results of the evaluation of the ***shrub layer*** *detection based on the* ***leaf-on*** *ALS data. Each chart shows the variation of gridsize and significance level at consistent stepsizes.*

Evaluation of the detection of intermediate layers

Close investigations of the results revealed that intermediate layers were most often detected by the threshold-based decision strategy (see Sec. 5.2), rather then by a detectable gap in the foliage mass (i.e. an empty density slice). If a distinct shrub layer and a top or dominant tree layer are present, the shrub layer usually distinguishes itself through an obvious gap in the foliage mass, which has proven to be reliably recognizable in the point cloud. However, if additionally an intermediate layer is present, it is often connected to the shrub layer, or the intermediate layer grows into the top tree layer. The gaps, if any, are then not as clearly pronounced as if only two layers were present and the gap detection becomes more challenging.
Consequently, the proposed method does not achieve comparable results in terms of completeness and correctness for the detection of sub-dominant tree layers as for the shrub layers. In most cases, large trade-offs between completeness and correctness can be observed, e.g. close to 100% completeness but only moderate correctness at 60%.

Completeness shows an upwards trend for increasing gridwidths and drifts further apart from correctness. Additionally, another interesting effect can be observed for the completeness, which tends to increase with increasing significance level. Although this seems paradox at first, it is a rather logical behaviour. Higher significance levels mean less density pixels will pass the significance threshold. As a consequence, the chance for a 0-density slice to be produced is higher. A gap will be the result and a multi-layered structure is detected. This may however not be accurate, which is also indicated by the corresponding correctness levels not sharing this increase and remaining at a more or less equal level.

Similar to the results for the shrub layer, leaf-on and leaf-off data achieve comparable quality, especially for gridwidths larger than 10 x 10 m^2. For small gridwidths (< 10 m), only combinations of small stepsize (5%) and low significance level (< 10%) are more accurate. A possible reason for this trend is that the intermediate layer during leaf-off conditions consists mostly of scattered foliage parts and branches, and consequently many small gaps. Increasing the stepsize at constant gridwidths and significance levels will lead to the detection of fewer gaps. Thus more continuous canopies are detected, evidently suppressing the recognition of sub-dominant tree layers. This leads to the apparent conclusion that the detection of intermediate layers during leaf-off conditions is mostly dependent on the detection of small gaps, which are easier detected with small density pixels.
Besides, it is noteworthy that a stepsize of 25% for the leaf-on data achieves the most constant quality throughout all parameter combinations. This might be explained by phenological behaviour. Contrary to the leaf-off period, the sub-dominant tree layers are grown to their maximum extent during leaf-on season and are thus best pronounced in that time of year, having a good chance of forming distinct foliage masses. Simultaneously also the gaps, if and when present, become easier recognizable for the automatic method. However, with a stepsize of 25% the chance for actually finding a gap is small, as the gap then has to be very big. The more obvious reason for the detection rates being better during leaf-on season and larger density pixels is that more continuous foliage masses ranging from the ground to above the shrub level are detected. This was already pointed out at the beginning of the section. In the threshold-based decision step, these layers, which were first derived as single ones, are then often separated, because their height extents were too large.

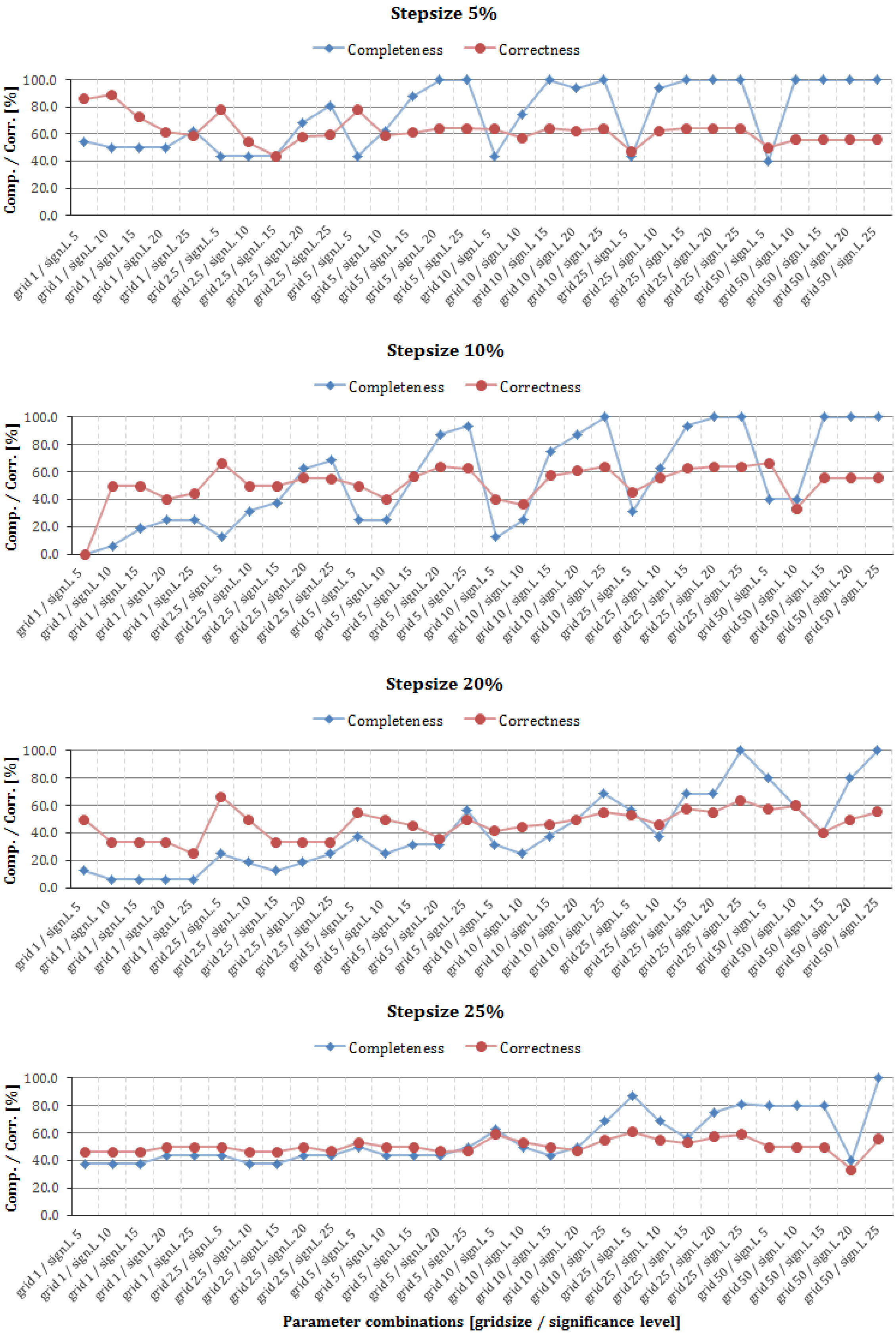

Figure 5.9: Pairs of completeness and correctness as results of the evaluation of the ***intermediate or sub-dominant tree layer*** *detection based on the* ***leaf-off*** *ALS data. Each chart shows the variation of gridsize and significance level at consistent stepsizes.*

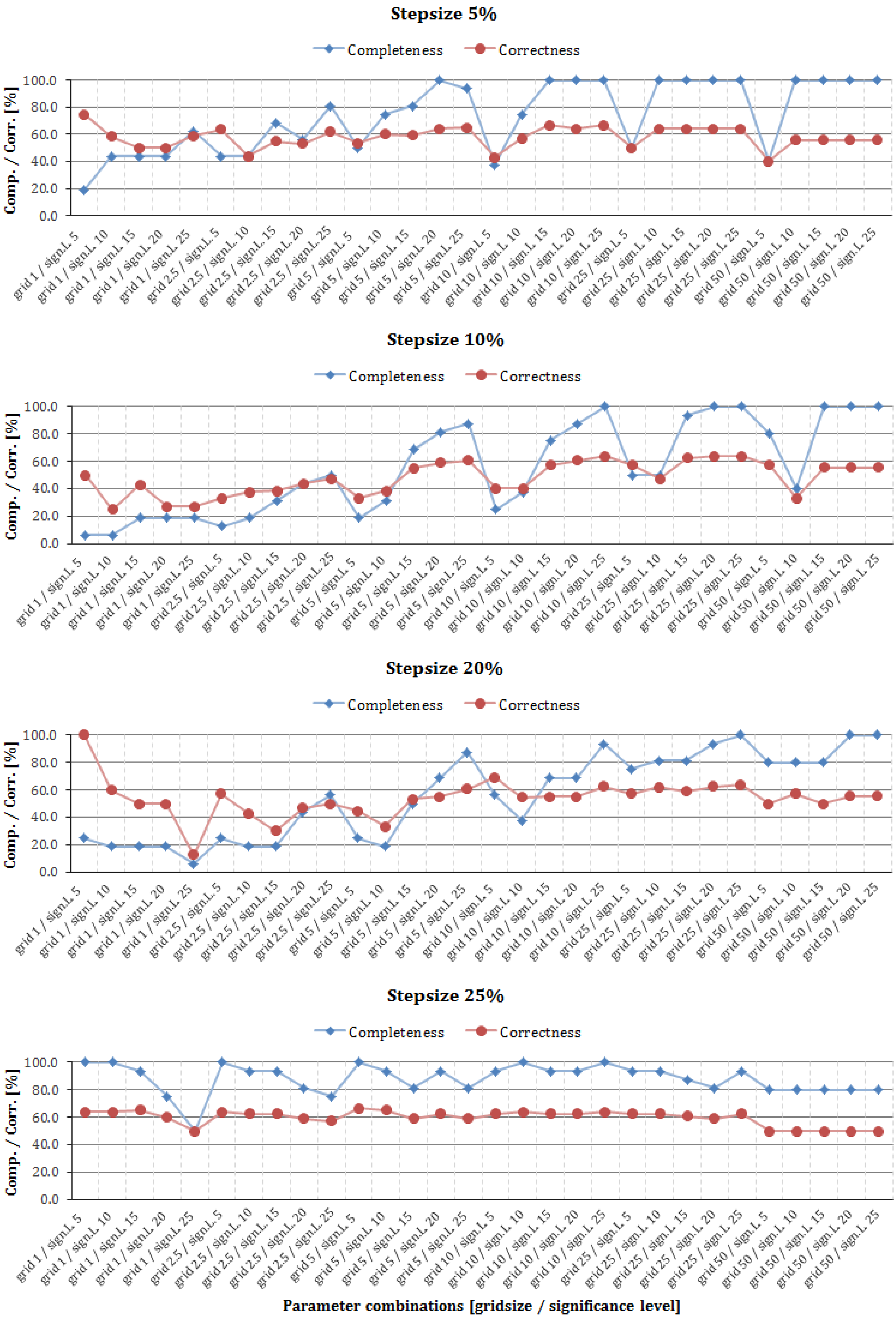

Figure 5.10: Pairs of completeness and correctness as results of the evaluation of the ***intermediate or sub-dominant tree layer*** *detection based on the* ***leaf-on*** *ALS data. Each chart shows the variation of gridsize and significance level at consistent stepsizes.*

5.4 Conclusion

This chapter presented a method for automatic detection of vegetation layers, starting from the ALS point cloud and subsequently employing raster-based operations. Based on the presence and absence of clusters of ALS echoes, the method was able to estimate the stratification of vegetation, which confirms the underlying hypothesis stated at the beginning of the chapter. The shrub layer could be identified with good quality and little dependency on the involved parameters or data acquisition times. The detection accuracy for intermediate layers overall featured higher variations of completeness and correctness than for the shrub layer, and the quality was significantly weaker for both, leaf-on and leaf-off data.

It was found that the composition of the foliage, especially the abundance of foliage gaps inside the canopy, was crucial for accurate detection results for all layers, but especially for sub-dominant tree layers. This points out a major limitation of the method, namely that two layers have to distinguish themselves from one another by a foliage gap, otherwise there is no chance of identifying them directly as two distinct entities. A threshold-based strategy derived from field mapping methodology was included in order to identify the shrub layer out of one continuous layer and to overcome this limitation. This strategy in essence leads to a clearer geometric description of what a shrub layer looks like in the field and therefore its automatic identification becomes easier. In that sense, the biggest problem for accurate detection of sub-dominant tree layers is that no explicit geometric definition was available for this study and probably is also not for general practice.

Sometimes in forest inventories pre-defined height levels are used, describing intervals that have to be "filled" with foliage mass to a certain extent in order to be regarded as a layer. It was however the aim of this study to develop a method that is less (or even in-) dependent of predefinitions of that kind.

Taking the overall result of the evaluation into consideration, giving a recommendation for the best parameter settings for is not a trivial task. As the shrub layer detection was generally less sensitive to parameter variations for both data acquisition times, it can be reasoned that predominantly adjusting the settings so they produce good results for the intermediate layer is a constructive way to go. Still then it remains to be decided which parameter combination is most suitable for the sub-dominant trees. Contrary to the results for the shrub layer, there was not a single parameter combination which produced both, high completeness and correctness (> 80%) for the intermediate layer. Whenever one of both exceeded the 60%-mark, the trade-off became large (>20%).
As it is the general idea of this thesis to develop methods that support the manual assessment process, but not necessarily completely replace it, it may be a possible solution to aim for maximum correctness. In the view of N 2000, vertical stratification of the foliage is desirable and positive, whereby it generally applies that the more is the better. If this is not the case for a certain habitat, management actions are usually advised or taken. Wrongfully detecting sub-dominant layers in a large number of assessment areas might lead to the erroneous assumption that everything is in accordance with N 2000 recommendations. In the worst case, this supports further degeneration of the respective areas without the responsible people noticing. On the other hand, identification of less but truly multi-layered areas will at the most lead to the decision to preferentially visit exactly these areas during ground survey, in order to get a clear picture of the scene. In the case management steps need to be taken, this visit might anyway be essential.

Following this argumentation, the presented ALS-based method for detection of understory vegetation is able to deliver a valuable input for the planning of N 2000 ground surveys, in order to optimize involved processes (e.g. identify areas of significant change, where to go first, etc.). Moreover, it enables the derivation of vegetation layer structure estimates in resolutions and area extent on a highly objective basis, which is not simply doable with manual assessment.

6

Identification of Deadwood

6.1 Aims

The role and the importance of dead wood for biodiversity in forests was outlined in section 3.2. In this chapter, the ALS point cloud is investigated with respect to the information content for identification of standing dead and downed trees. Based on the findings, an automated method for the extraction of deadwood locations is developed. Wherever possible, full-waveform ALS data is exploited in order to derive parameters describing distinctive features of dead trees. The deadwood analysis are conducted on the Uckermark and Nagyerdö test sites.

6.2 Methods

6.2.1 Visual examination of the point cloud

To identify downed stems in a standard 3D viewer, various subsets of the ALS point clouds from study sites with known amounts of downed stems were exported. Starting with all echoes, more and more echoes were removed consecutively using the echo number (i.e. the continuous number for all echoes within a laser shot) and the normalized point heights, with the aim of eliminating as much echoes not belonging to downed stems as possible to make them visible in the point clouds. Figure 6.1c shows an example of 3D visualisations, where the fallen trees became visible through extraction of only the last echoes with normalized heights smaller than or equal to 2 m above ground. These visualisations also give promising evidence that downed stems are picked up by the laser scanner and are included in the ALS point cloud to a sufficient degree of detail to make an automated detection possible. In figure 6.2 terrestrial photographs taken during a field trip in one of the Uckermark study sites are shown to give an impressions from a forest with significant amounts of deadwood featuring all degrees of decay.

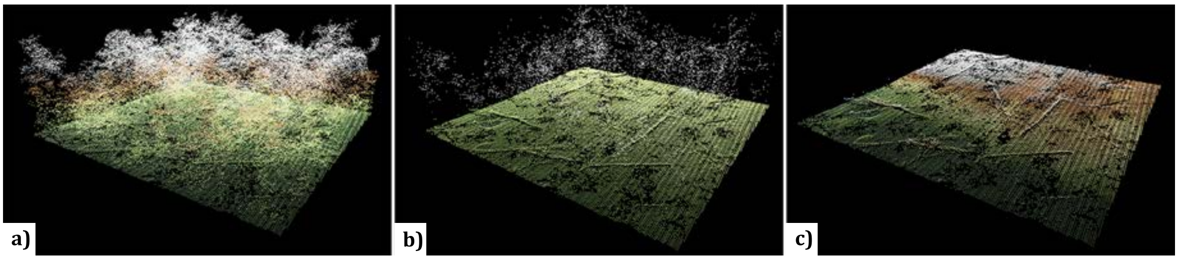

Figure 6.1: This 3D visualisations of the ALS point cloud show a part of forest with multiple vegetation layers. (a) all echoes from the leaf - off flight, (b) all last echoes, and (c) all last echoes with normalized heights smaller than or equal to 2 m above ground clearly make downed stems visible which are taken up by the laser scanner.

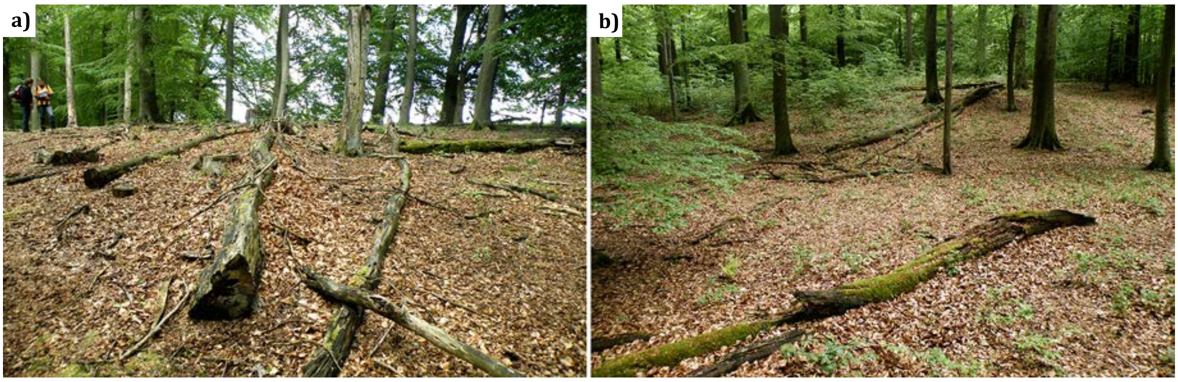

Figure 6.2: Terrestrial photographs taken at one of the Uckermark study sites during the field trips. Impressions from a forest with significant amount of downed stems, featuring several degrees of decay.

To investigate the representation of standing dead trees in the ALS point cloud, sample trees had to be located in the study area. In contrast to downed stems, which usually lie on the forest ground, standing dead ones are not so straight forwardly distinguishable in the point cloud. To support the process, the field-measured GNSS locations were used to locate them. From experience, it was expected that these measurements were error prone due to the generally difficult circumstances for GNSS measurements in forests (e.g. shadowing effects from branches and foliage, multipath effects, etc...). Therefore, the GNSS locations were only used as initial locations for coarse positioning, after which the point cloud was browsed manually in search for the standing deadwood. As documented in section. 4.2.1, the height and diameter of the tree, as well as the information whether it still had a crown, were noted during the field data collections. Together with the terrestrial photographs from the dead trees, which were also taken (examples see Fig. 6.3), this information could be used for identification of the trees.

Twelve standing dead trees that distinguished themselves clearly (two of which still had a crown) could be selected visually. Due to the high point density and penetration rate, the stems of the standing trees were depicted in the point cloud by at least one line of ALS echoes along the side of the respective trees (see Fig. 6.4b). The approximate position of the stem centre, which was manually extracted from the ALS data, was used for correction of the GNSS locations of the trees.

Actually, more standing dead trees were found in the field by the ecologists (see Fig. 4.2), however most of them were short snags (height <= 5 m). Although the detail in which the other twelve standing dead trees are depicted in the ALS data suggests that also these short snags are included, they could not be identified through 3D visualization. For a comparison in the point cloud analysis,

Figure 6.3: Terrestrial photographs of standing dead trees found in one of the study sites in the Uckermark. (a) and (b) show trees that still have a crown reaching through the canopy. Whereas (c) shows a snag without a crown, which is overgrown by the surrounding trees.

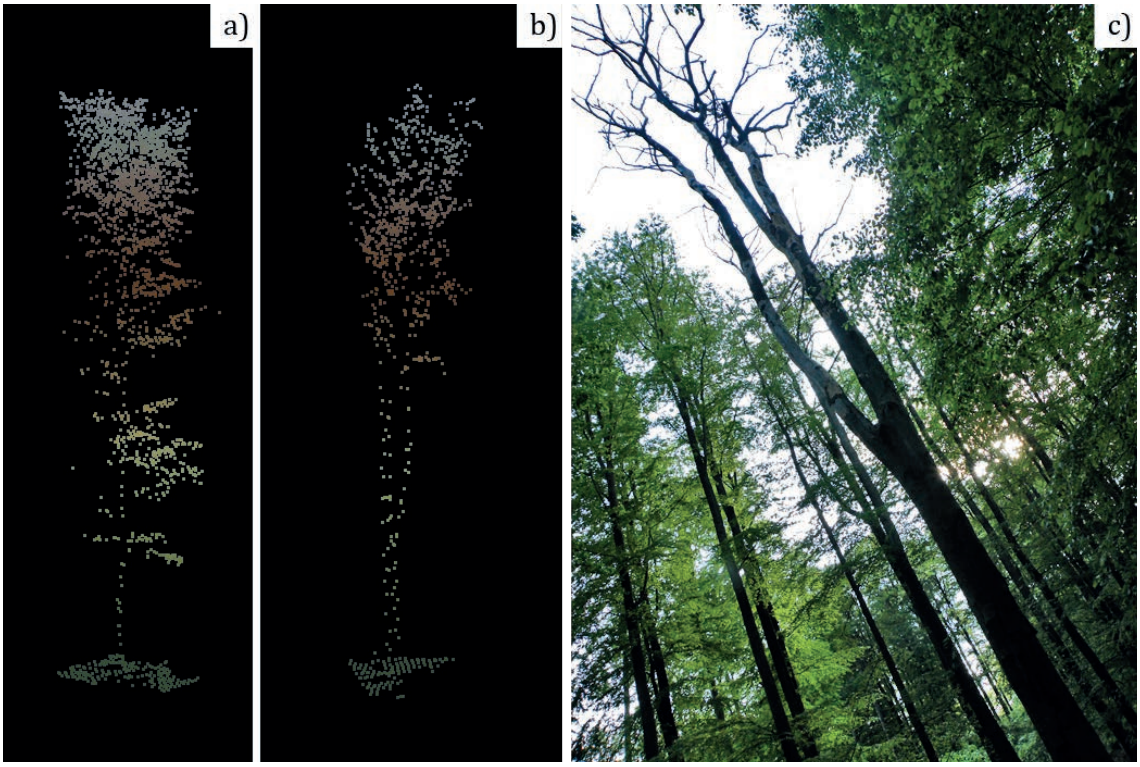

Figure 6.4: Extract of the ALS point cloud for a standing (a) vital and (b) dead tree. The vital tree exhibits a higher point density in the upper parts of the crown, when compared to the dead one. (c) shows a terrestrial photograph of the same standing dead tree as depicted by the ALS points in (b). It can be seen that the "dual" main branch structure is very clearly represented in the point cloud.

twelve arbitrarily chosen vital trees were selected and their stem locations noted. An example of how these vital trees look like in the point cloud is given in figure 6.4a.

The locations of the manually selected stems were used as centre points for a cylindrical extraction with a radius of 2.5 m of the ALS data. The cylinder radius of 2.5 m was empirically derived and visually confirmed as adequate for selecting a single deciduous tree in the study area, as they were high growing with only slightly overhanging crowns. For the extracted 24 data sets exploratory point cloud analysis was carried out. The different representations of vital and dead standing trees concerning the point distribution (i.e. number of echoes in a certain height interval), as well as potential differences in their FWF attributes echo width and amplitude were investigated per sample tree. The investigations were carried out for the leaf-off and the leaf-on data set, likewise. For visualization purposes box plots were created, showing the distribution of the tested echo attributes with respect to the corresponding normalized point height.

6.2.2 Concept and workflow for downed stem detection

The findings of the visual data examination have shown that downed stems are likely to present themselves as mere parts of the forest ground, however they are often distinguished by a clearly developed cylinder-like shape. Thus, it is reasonable to use the leaf-off ALS data set for the detection process, as it usually features better penetration rates and gives a better representation of the forest ground (c.f. Sec. 4.3.1). The basic idea behind the process for the detection of downed stems is to create a DHM which includes and preserves these shapes of downed stems as good as possible, so that the stems can be extracted. For this purpose, all the echoes from vital vegetation possibly covering or overgrowing the fallen trees need to be removed in order to expose them.

Considering downed stems as parts of the forest ground, the hypothesis is that these surfaces can be distinguished from vegetation through their more homogeneous surface characteristics (i.e. surface roughness). Following the concept proposed by Hollaus et al. 2011b, roughness can be described in multiple scales using ALS data. Firstly, high-density small-footprint ALS point clouds, like the one used for this study, represent surface roughness through the distribution of the echoes. Normalized heights of neighbouring echoes will be more divergent in vegetated areas than on bare ground. Given adequate penetration of the foliage, this characteristic can be exploited for discrimination of ground and low vegetation [e.g. Vetter et al. 2011]. Secondly, full-waveform ALS data additionally provides the width of the reflected pulse (i.e. echo width), which relates to small height variations of scattering elements within the footprint of the laser beam [Wagner et al. 2008]. Essentially this means that the echo width tends to widen up compared to the emitted laser pulse if it is reflected from a more inhomogeneous (i.e. rough) surface. It can therefore be understood as a measure of sub-footprint roughness.

The echo width is available for every return as a result of the Gaussian decomposition, so it always relates to a specific ALS echo. It does not need any further processing and can be used instantly as a selector for a single return. The discriminative power of the echo width for different types of surfaces or landcover was already investigated by several research papers [Alexander et al. 2010; Doneus et al. 2008; Hollaus et al. 2011b; Lin and Mills 2009; Mücke et al. 2010c; Rutzinger et al. 2008]. Using the normalized heights, a sample data set was divided into terrain and off-terrain (including among others vegetation) points and their echo width distributions were investigated (see Fig. 6.5 a). Echoes with normalized heights smaller than or equal to 0.1 m were classified as terrain, above as off-terrain. Although the two classes exhibit an overlap to a threshold of 4.75 ns, above that a clear distinction becomes evident. Additionally, the echoes from 35 downed stems were manually extracted from the ALS point cloud and their echo width distributions were compared to those from the terrain and off-terrain samples (see Fig. 6.5 b). Similar to the ones from the forest ground, a significant proportion of the echoes from the downed stems feature widths smaller than 4.75 ns. This indicates that the the downed stems appear also as a smooth surface in relation to the footprint size of the incorporated laser scanner and that the echo width can be used to differentiate between the bare forest ground or the downed stems and the shrub or herbaceous vegetation layers.

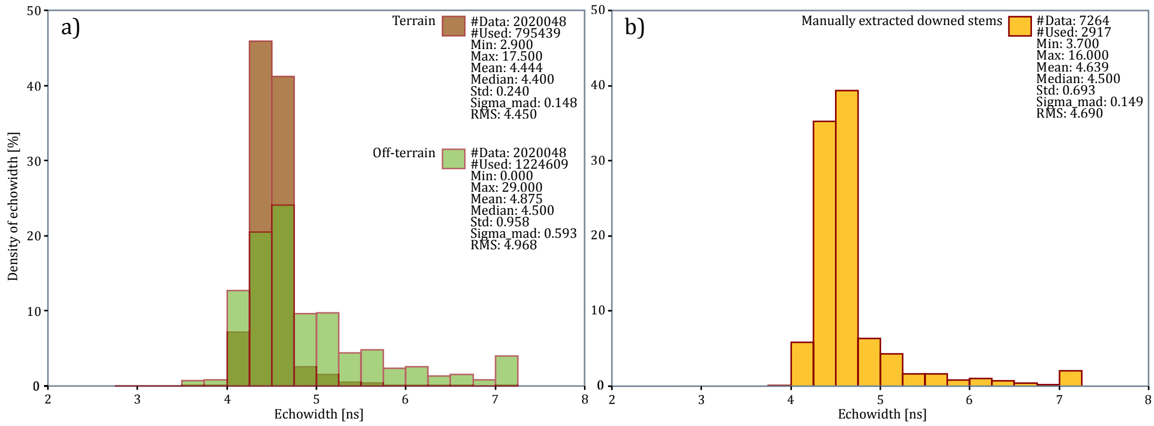

Figure 6.5: (a) Distribution of echo widths for terrain (brown) and off-terrain (green) echoes created from sample data from the Nagyerdö study site. Above a threshold of 4.75 ns a distinction is obvious. (b) Distribution of echo widths from manually extracted downed stems. A significant proportion is below 4.75 ns, indicating that these echoes appear as smooth surfaces in relation to the footprint size of the laser beam.

In the proposed approach for deadwood detection the echo widths are employed in two ways: (1) directly, as a threshold filter for ALS echoes with normalized heights less than 2 m and echo widths less than 4.75 ns, in the initial step of the process to partition the data set. And (2) as a 1 x 1 m^2 grid model of the echo width variance of the echoes in between 0.1 and 2 m distance to the DTM (referred to as EW_{var}) for classification purposes in the last step (see Fig. 6.6). The 2 m normalized height threshold is motivated by the fact that the biggest occurring uprooted stems and their vertical root plates are smaller than that. However, shrub vegetation would still be included in this subset and needs to be removed. This is largely, but not entirely, achieved with the echo width threshold of 4.75 ns, which means that only echoes with a small widening of the echo are accepted for this initial step. The necessary steps to further eliminate areas representing near-ground vegetation are described in the following and schematically depicted in figure 6.6.

A DHM is created from the selected echoes by moving least squares interpolation (further referred to as DHM_{cand}, meaning a DHM depicting the stem candidates, grid size 0.25 x 0.25 m^2). It clearly shows the locations of the downed stems as elongated features (see e.g. Fig. 6.7 c). Then a difference model, a so-called normalized DHM_{cand} ($nDHM_{cand} = DHM_{cand}$ - DTM) is calculated, on which a height threshold of 10 cm (to exclude terrain echoes) is applied to separate the downed stems as non-terrain features. The resulting model is binary classified (1 if $nDHM_{cand} > 0.1$ m, else 0) and morphological closing is applied to connect stem areas that have been separated by the height

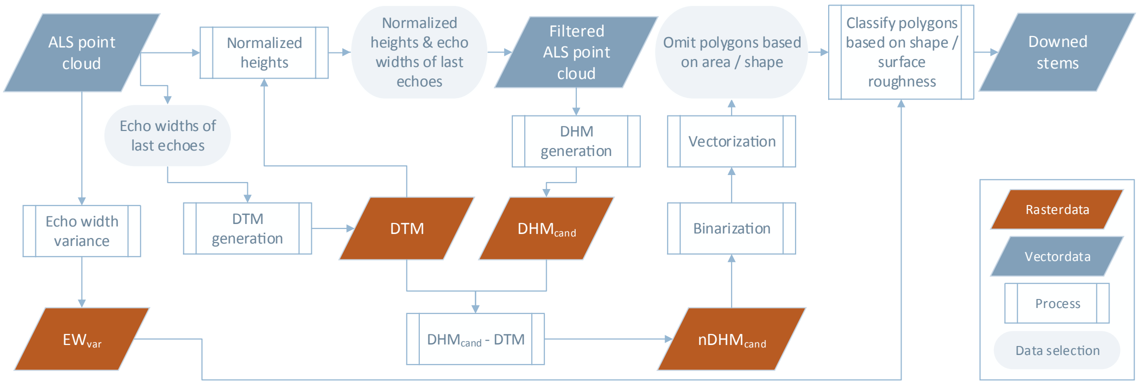

Figure 6.6: Depiction of the proposed workflow for the detection of downed stems based on ALS data.

thresholding and to fill holes. The resulting binary image includes elongated areas presumably representing the downed stems and spot-like features which are assumed to result from the stems of standing trees or remaining near ground vegetation (see Fig. 6.8 c). The binary image is subsequently converted to vector format (ESRI shape file). In the next step, an area-perimeter-ratio (ap_{ratio}) is computed in order to identify elongated features (see Eq. 6.1).

$$ap_{ratio} = 4 * \pi * a / p^2 \tag{6.1}$$

where a is the area and p the perimeter of the vectorized object. The resulting value for ap_{ratio} is closer to one for round (circle-like) polygons and closer to zero for elongated polygons. To eliminate the afore mentioned spot-like areas that presumably represent stems of standing (vital or dead) trees, empirically derived thresholds of $ap_{ratio} \geq 0.3$ describing a circle-like shape and areas smaller than 4 m^2 are applied and the respective polygons are omitted.

The remaining vector map is spatially intersected with the EW_{var} raster map to assign roughness values to every object (i.e. downed stem outline). In the last step a classification scheme is introduced, which is intended to identify well detectable stems (featuring low surface roughness) and distinguish them from the rest, which are possible stem candidates but cannot be clearly identified as such due to their surface roughness (because they are probably overgrown). The thresholds used were empirically derived during exploratory data analysis and the scheme is defined as follows:

- **Class 1:** Elongated and low surface roughness: $ap_{ratio} < 0.3$ and $EW_{var} < 1$.
- **Class 2:** Elongated and intermediate to high surface roughness: $ap_{ratio} < 0.3$ and $EW_{var} > 1$.
- **Class 3:** Not elongated and intermediate to high surface roughness: $ap_{ratio} >= 0.3$ and $EW_{var} > 1$.

Class 1 is designed to represent well detectable downed stems, whereas class 3 comprises areas featuring high surface roughness and should thus represent near-ground vegetation. Class 2 should hold the downed stems that are identified by their lengthy shape, but have high surface roughness due to the fact that they are partly or fully overgrown by near ground vegetation. Applying the suggested method on the point clouds of the study sites results in a final vector map, which represents the outlines of the identified downed stems (see e.g. Fig. 6.9 a).

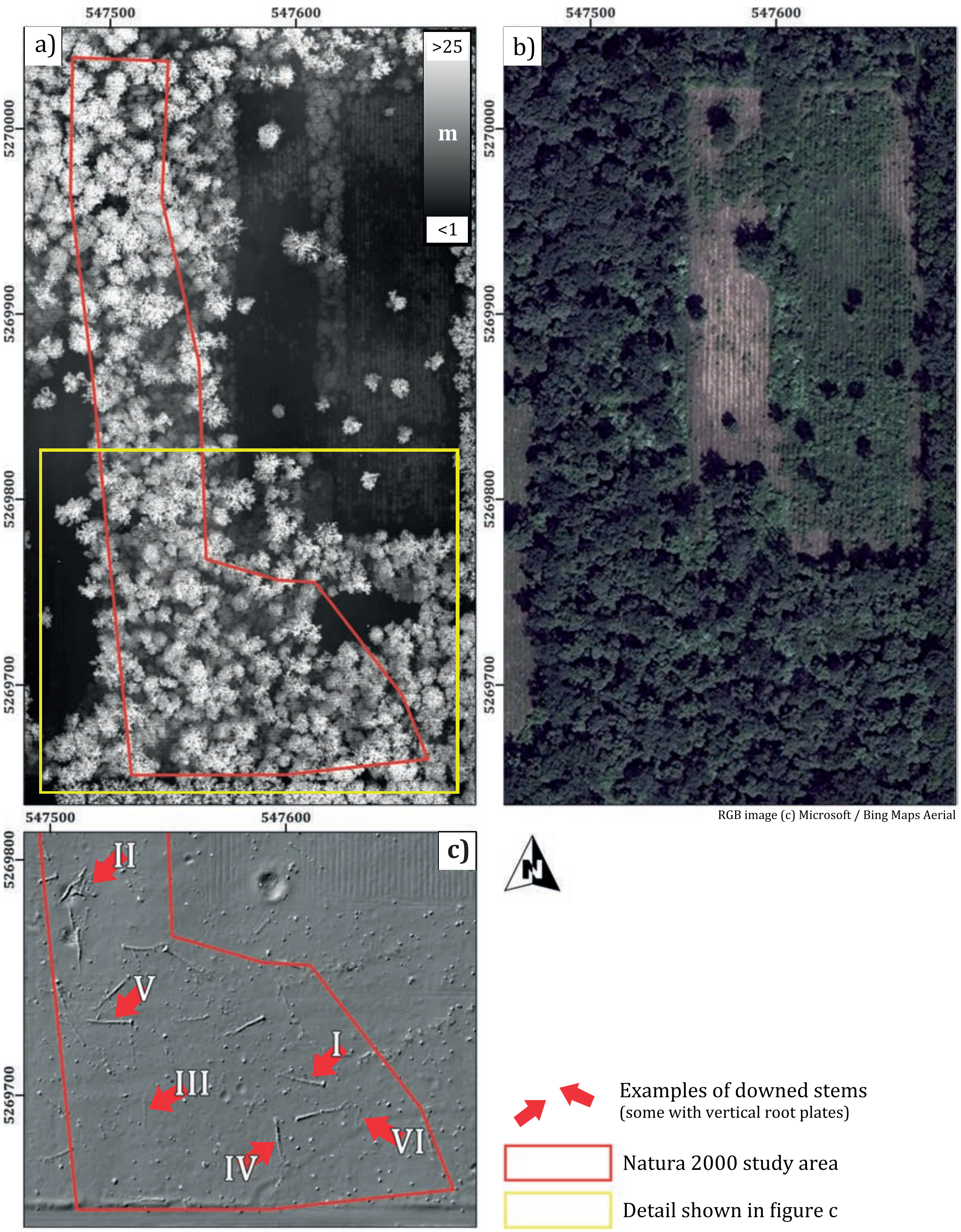

Figure 6.7: The Nagyerdö study site. (a) nDSM of N 2000 site (outlined in red) with detail (yellow rectangle) depicted below in (c); (b) true-colour orthophoto; (c) shaded DHM_{cand}, the red arrows indicate examples of downed stems, which are shown in the photographs presented in Fig. 6.10.

All the above described data analysis and processing was conducted using SCOP++ [SCOP++ 2008], Matlab [Mathworks 2013], OPALS software packages [OPALS 2013] and ArcMap [ESRI 2013]. The described approaches were developed and tested based on the Uckermark ALS data set. Improvements on the method for the delineation of downed stems, e.g. consideration of the decay classes, were included during the processing of the Nagyerdö test site, as the respective reference data from this site was more extensive.
Only the Uckermark ground truth data contained information on standing dead trees. Therefore the following description and results of the identification of standing dead trees and corresponding figures are based on the Uckermark site, whereas the results for the delineation of fallen trees, as well as all provided figures are based on the Nagyerdö site. A comparison of the outcome for the downed stems delineation for both study sites is given in the discussion section.

6.3 Results and discussion

6.3.1 Delineation of downed stems

Visual comparison of the field-measured locations of the downed stems and the DHM_{cand} revealed positional deviations of 0.5 m to 3 m (see Fig. 6.9 b). On board the ALS acquisition aircraft a geodetic grade dGNSS receiver was used in order to provide an accurate flightpath for the post-processing and georeferencing of the ALS point cloud. To evaluate the georeferencing usually ground truth data is surveyed in the form of geocoded planes (i.e. roofs, slopes, etc.) in various directions. They are compared to surface models created from the ALS point cloud, which identifies possible discrepancies caused by shifts, rotations or even distortions of single ALS strips or whole groups of strips [e.g. Kager 2004]. For the CH2 studies, no such ground truth measurements of artificial or natural planes outside the forests in differently exposed positions were available. However, the geometric accuracy of the ALS point cloud could be evaluated by visual comparison of the derived DSMs (grid size 0.25 x 0.25 m^2) and orthophotos at hand, which were available from online resources (e.g. ESRI web mapping services, national web mapping services). The fit was checked manually and visually in different locations distributed across the whole study areas and the deviations were found to be less then a pixel.

Therefore those considerable differences between the automatically detected and terrestrially measured stems resulted most likely from shadowing effects caused by overhanging crowns blocking the sky during the GNSS observations on the ground. A common situation when measuring with GNSS in vegetated areas, as opposed to the GNSS observations on board flying aircrafts, which do not have to deal with this problem. Another reason could have been bad satellite constellations, or other accuracy diminishing effects (e.g. multipath effects, etc.), but as only the final acquired positions and not the raw GNSS data were available for comparison, this remains as speculation.

Thus, a straight forward (automatic) comparison of the reference data and the automatic identification result (e.g. on pixel or object level) was not possible. However, a human interpreter was able to assign the field-measured trees to corresponding ones in the DHM_{cand}. Both had to be (1) in close proximity to each other and (2) a similarity in shape, length and (or) direction had to be observed in order to allow an assignment. Manual accuracy assessment following these rules was chosen and a stem was defined as

- found, if the lengthwise agreement of ALS-derived outline and assigned reference tree was bigger than 75%.
- partly found, if the lengthwise agreement of ALS-derived outline and assigned reference tree was less than 75%.
- not found, if no corresponding reference tree could be found for the ALS-derived outline.

Based on this assessment a basic performance evaluation was conducted. A stem found in the automatically derived result and also present in the reference data is called a True Positive (TP). A stem found by the automated approach, which is not in the reference data, is called a False Positive (FP) and a stem not found by the automated approach but present in the reference is called a False Negative (FN). To estimate the quality of the results, the two metrics completeness and correctness were computed as described in section 5.2.

As mentioned in section 6.2.2, for the Nagyerdö test site the ground truth data additionally contained information on the decay state of the downed stems. The evaluation method was thus extended to make use of this knowledge. According to the above-described method of manual accuracy assessment, a classified object was counted a TP if it was found (agreement $> 75\%$) and its decay state was 1, 2 or 3. It was also counted a TP if it was partly found (agreement $< 75\%$) and its decay state was 2 or 3.

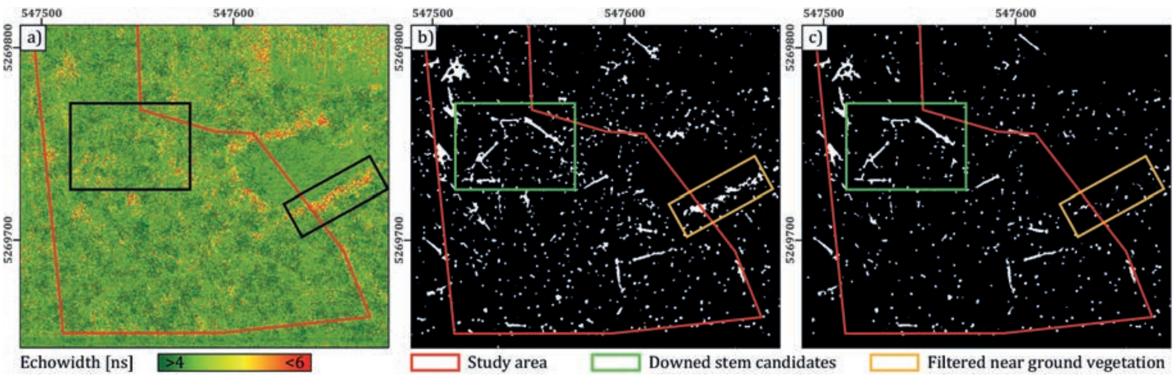

Figure 6.8: (a) Raster map of echo widths for visualization of surface roughness; (b) binary representation of $nDHM_{cand}$ after morphological image processing without echo width information; (c) binary representation of $nDHM_{cand}$ after morphological image processing with echo width information.

The normalized height and echo width filter applied together in the first step of the identification process significantly reduced the amount of data, while still including the echoes relevant for stem detection. Figures 6.8 b and c show binary representations of the $nDHM_{cand}$ after the morphological image processing and the differences without (Fig. 6.8 b) and with (Fig. 6.8 c) the echo width threshold applied for the filtering. The elongated features (stem candidates) in the area are still included (e.g. green rectangle), while a significant amount of spot-like features was eliminated by this simple initial thresholding on the echo widths (e.g. orange rectangle). However, there are still a lot of these spot-like areas left in this binary image. The subsequent classification step, which applies a combined shape and roughness criterion on the vectorized image, successfully identified most of these features. Figure 6.9 shows the final outlines of the downed stem candidates including

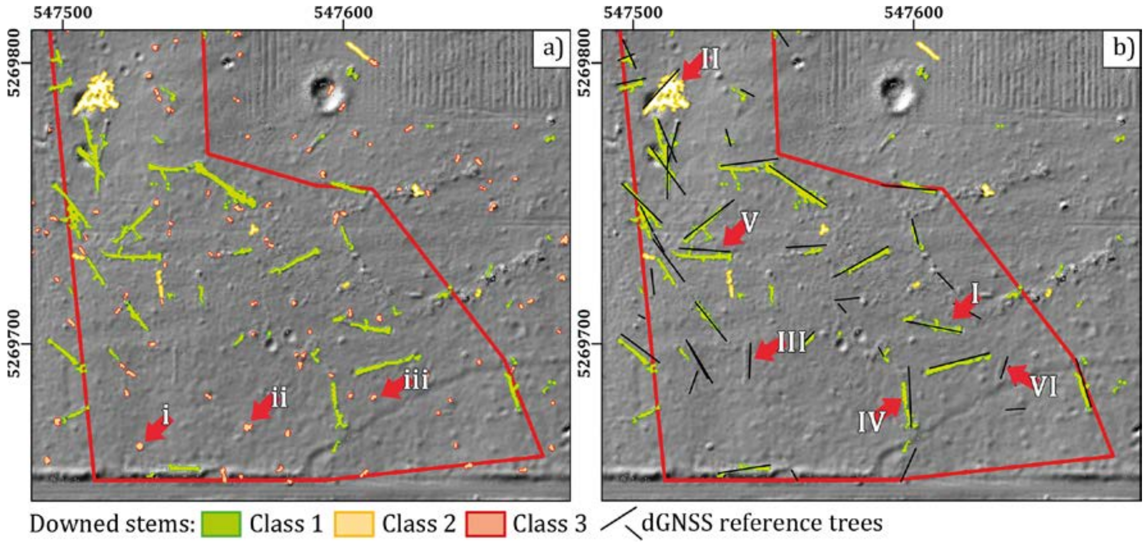

Figure 6.9: (a) Outlines of classified downed stems with locations (i-iii) of objects eliminated by shape and roughness criterion (class 3), corresponding photographs are shown in Fig. 6.11 (i-iii); (b) final outlines of downed stems (class 3 polygons omitted) overlaid by reference class (black), corresponding photographs are shown in Fig. 6.10 (I-VI).

the classification result based on the surface roughness and shape criterion (class 1 = green, class 2 = orange, class 3 = red) (c.f. Sec. 6.2.2). Through investigation of the terrestrial images taken during the field work, as well as visual interpretation of the ALS point cloud, this classification scheme could be evaluated. Class 1 (green) represents the areas that are very likely downed stems (see e.g. Fig. 6.10 I and IV). Class 2 (orange) was found to include mostly FWD or downed stems densely covered with FWD (see e.g. Fig. 6.10 II and V). Class 3 (red), which is supposed to highlight not-elongated

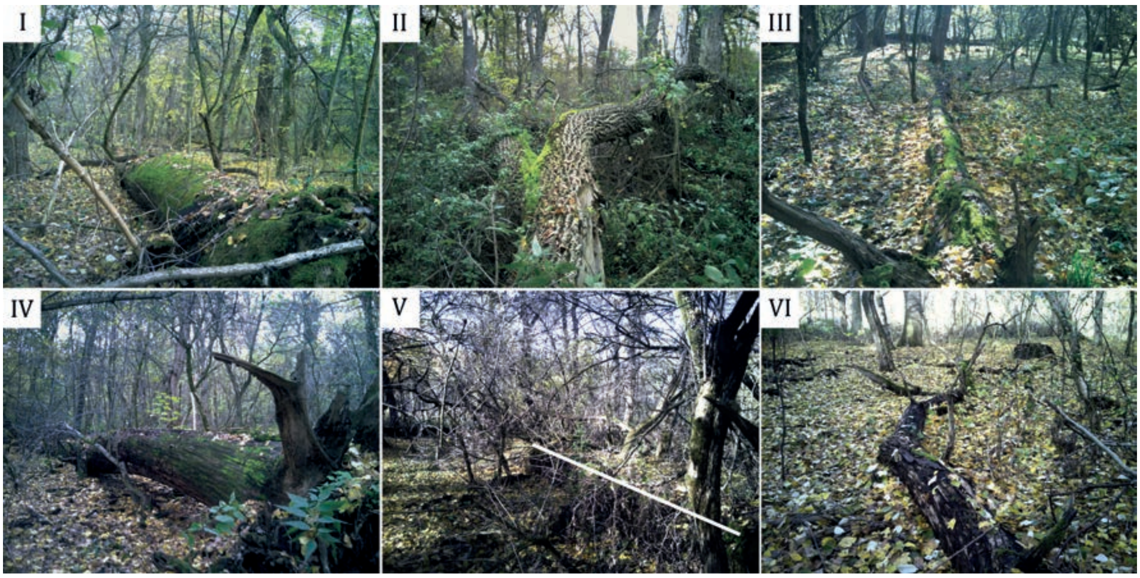

Figure 6.10: Examples of photographs from downed stems taken during field data acquisition. The locations where these images were taken and the outlines of the corresponding stems are shown in Fig. 6.7 c and Fig. 6.9 b. In (V) a white line is drawn to indicate the downed stem, as it is densely covered by FWD.

features with intermediate to high surface roughness, most often represents near-ground vegetation (dense herbaceous layers) and stems of vital standing trees (including their emerging root area right above the ground) (see e.g. Fig. 6.11 i - iii). It also includes some separated parts of downed stems that are often partly or fully overgrown, although to such a small amount that its influence can be neglected.

Consequently, class 3 polygons were omitted from the result, as they were most likely not downed stems. It was found that actually only classes 1 and 2 could be considered for further analysis of assessment of downed stem quantity. Figure 6.9b shows the final result (after omitting the class 3 polygons), overlaid with the reference class (i.e. the GNSS measured ground truth). In total, 62 TPs, 7 FPs and 20 FNs were determined, which resulted in completeness of 75.6% and correctness of 89.9% (see also Tab. 6.1). Elongated and well-preserved stems (i.e. decay states 1 and 2) were reliably detected (31 out of 40), whether they were covered by FWD or not (see e.g. Fig. 6.10V). The more decayed the stem was or the smaller its diameter, the less distinct was its outline and the less likely it was to be found by the automatic process.

The final outline map does also still include some spot-like polygons, which could not be associated with nearby downed stems or other downed stems in the reference class. Examination of the field photographs has shown that they either represent (1) near-ground vegetation (shrubs and herbaceous layer), (2) piles of twigs or FWD, and (3) vertical root plates of nearly fully decayed downed trees. At this point it can be assumed that (1) and (2) were very densely entwined (i.e. having a very complex structure with a lot of crossing branches), therefore impenetrable for the laser and hence featured comparable surface roughness to the downed stems. Case (1) is obviously problematic, as those are vital plants which should not be contained in the final result. On the other hand, cases (2) and (3) would be correct and in principle a desirable result.

Figure 6.11: Examples of photographs of FWD taken during field data acquisition. The locations of the images taken and their corresponding outlines are shown in Fig. 6.9a (i-iii).

The approach presented by Blanchard et al. [2011], who did not have waveform data at hand, features certain conceptual similarities, but less and different input parameters derived from the FWF-ALS were used in this study. Also, Blanchard et al. [2011] applied their approach on a mostly open area (i.e. only a small part was covered by forest). They achieved a classification accuracy of 73%, a result that is per se comparable with this study. However, they stated that misclassification occurred most often in areas with clusters of downed logs and in areas of (lower) vegetation. If FWF-ALS data is at hand, as for this study, and is used in the identification process, then near ground vegetation is only a problem if it is very dense or densely entwined, as the echo width can help to filter out many echoes backscattered from low vegetation. Blanchard et al. [2011] also stated that the determination of the object segmentation and classification rule set and thresholds took rather long for their study site (several days), a fact which makes the method not easily transferable to other sites (probably with different characteristics). In contrast, the method described here was applied on the data sets from the

Uckermark and the Nagyerdö, which feature slightly different characteristics (e.g. the Uckermark study site has less herbaceous plants and less FWD, but more large old trees). An assessment of decay state was not available for the Uckermark test site, but for the well represented stems (diameter > 30 cm) the quality of the results are comparable (completeness of 70.5% and correctness of 75.6%, see also Tab. 6.1). This indicates the stability of the method, at least for certain forest types, and it was achieved without changing the implemented rules for the thresholding.

Table 6.1: Results of the quality evaluation in the Uckermark and Nagyerdö study sites.

	Comp. [%]	Corr. [%]
Uckermark	70.5	75.6
Nagyerdö	75.6	89.9

For the sake of completeness it has to be stated that different characteristics of applied sensors or flight mission parameters (e.g. footprint size, width of emitted pulse, etc.) will require a certain amount of adaption of the thresholds. However, the echo width is a physical quantity which can in principle be related to height measurements (or height variations of objects) and thus adequate thresholds are not expected to be difficult to derive (also c.f. Sec. 7).
A widening of the echo was also observed on the edges of stems. These are areas where height jumps of a few decimetres occur and multiple scattering surfaces contribute to one reflection (see Fig. 6.12). Nevertheless, the inner part of a stem usually does not feature height undulations in this magnitude. Therefore it can still be considered "smooth" with respect to the footprint size of the laser (as long as it is not significantly smaller than the footprint diameter).
An influence of local incidence angle on the echo widths was not investigated in this study.

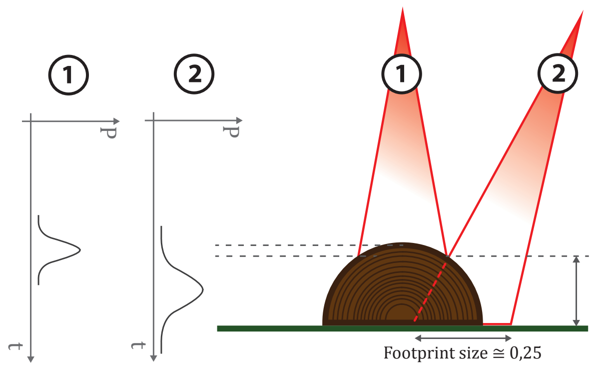

Figure 6.12: Illustration of the widening of the echo on the borders of downed stems (case 2). The "inner" part of the downed stem does not feature large height undulations and can be considered "smooth" with respect to footprint size (case 1).

6.3.2 Point cloud analysis for identification of standing dead trees

For the explorative point cloud analysis, the ALS data were divided into subsets holding only first, last, single and all echoes, in order to investigate the influence of the different return types. In concurrence with other existing studies, which were mentioned in the introduction, the echo distribution and the echo amplitudes were found to be the strongest indicators of discrimination between standing live and dead trees. However, significant differences between the different return types were not observed. On the contrary, the more echoes were included in the analysis, the better the discriminatory power turned out to be. The boxplot given in Fig. 6.13 shows that the echoes from dead trees are at both acquisition times more equally distributed than the ones for live trees. This is partly due to the high number of dead sample trees without a crown in our study area. Nevertheless it can serve as an indicator for trees at this stage of decay.

A relevant difference between leaf-off and leaf-on data could not be observed, although this was assumed to be a critical indicator for identifying standing dead trees that still have crown-forming branches, as it directly refers to vegetation phenology. Unfortunately, the subset of this tree type in our study area was too small to further elaborate on that matter.

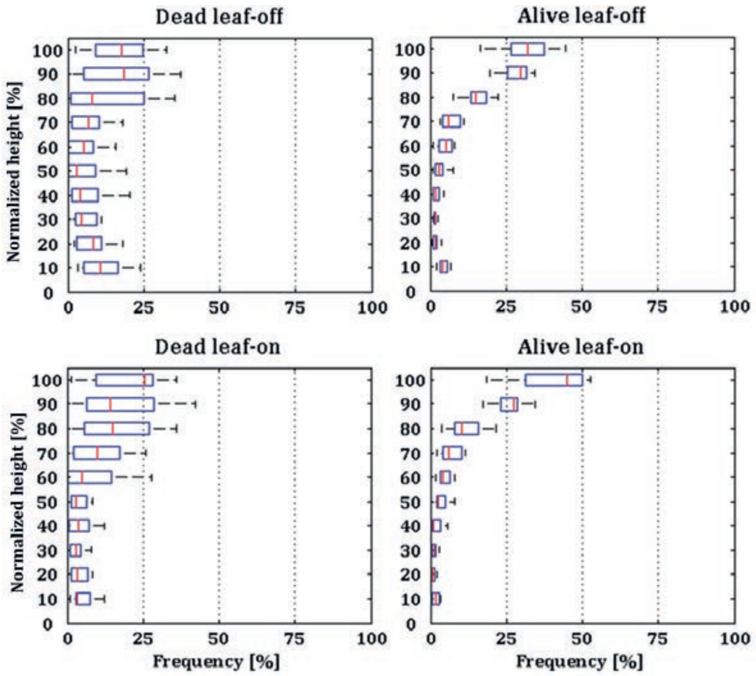

Figure 6.13: Boxplots showing the point distribution of all ALS echoes from the leaf-off and leaf-on data for the selected standing live and dead trees (red mark = median, blue box = 0.25 to 0.75 quantile, black line = data range without outliers).

In contrast, the echo amplitudes feature significant differences for leaf-off and leaf-on data, which can be seen in Fig. 6.14. While again the distribution for the dead trees is rather equal for leaf-off and leaf-on, the trend for the live trees behaves contrarily. It shows significantly higher amplitudes in the top 30% of the echoes in the leaf-on than in the leaf-off, which is most likely caused by green foliage and its high reflectivity in the near infra-red. This is also the strongest discriminator if employed for identification of dead trees during leaf-off season and live trees during leaf-on season using only the echoes in the top 30% of the tree heights. The high amplitudes in the leaf-on data set in the top most parts of the dead trees are most likely caused by branches of surrounding live trees, partly-overgrowing or growing into the dead tree.

The echo width parameter was also examined. It did not show any relevant differences for all of the selected data samples. A possible reason for this could be the fact that the echo width is a measure that is highly influenced by geometry. It is very well suited for a parametrization of height differences smaller than the footprint size of the laser scanner. However, the results of the data analysis suggest that for this application a different scale is relevant. It is more the distribution of the echoes themselves and how they are (or are not) clustered along the stem of a tree. One could assume that the echo width would become more significant once the standing dead tree had a crown and, due to the phenological cycle, a difference because of the presence or absence of leaves would become evident. As already mentioned, this tree type (standing dead with crown-forming branches) was unfortunately under-represented in our test areas, so this could not be further investigated.

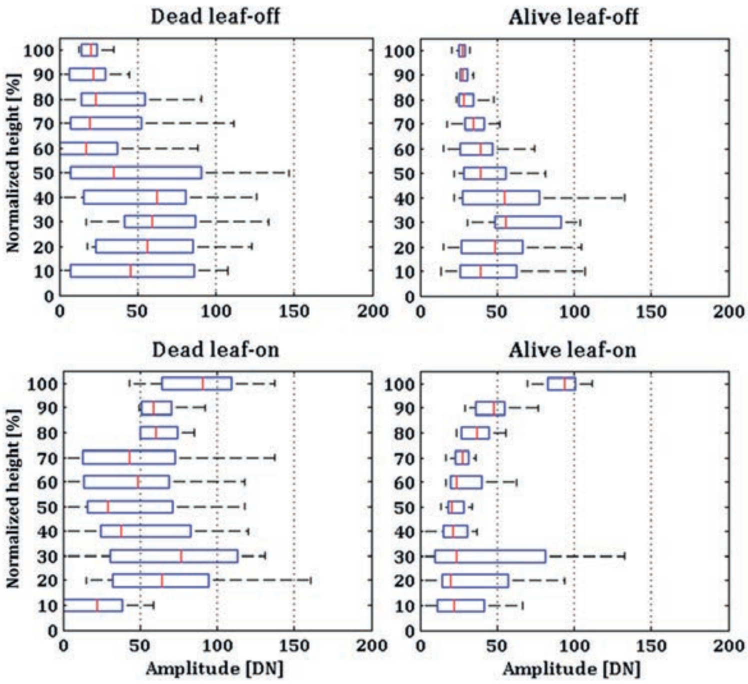

Figure 6.14: Boxplots showing the echo amplitudes of all ALS echoes from the leaf-off and leaf-on data for the selected standing live and dead trees (red mark = median, blue box = 0.25 to 0.75 quantile, black line = data range without outliers).

6.4 Conclusion

The capability of ALS for the identification of individual dead trees in forest ecosystems was investigated. A highly automated method for the detection of downed trees was presented and tested in two different study sites. It yielded comparable results for both test sites, thus highlighting the robustness of the approach.

The proposed method produces a vector map containing the outlines of downed stems, which can further be used for clipping the ALS point cloud and selecting only echoes from downed trees. Subsequently, cylinder fitting could be carried out in the 3D data to derive the dimensions of the stems. ALS with high spatial resolution as available for this study explicitly allows picking up of downed stems. With decreasing resolution the differentiation between CWD and low vegetation is expected to become more difficult. It was demonstrated that an identification of downed trees is possible with a completeness of 75% and a correctness of 90%, if downed trees with little to moderate state of decay are considered. Strongly decayed trees are more challenging to identify because they are less distinct from the forest terrain surface.

Provided that efficient data structures for the storage and access of the ALS data are available as in the incorporated OPALS software modules [Pfeifer et al. 2013], the echo selection process and subsequent raster derivation is not time-consuming. After the initial echo filtering the remaining parts of the method are raster based and therefore not computationally extensive. The processing of an approximately 1 x 1 km^2 area (the Uckermark data set) took around 6 minutes on a standard PC (QuadCore CPU, 8 GB of RAM). Therefore, it can be assumed that with significantly more powerful state-of-the-art workstation computers at hand, also large area processing is possible in a reasonable time.

As opposed to that, the efforts taken for a direct (and also automated) estimation of standing dead trees in the point cloud were inconclusive up to now. Although a large number of specimen was found in the Uckermark test site in the field, it was only possible to locate less than a quarter of them in the ALS data due to (1) GNSS inaccuracies and (2) the general difficulty to differentiate visually between vital and dead standing trees in the ALS point cloud. Nevertheless, the results of the exploratory point cloud analysis were given in this study and they show potential which should be subject to further investigation.

All of the proposed methods support ecologists to gain an overview on the state of an ecosystems or habitat. A downed tree needs a certain amount of time to "evolve" from decay state 1 to states 2 (approximately 3-5 years) and 3 (usually longer than 10 years), which allows the conclusion that the time frame to detect a newly downed tree by ALS with good completeness and correctness is (at least) a few years. Assuming multi-temporal data were acquired and available, the proposed methods could highlight areas where significant amounts of deadwood are present. Areas with high volumes of deadwood indicate habitats with low levels of anthropogenic disturbance and good habitat quality. Furthermore, it can refer to certain changes in the structure and function of the ecosystem or the way of management. This new method enables ecologist experts of N 2000 monitoring to prioritize field-work efforts. They can pre-select forest stands with possibly high naturalness and conservation value, in that way determine where field work efforts should be focused, and identify degraded stands with lower conservation value, which in turn have lower priority during habitat assessment.

7

Point Cloud Classification and DHMs in Wetlands

7.1 Aims

As described in section 3.3, terrain determination in wetland areas, which usually have a very low relief energy, is not a straightforward task. Especially dense and near-ground vegetation makes the identification of the true ground level with remote sensing methods difficult. This chapter deals with the correct ALS-based estimation of vegetation heights in wetlands, which is very much dependent on the composition of the plant communities and their foliage (see Sec. 3).

In vegetated areas, the penetration of the foliage by the laser beams is a critical issue, as it is directly related to the measurement quality and accuracy of the terrain and, consequently, the vegetation heights. Short growing plant species (heights < 0.5 m), which are typical for wetlands in general, pose special challenges for elevation modelling.
Firstly, the determination of the ground level with ALS is difficult in areas of dense vegetation due to the sheer absence of ground reflections. Moreover, modern ALS systems emit pulses with lengths of typically 5 to 10 ns, which corresponds to unambiguously measurable distances of 0.75 to 1.5 m (i.e. range resolution) [e.g. Baltsavias 1999]. Vegetation falling below this height threshold is bound to cause not two (or more) clearly distinct echoes, but only one. It will result from an overlap of all distance measurements within the laser beam, which leads to inaccurate range estimations.
Secondly, particular emphasis must be put on the discrimination of ground and vegetation echoes (i.e. filtering) and the choice of rasterization or interpolation method for DSM and DTM creation. Echoes from low vegetation tend to be mistaken for ground echoes due to their small differences in elevation from one another. If they are included in the point cloud used for terrain modelling, the resulting surface might run right through them and therefore be to high. Especially in areas that are widely occupied by low vegetation, elevation errors in the order of a few decimetres are critical, as they might result in a complete loss of information on these vegetation heights [e.g. Rose et al. 2012]. Consequently, the estimation of plant heights or other indicators of ecological relevance (e.g.

vertical structure, biomass, etc.) will be erroneous. An important question in this context, which needs to be taken into account, is the vertical accuracy of the ALS-derived height measures.

Both selected study sites in the Seewinkel are predominantly occupied by the same plant communities, however in the Zicklacke only high reed (1.5 to 3 m) is present. Therefore, this study is structured so that first the interaction of the laser with the low vegetation from the grey cattle paddock is analysed and influences on terrain echo selection and DTM generation are investigated. Secondly, the behaviour in the high vegetation of the Zicklacke and also consequences for terrain modelling are explored. Influences of different interpolation methods for DSM generation and the consequences for vegetation height estimation are studied in the Zicklacke.

7.2 Methods

7.2.1 Exploratory point cloud analysis and DTM generation

The grey cattle paddock is mainly occupied by sawtooth sedge and sea rush. Only small patches of common reed were found during the field trips in the area. To study the penetration capability of the applied laser scanner with respect to the three plant species, echoes in close proximity to the GNSS reference measurement locations were extracted from the point cloud. The point density permitted a minimum circular neighbourhood of 0.5 m around each GNSS reference for the selection of echoes and computation of statistics of their elevation differences to the GNSS elevation. Given the average point density in the study site, a 0.5 m circular neighbourhood would hold at least three echoes, which is sufficient for plane interpolation. The main interest lay in the selection of ground echoes, which in the case of ALS are usually the lowest ones, so the respective statistics contained the minimum and mean differences of all last echoes for every location. As sawtooth sedge and common reed tend to form large clusters, additional radii of 1.25 and 2.5 m for the neighbouring echo selection were chosen. This was done in order to increase the chance of including a true ground echo in case of low penetration, and to gain an estimate of the grid resolution dependency for DTMs, which should be derived in the next step. First, the lowest ALS elevation within a certain neighbourhood was selected and a DTM was created using a simple nearest neighbour interpolation method, in order to investigate the results from a strategy without involvement of complex filtering algorithms. Second, robust filtering [Kraus and Pfeifer 1998], as described by Pfeifer et al. [2001], was selected to create an additional, methodically more advanced DTM. Robust filtering has proven to provide good results in areas of low vegetation [e.g. Sithole and Vosselman 2003] and it is also implemented in the software at hand for this study [SCOP++ 2008]. DTMs with grid resolutions of 1, 2.5 and 5 m were derived from the last echoes using both above described methods. The elevations of the GNSS reference points were subsequently compared to the DTM elevations at the corresponding grid positions.

It was to be expected, based on the findings from other studies (see Sec. 3), that especially the lowest vegetation clusters (heights less than 0.5 m) would be problematic for DTM generation. This sort of vegetation is usually too short for the scanner's range resolution to cause two distinct echoes. Therefore, the echo width and amplitude were studied as a means of distinguishing between echoes representing terrain and vegetation, i.e. sea rush, sawtooth sedge and common reed. The mean echo width and amplitudes of the selected last echoes in 0.5, 1.25 and 2.5 m circular neighbourhoods of the GNSS references were calculated and examined for possible correlations with the elevation differences between reference and ALS points. Assuming accurate georeferencing of the GNSS field and ALS measurements, occurring offsets between elevations should result from impenetrable vegetation and thus correspond to vegetation height. If a significant difference in amplitude and echo width could be observed for echoes with large and small residuals (i.e. from terrain and above terrain), then it could be used as an a-priori selector for vegetation and non-vegetation echoes.

The hypothesis of correlations of plant growth pattern and echo width was investigated by comparing the height densities with the ALS-based mean echo width. The vegetation height densities were estimated for every terrestrially measured vegetation patch (c.f. 4.2.2). This was also performed for three neighbourhood radii of 0.5, 1.25 and 2.5 m. Several studies describe improvements of DTM quality through inclusion of echo widths [Doneus et al. 2008; Lin and Mills 2009], and echo widths and amplitudes in the filtering process [Bretar et al. 2009; Mandlburger et al. 2007; Mücke et al. 2010c]. So based on the findings of the above described analysis, a threshold-based filter was used to eliminate echoes that had a high likelihood to represent low vegetation (featuring large echo widths) and create an additional DTM using the above mentioned method. Likewise, this DTM was also compared with the GNSS elevations for an accuracy assessment.

In the Zicklacke, which was mainly covered by common reed, no ground truth measurements were available. To investigate whether full-waveform ALS offered a benefit for the purpose of reed structure mapping, the focus in the data analysis was laid on the echo width and amplitude of reflections close to the water and terrain surface (representing the optimal input for DTM generation), and above the water and terrain surface (likely resulting from reed stems or leaves, not to be used for DTM generation). Obtaining such a discrimination of echoes in the two mentioned classes without any reference measurements made an approximate description of the water and terrain surface necessary. As explained in the introduction (c.f. Sec. 3), water acts as a specular reflector, meaning that the majority of incident laser beams are mirrored by the surface and scattered away from the laser scanner's detection unit. However, it was found that for a very narrow area directly below the aircraft's flight path, exactly this mirroring effect is responsible for an orthogonal reflection of pulses right back to the detector, so that some range measurements to the water surface are available. This characteristic was exploited to derive the water surface level (as the mean height of all the available echoes in the homogeneous water areas according to the RGB image) and divide the point cloud into echoes above the water level ($\Delta_z > 0.1$ m) and echoes close to the water level ($\Delta_z <= 0.1$ m). The 0.1 m threshold was motivated by the fact that the documented ranging accuracy of the laser scanner for this flight was $\pm$ 0.1 m. Echoes from three small sample areas, as indicated in Fig. 7.1, were extracted and histograms of their amplitudes and echo widths, as well as raster maps for visual interpretation were created. The last echoes in the study site were selected and two DTMs were created: one with conventional hierarchic robust filtering and a second one using the same method but a pre-filtered point cloud based on derived echo width thresholds as input. As the point density of the ALS data from the Zicklacke was higher than for the grey cattle paddock, a resolution of 0.5 m was chosen for the DTM.

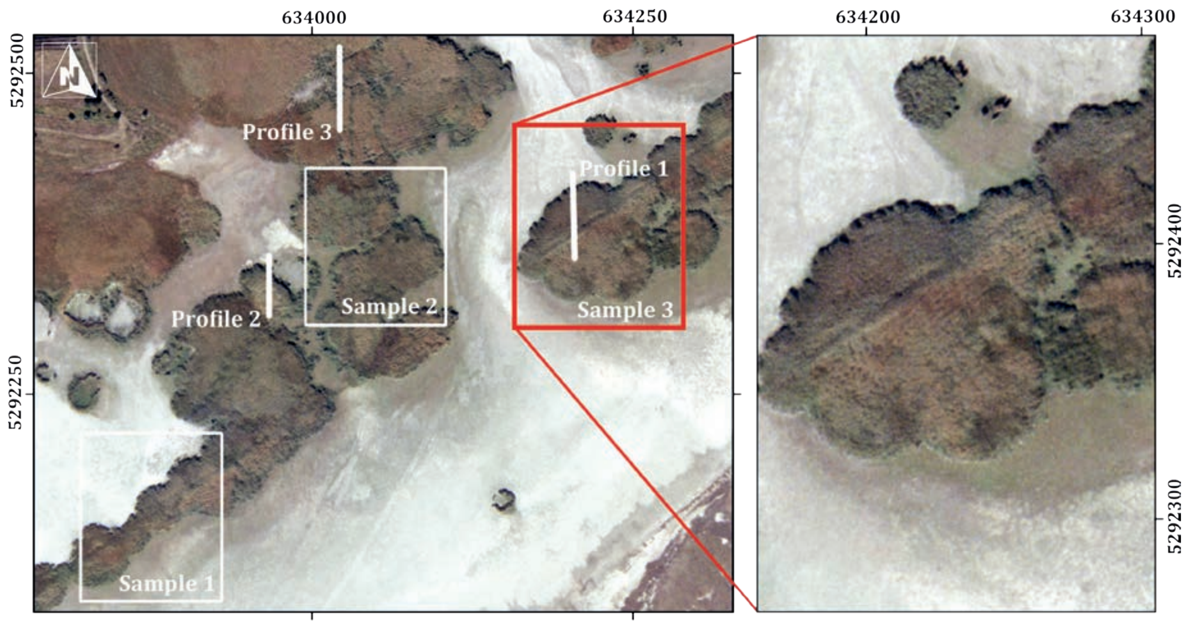

Figure 7.1: True colour aerial photograph of the Zicklacke (GSD = 25cm) with locations of sample areas 1 to 3 and profiles 1 to 3. The enlarged detail on the right shows weakly emphasized tracks caused by tractor-mowing. The image was acquired without surface water present, so the lake basin appears white because of the highly saline soil.

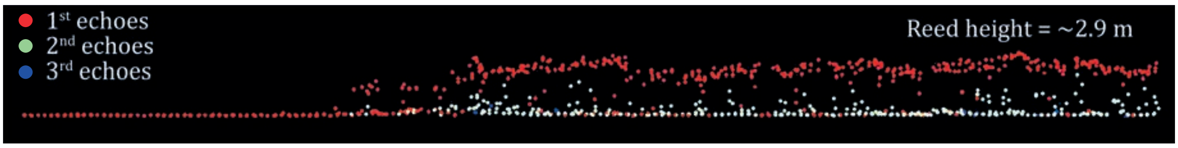

Figure 7.2: Profile 1 (c.f. location in Fig. 7.1) showing the ALS data of the Zicklacke. The red dots represent first, the green second, and the (very few) blue dots third echoes. The width of the profile is 50 cm, the length is approximately 60 m, extending to the open water surface on the left.

7.2.2 DSM generation

Algorithms for derivation of DSMs from ALS data appear trivial when compared to most strategies for DTM computation. However, in the case of DSMs in vegetated areas it was found that this task requires careful consideration, as well. A small footprint laser scanner is likely to miss the topmost parts of the foliage and reflections are easier caused by the "flanks" of the canopy [e.g. Hill 2003; Hyyppä et al. 2004]. Although wetland vegetation often appears as quite homogeneous surface with only low height variations, when considering the footprint size and sampling density available in this study even these surfaces appear inhomogeneous (see Fig. 7.2). Essentially, this poses the same problems as with DTM generation, only in the opposite direction: if a large number of echoes, which resulted from too far down in the canopy, contributed to the DSM generation (e.g. for interpolation), the DSM is likely to run too low through the canopy, as these echoes tend to pull the interpolated surface downward. This behaviour equals to a smoothing effect, consequently the plant heights will be underestimated and wrong. Following the approach presented by Hollaus et al. [2010], two different DSMs based on the first echoes were derived to demonstrate this effect. One DSM was calculated using moving planes (i.e. moving least squares) interpolation (so-called DSM_{mls}). This interpolation method uses a certain number of ALS echoes around one grid point (e.g. in this case eight neighbouring echoes) and estimates a best fitting plane (minimizing the vertical distances of the points to the plane). The height at this respective grid point in the DSM results from the height of the plane in that location [Kraus 2000]. For comparison, a second DSM was created using the highest point within a defined grid cell and assigning this height to the grid point (so-called DSM_{max}). The DSMs in the Zicklacke were created with 0.5 m resolution. Difference models of the DSMs created from the different methods were produced in order to investigate their offsets.

7.3 Results and discussion

7.3.1 Exploratory point cloud analysis and DTM generation

In the grey cattle paddock the differences of ALS point and DTM based elevations were compared with the GNSS reference elevations. For visualization purposes bar plots were created, where each bar represents the residuals of one assessed vegetation patch. Additionally, the bars in the plots were grouped corresponding to spatial proximity of the patches in the field. The resulting bar plots of the selected ALS echoes are shown in Fig. 7.3 and 7.4. The nomenclature in the plots consists of four digits and is defined as follows:

Digit 1. **Species**: A...Sea rush, B...Sawtooth sedge, C...Common reed

Digit 2. **Coverage**: D...dense, M...medium, S...sparse

Digit 3. **patch number**

Digit 4. **patch number**

The patches with three digit numbers R01 - 05 are reference height measurements and were measured in completely open terrain (i.e. only very low grassland) in order to assess the vertical discrepancy of the ground truth data and the ALS data (see e.g. Fig 4.12). They exhibit residuals of maximum 0.06 m, which were achieved through application of identical Helmert transformation parameters for the ALS and ground truth measurements. The small offsets document the spatial consistency of both data sets. Visual examination of the ALS point clouds representing the vegetation patches showed that only single echoes occurred in these areas. As mentioned earlier, a possible reason for that is the fact that encountered vegetation heights for the dominant species in the area were shorter than or very close to the range resolution of the laser scanner. This makes the detection of a distinct consecutive echo within this range impossible.

Investigations of the three different echo selection radii yielded small, but noteworthy differences between the residuals of the three radii of 0.5 m, 1.25 m and 2.5 m. The largest improvement (i.e. smaller residuals) was observed for the 2.5 m radius when compared with the 0.5 m radius, when selecting and comparing the lowest ALS echo with the GNSS reference (see column of the respective minima in Tab. 7.1, as well as Figs. 7.3a and 7.4a). The improvement largely disappears through averaging over all available ALS echoes within the neighbourhood (see column of the respective means in Tab. 7.1, as well as Figs. 7.3b and 7.4b).
Obviously, the chance of selecting a lower ALS echo increases with bigger radii for selecting the echoes. In the case of very flat and horizontal terrain, as it is characteristic for most wetlands, this also means an increasing chance of selecting a lower and thus more accurate ground echo. It has to be noted that choosing an adequate echo selection radius depends on ALS point density and size of

vegetation patches on the ground. Both, a higher point density in combination with smaller spatial extent of the vegetation patch resulting in less ground coverage, increases the chance for producing a true ground echo. This consideration is supported by the bar plots, which show that significant improvements in height accuracy were achieved for the densely covered patches when the radii were increased. This yields to the conclusion that a radius of 0.5 m was simply to small to contain an adequate ground echo in these patches. Whereas for some patches (e.g. BD01 - 06 and BD11 - 18) the residuals could be reduced by as much as 0.25 m if a radius of 2.5 m was selected.
The main intent of investigating different selection radii was to gain knowledge about which neighbourhood size is needed in order to accurately depict the terrain for DTM interpolation. The relevant question in this case is whether a coarser (i.e. lower) resolution will still adequately represent the topography of a typical wetland. An answer to this question will be considerably defined by the application for which the DTM is generated, so there will not be an universally applicable solution. For this study it was chosen to exploit the optimum potential of the ALS data at hand to derive fine-scaled surface undulations. So it was decided to proceed with the finer (i.e. higher) selection radius of 0.5 m, which corresponds to a 1 x 1 m^2 grid resolution and which was assumed to depict the surface with the highest possible detail.

For a number of vegetation patches (e.g. AS08 - 11 or BS07) the elevation residuals were found to be negative. This would mean that the GNSS measured elevations are higher than the ALS elevations (residuals $<$ - 0.5 m). The fact that this is only the case for a subset of the sparsely vegetated patches can be explained by standing surface water during the time of ALS data acquisition, which is common in the grey cattle paddock. Standing surface water leads to a mirroring of the laser beam and reflections from surrounding vegetation. Thus, the run-time measurement of the pulse and consequently the range estimations are too long and erroneous. However, ground truth information on water levels, especially in the grey cattle paddock, are not available for this study, so this explanation remains a hypothesis.

Generally, the residuals are smallest for the sparsely covered patches, which indicates sufficient penetration in these areas. The biggest residuals ($>$ 0.5 m and up to 1.65 m) occurred for medium and densely covered sea rush and sawtooth sedge patches (AM01 - 06 and BD01 - 06). In these patches it can be assumed that due to the impenetrable foliage not the ground, but the top most part of the plants is depicted in the ALS data. For such cases the residuals should correspond to the vegetation heights measured in the field, however they do not for most of the patches (see Tab. 7.1). The most probable cause for this lies in the temporal offset between ALS and ground truth data acquisition, which was (sub-optimally) two years. Differences resulting through cutting or extensive grazing between the acquisition times cannot be conclusively accounted for, as there is no information available on that matter. However, the measured vegetation heights of the patches in question indicate exactly that, as the discrepancies range from 0.5 to 3 m (see Tab. 7.1), a magnitude that is highly unlikely being caused by a random or systematic error of the measurement method (e.g. bad satellite constellations, inadequate georeferencing, etc.) considering the good correspondence with the reference height measurements. The few reed patches that were measured in the grey cattle paddock do also show large residuals (patch names CD01-05, height differences of 1.5 - 2 m, see Tab. 7.1), so it is reasonable to presume that they were also mown some time before the ALS acquisition

Table 7.1: Results of the accuracy assessment for every vegetation patch. Height [m] refers to the vegetation height measured in the field.

Patch No.	Radius [m] 0.5 min.	0.5 mean [m]	0.5 σ	1.25 min.	1.25 mean [m]	1.25 σ	2.5 min.	2.5 mean [m]	2.5 σ	Height [m]
AM01	1,19	1,31	0,13	1,16	1,29	0,12	1,16	1,30	0,10	0,55
AM02	1,20	1,32	0,06	1,19	1,30	0,05	1,16	1,30	0,06	0,65
AM03	1,28	1,34	0,05	1,22	1,34	0,05	1,21	1,36	0,06	0,60
AM04	1,18	1,24	0,06	1,17	1,29	0,11	1,17	1,30	0,09	0,50
AM05	1,23	1,35	0,07	1,20	1,31	0,07	1,18	1,31	0,08	0,40
AM06	1,09	1,15	0,06	1,07	1,20	0,06	1,05	1,20	0,07	0,65
AS07	0,47	0,47	0,00	0,39	0,47	0,02	0,39	0,47	0,01	0,50
AS08	-0,31	-0,30	0,00	-0,33	-0,29	0,06	-0,39	-0,30	0,04	0,50
AS09	-0,29	-0,27	0,01	-0,29	-0,26	0,02	-0,29	-0,24	0,06	0,60
AS10	-0,32	-0,31	0,01	-0,35	-0,31	0,02	-0,40	-0,30	0,03	0,40
AS11	-0,38	-0,35	0,02	-0,40	-0,37	0,02	-0,43	-0,37	0,01	0,50
BD01	1,68	1,80	0,12	1,46	1,80	0,18	1,39	1,75	0,17	1,90
BD02	1,56	1,70	0,12	1,41	1,73	0,18	1,41	1,76	0,21	1,80
BD03	1,27	1,59	0,40	1,09	1,39	0,21	1,09	1,42	0,23	1,90
BD04	1,07	1,33	0,13	0,88	1,19	0,17	0,81	1,18	0,25	1,40
BD05	0,82	0,97	0,12	0,82	1,12	0,25	0,77	1,14	0,31	1,00
BD06	0,88	0,96	0,06	0,88	1,09	0,17	0,83	1,08	0,19	1,00

Patch No.	Radius [m] 0.5 min.	0.5 mean [m]	0.5 σ	1.25 min.	1.25 mean [m]	1.25 σ	2.5 min.	2.5 mean [m]	2.5 σ	Height [m]
BS07	-0,35	-0,24	0,09	-0,41	-0,23	0,17	-0,43	-0,26	0,14	1,65
BS08	0,31	0,42	0,07	0,29	0,41	0,15	0,23	0,43	0,18	1,60
BS09	0,43	0,65	0,22	0,36	0,57	0,23	0,31	0,56	0,23	1,90
BS10	0,68	0,86	0,14	0,62	0,89	0,17	0,53	0,87	0,21	1,80
BD11	0,15	0,28	0,06	0,06	0,26	0,13	0,02	0,27	0,13	1,60
BD12	0,21	0,27	0,05	0,11	0,27	0,07	0,10	0,30	0,12	1,50
BD13	0,33	0,53	0,09	0,15	0,45	0,15	0,07	0,40	0,14	0,60
BD14	0,17	0,32	0,07	0,17	0,40	0,21	0,11	0,38	0,16	0,60
BD15	0,30	0,38	0,06	0,12	0,33	0,08	0,11	0,36	0,13	1,50
BD16	0,34	0,35	0,02	0,27	0,41	0,10	0,18	0,40	0,12	1,30
BD17	0,42	0,53	0,10	0,18	0,41	0,15	0,11	0,36	0,14	1,30
BD18	0,38	0,42	0,04	0,18	0,43	0,13	0,18	0,46	0,11	1,50
BS19	-0,01	0,10	0,06	-0,01	0,09	0,05	-0,01	0,08	0,05	0,70
BS20	0,01	0,05	0,04	-0,03	0,04	0,05	-0,03	0,09	0,06	1,30
AS12	0,06	0,08	0,03	0,05	0,07	0,01	0,03	0,07	0,02	0,50
AS13	0,05	0,12	0,05	-0,04	0,05	0,07	-0,04	0,02	0,04	0,70
AS14	0,10	0,22	0,11	-0,03	0,14	0,09	-0,03	0,11	0,08	0,70

Patch No.	Radius [m] 0.5 min.	0.5 mean [m]	0.5 σ	1.25 min.	1.25 mean [m]	1.25 σ	2.5 min.	2.5 mean [m]	2.5 σ	Height [m]
R01	0,05	0,13	0,05	0,03	0,12	0,05	0,01	0,12	0,04	0,00
R02	0,03	0,10	0,04	0,01	0,09	0,04	-0,04	0,09	0,05	0,00
R03	-0,01	0,10	0,09	-0,05	0,06	0,07	-0,05	0,05	0,06	0,00
R04	-0,04	0,05	0,07	-0,07	0,04	0,08	-0,07	0,02	0,06	0,00
R05	0,00	0,04	0,04	-0,04	0,06	0,06	-0,05	0,05	0,06	0,00
AS15	0,02	0,05	0,03	-0,01	0,05	0,03	-0,01	0,07	0,04	0,08
AS16	0,00	0,04	0,03	0,00	0,05	0,02	0,00	0,06	0,05	0,10
BS21	0,24	0,29	0,03	0,15	0,26	0,04	0,13	0,24	0,05	0,60
AS17	0,05	0,08	0,03	0,02	0,08	0,02	-0,02	0,07	0,03	0,12
AS18	0,11	0,16	0,04	0,08	0,15	0,03	0,08	0,16	0,03	0,15
BS22	-0,04	-0,01	0,01	-0,04	-0,01	0,02	-0,08	-0,01	0,03	0,00
CD01	0,00	0,06	0,04	-0,01	0,15	0,12	-0,04	0,28	0,24	3,20
CD02	-0,07	0,00	0,09	-0,13	0,07	0,16	-0,19	0,27	0,39	3,20
CD03	0,00	0,07	0,07	-0,13	0,11	0,18	-0,20	0,33	0,49	2,80
CD04	0,04	0,08	0,03	-0,16	0,15	0,22	-0,18	0,25	0,34	3,00
CD05	0,04	0,07	0,03	0,01	0,11	0,08	-0,02	0,21	0,22	3,40

in April 2010 and grew to a height of more than 2.5 m by the end of March 2012. Growth like that is not atypical for common reed, even within one year, if the environmental conditions are optimal.

Fig. 7.3c and 7.4c show that larger residuals (> 0.5 m) tend to correlate with larger echo widths (> 5 ns). This indicates that portions of the laser beam do penetrate also the dense canopies, but too much energy is lost in the upper parts of the foliage to cause another distinct echo from deeper down or the ground itself, if it is not entirely covered anyway (Fig. 7.5). This is the case for all the sawtooth sedge patches (patch names Bxxx), and all but one sea rush patches (AM04).

Furthermore, most of the sea rush patches feature lower mean echo widths and also standard deviations than the sawtooth patches. This might be founded in the different growth patterns of the plants. The sharp and thin stems of sea rush do not get picked up by the laser scanner because they are too small. It is thus rather the bulky bottom part of the plant which causes the reflections and yields a more homogeneous surface for the laser scanner with respectively lower echo widths (Fig. 7.5c). Due to their size, the much bigger leaves of the sawtooth sedge may very well constitute a big enough target to widen up the return pulse (Fig. 7.5b).
The growth pattern is reflected by the field measured height densities. These height densities are not largely influenced by temporal offsets of the acquisition times, as they refer more to the phenological states, which were essentially the same. The investigations of the echo widths and the estimated height densities show strong correlations. The echo widths tend to widen up with increasing stratification of the foliage (see Fig. 7.6).

In keeping with the insight from the above described analyses (i.e. smaller echo widths correspond to the smaller residuals), an echo width filter was applied on the point cloud for DTM generation. To determine the magnitude of the threshold, the patches that represented bare earth were consulted. These were the reference patches (R01 - 05), the mown reed patches (CD01 - 05), as well as a group of sea rush patches which consisted only of dead plants (AS15 - 18) and a mixed group of sparsely distributed sea rush and sawtooth sedge patches, which were very short in heights (BS19 - 20 + AS12 - 14). The statistics showed that all of these patches featured mean echo widths of less then 4.7 ns, so this threshold was selected and applied on the point cloud in order to eliminate echoes that resulted from vegetation.
All last echoes with echo widths smaller than 4.7 ns were used for the generation of DTMs. The result of all created 1 x 1 m^2 DTMs compared to the GNSS reference elevations are shown in Fig. 7.7. The DTM_{min} refers to the model created from the lowest last echoes within a grid cell, DTM_{rob} refers to the DTM created from all last echoes with hierarchic robust filtering, and DTM_{EWfilt} refers to the DTM calculated on the basis of the point cloud after the echo width thresholding. The magnitude of the residuals between the DTM and the GNSS references matches those from the point-based investigations (c.f. Fig. 7.3). When compared to each other, the three different methods for DTM calculation show only small differences, the biggest being in the range of a few centimetres (e.g. patch names BD11 - 18). The best results with regards to the GNSS elevations were achieved with the DTM_{EWfilt}. The largest relative differences between the DTMs were 0.19 m (DTM_{min} - DTM_{EWfilt}) and 0.10 m (DTM_{rob} - DTM_{EWfilt}).

The presented results demonstrate that for low vegetation in wetlands, like sawtooth sedge and sea rush in the study site, the penetration of the laser beams through the foliage and down to the ground

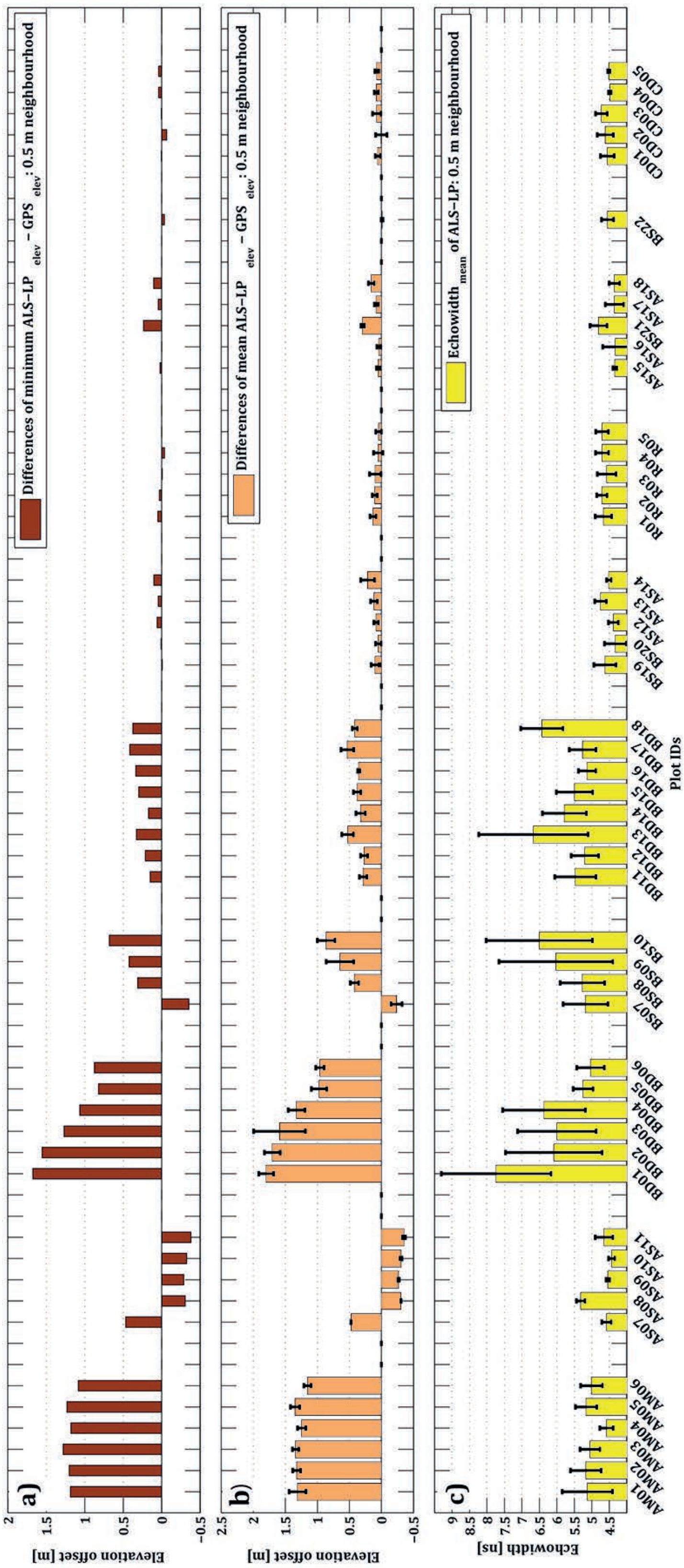

Figure 7.3: Differences of GNSS reference elevation and (a) minimum ALS elevation, and (b) mean ALS elevation. (c) shows the corresponding mean echo widths per vegetation patch. The black lines correspond to the respective standard deviations. ALS echoes were selected in a 0.5 m circular neighbourhood.

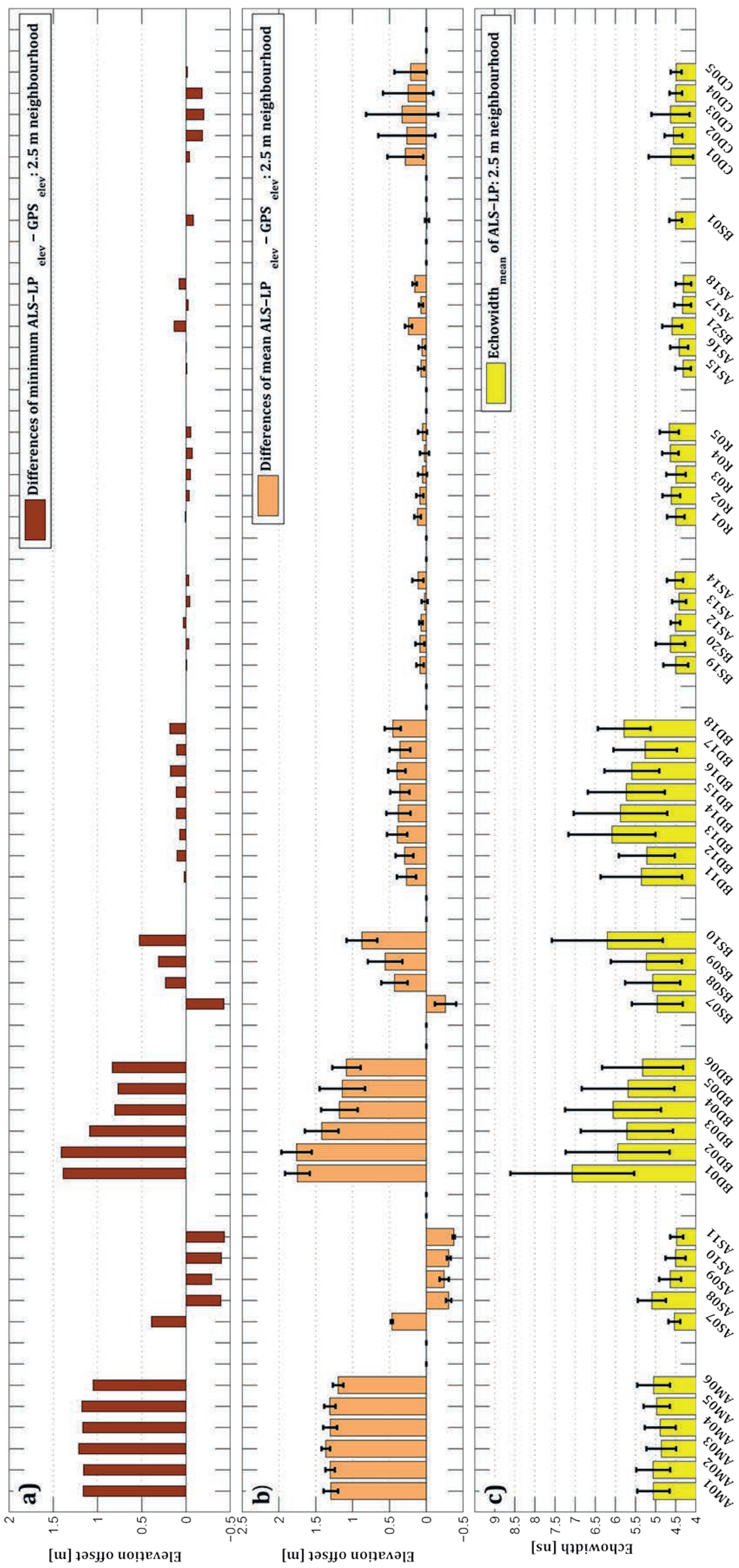

Figure 7.4: Differences of GNSS reference elevation and (a) minimum ALS elevation, and (b) mean ALS elevation. (c) shows the corresponding mean echo widths per vegetation patch. The black lines correspond to the respective standard deviations. ALS echoes were selected in a 2.5 m circular neighbourhood.

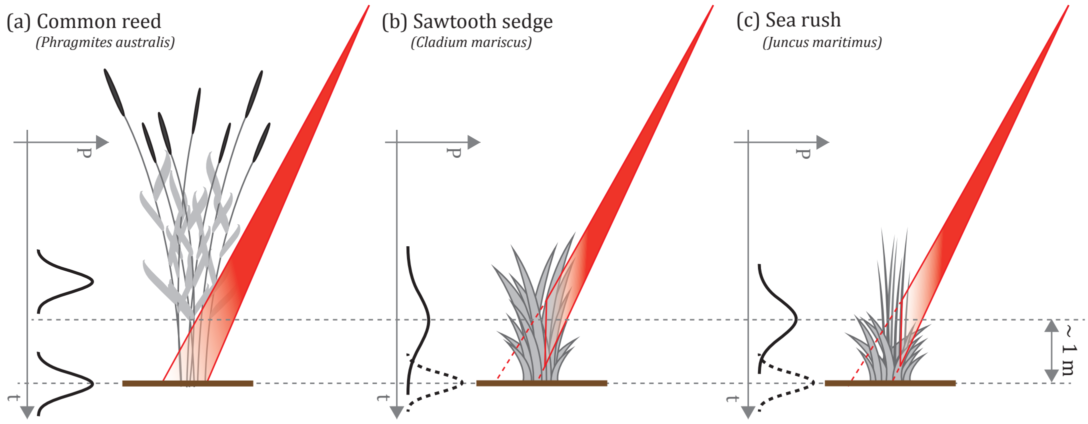

Figure 7.5: Illustrations of different situations causing variations in the widths of the backscattered pulses. Exemplary vegetation growing structures for (a) common reed with (comparably) open canopy causing two distinct reflections, one from the stems and one from the ground; (b) sawtooth sedge with dense and large leaves, which comprise a number of scattering surfaces of different height distribution causing the echo to widen up, while the ground is covered entirely and no echo is reflected, and (c) sea rush with thin tall leaves that do not cause distinct reflections, but the bulky bottom part does, which is also too dense to let the laser beam penetrate and reach the ground.

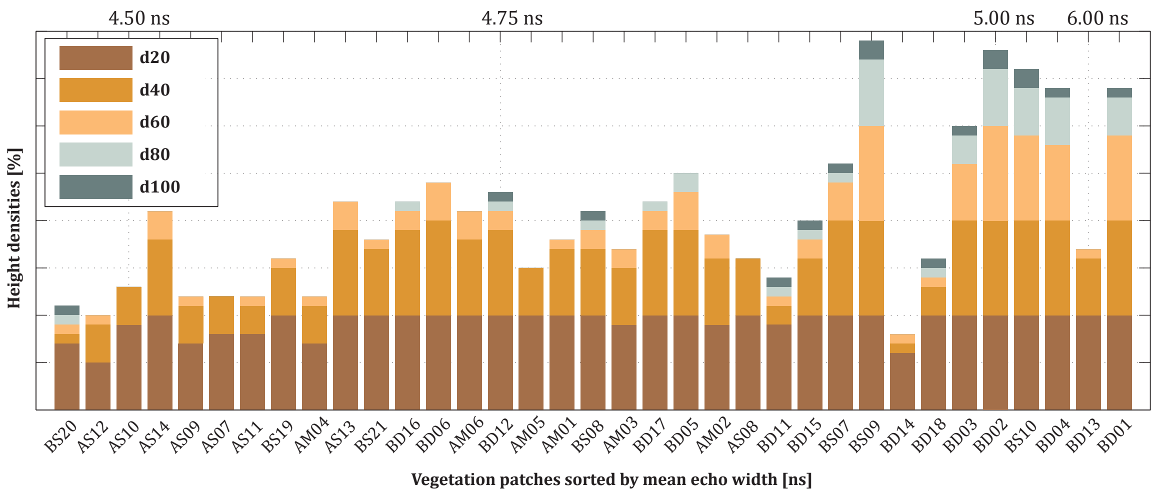

Figure 7.6: Mean echo widths (neighbourhood 0.5 m) of vegetation patches calculated from ALS echoes and compared to height densities measured in the field. Larger echo widths correlate with stratification of the foliage. Bare earth plots were removed.

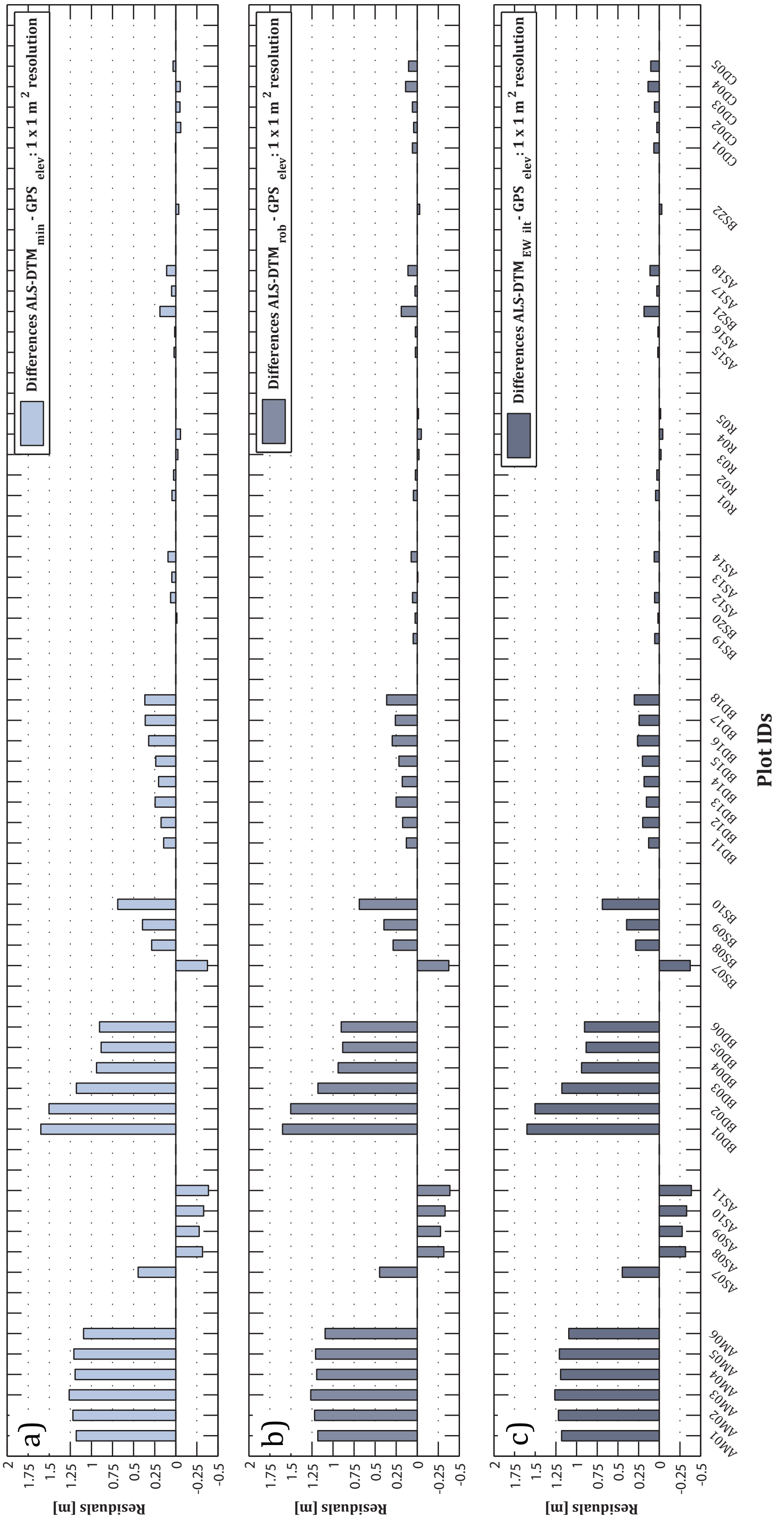

Figure 7.7: Differences of GNSS reference elevation and DTM created (a) from the lowest ALS LP elevation within 1 x 1 m², (b) with hierarchic robust filtering from all ALS LP elevations, and (c) with hierarchic robust filtering from ALS LP elevations after echo width thresholding (EW <= 4.75 ns).

has the essential influence on the quality of the DTM. Out of the three methods for DTM generation tested in this study, none produced outstandingly better results than the other. In this case the choice of DTM generation method had only minimal effect. However, there are other filtering techniques [e.g Sithole and Vosselman 2003], some of which to the author's knowledge have not been tested on wetlands and which might improve the quality. The modification of the grid resolutions did also not have any noteworthy influence on the accuracy of the models.

As described in section 7.2.1, the amplitudes have also been investigated. They showed very high inhomogeneities across the whole acquisition area. The amplitude is a measure which is largely influenced by radiometric properties of surfaces (e.g. reflectivity of materials, water content, etc.). As there was no information on soil properties available for this study, the large inhomogeneities in the non-vegetated parts of the study site could not be investigated or explained. They may result from different states of water saturation of the bare earth or also standing surface water. Neither a conclusive correlation of amplitude and ground coverage, nor amplitude and vegetation species or growth patterns could be found. Informations on errors during data acquisition (e.g. faulty settings or calibration, etc.) or caused by data processing (i.e. settings in the full-waveform decomposition) cannot be excluded, but also not be investigated, as the raw waveform data was not at hand for this study. At this point it can only be speculated that maybe site or sensor specific characteristics were the reason why the amplitudes were unreliable in this case. The amplitudes were therefore not considered for further analysis. It shall be noted that in another study on wetland vegetation mapping with ALS, the amplitudes have indeed successfully contributed to classification tasks [e.g. Zlinszky et al. 2012].

In the Zicklacke exploratory point cloud analysis and visual interpretation of the 3D ALS point cloud show that despite the dense growing structure of the reed in the study site, still a significant number of second and / or last echoes occurs. Also it was observed that the second or last echoes, even if they were reflected close to the water level, were very likely to result from reed stems (see Fig. 7.2). Furthermore, the following three possible situations were identified to cause ALS reflections in the lower parts of the reed, near the water surface (see Fig. 7.10c):

1. the lowest echo results from inside the reed stems, caused by an overlap of reflections from foliage components of different height and, as a result, it is too high.
2. the lowest echo results from uneven ground, where the reed is growing on or which is formed by the basal area of the reed.
3. the lowest echo is reflected from smoother ground, which is likely the case if the reed stems are not too densely grown and are not in the water.

The DTM created with the standard hierarchic robust filtering approach showed many bumps (i.e. surface irregularities with heights ranging from 0.5 to 1 m), some of them well inside densely overgrown areas (white rectangle in Fig. 7.10a). It can be speculated that accumulated silt or organic litter, which is transported in or on the open water, is most likely to happen in the outer parts of the reed, on the reed-water edge. Following this argumentation, the bumps in the outer parts have (at least) partly natural causes and are therefore correct. In the inner parts accumulation of litter through flowing water is less likely as there is usually little water flow. However, due to the way reed

regenerates itself (it dries out, dies, then bends and finally falls, to grow again from the same plant in yearly cycles), the reed's basal area gets thicker and thicker. In this stage it does not allow any more water flow, which slowly leads to aggradation.
To identify the echoes causing the bumps and whether they represent vegetation or non-vegetation, the amplitude and echo width information should be used. The raster maps of the amplitudes showed a very inhomogeneous image with very high amplitudes in the strip centre. The obvious reason for that is the direct (mirrored) reflection from the water surface, which causes very strong backscattered signals, probably resulting in over-modulation (i.e. saturation) of the detection unit, which could also be observed in other data sets from different scanners [e.g. Zlinszky et al. 2012]. However, in this case the resulting amplitudes in the strip centres were fifteen to twenty times larger than anywhere else in the strip. In fact, this could also be observed in the reed areas with only little to no open water, where this kind of over-modulation was not to be expected. To exclude the possibility of errors that might have occurred during recording or post-processing and caused this unexpected characteristics, other non-wetland areas were investigated. It was found that such unlikely high amplitudes only appeared on the wetlands, or more general, areas with high water content or even surface water. Furthermore, no significant difference between amplitudes from echoes close to the water level and above the water level could be observed. This unpredictable behaviour of the recorded amplitudes led to the conclusion not to make use of them for further analysis or the DTM generation.
The range estimation in the full-waveform data recording and processing are also connected to the amplitudes. First, a backscattered signal has to exceed a (usually) proprietary pre-defined signal strength (i.e. amplitude) threshold in order to trigger the detector. Second, during post-processing another user-defined threshold is applied in order to identify a single echo if the signal forms a clearly distinct amplitude peak. Therefore it is logical to assume that possibly incorrectly registered amplitudes might also go along with erroneous range estimations. As no ground truth measurements were available for this study site, this matter could not be investigated in detail through comparison with terrestrial elevations. However, a check of elevations of several neighbouring ALS point clusters inside and outside the areas of these unusually high amplitudes did not show any significant differences, at least none that would go beyond the ranging accuracy of the scanner or the georeferencing accuracy of the flight.

The signature analysis of the echo widths showed that echoes near the water level had a smaller width than the echoes above the water level. Although there is an overlap of both signatures present below the threshold of 5 ns, between 5 and 5.5 ns less than 10% of the echoes close to the water level are present, and above 5.5 ns only the echoes above the water surface remain. For a small sample area this is also illustrated in Fig. 7.9, which shows a 0.5 x 0.5 m^2 raster map created from the mean values of all echo widths within a raster cell for both, the echoes near and above the water level. This indicates that using the echo width information for further discrimination of the point cloud into vegetation and non-vegetation echoes could potentially eliminate echoes from reed stems, which could not be removed with the conventional approach.

Based on the above described observations, an echo selection step was introduced prior to the DTM filtering, neglecting last echoes with large echo widths (EW >= 5.5 ns) because they were likely to represent reed stems (case 1 in Fig. 7.10c). Lower echo widths (EW < 5.5 ns), which were assumed

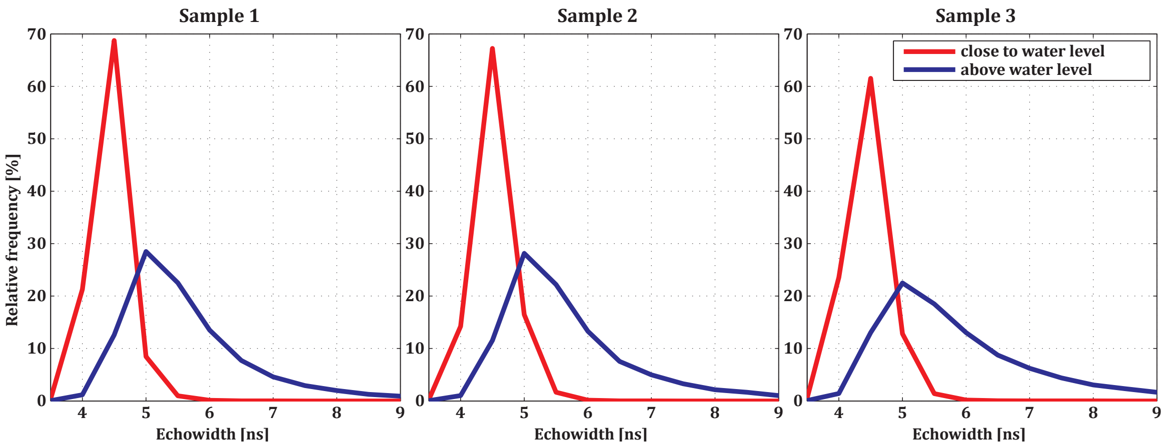

Figure 7.8: Signature analysis of echo widths from ALS point clouds in three different samples.

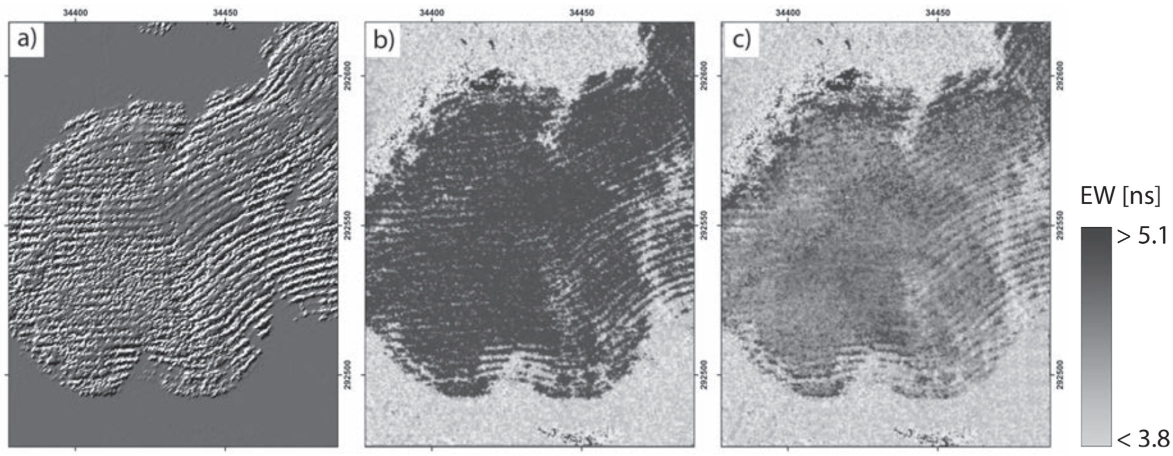

Figure 7.9: (a) DSM shading of small sample site No. 3, tracks caused by tractor mowing are visible, (b) colour-coded raster model of the echo widths generated from points above the water surface (δ_z > 10 cm), and (c) echo widths of points close to the water surface (δ_z <= 10 cm). Grid size of all models = 0.5 x 0.5 m^2.

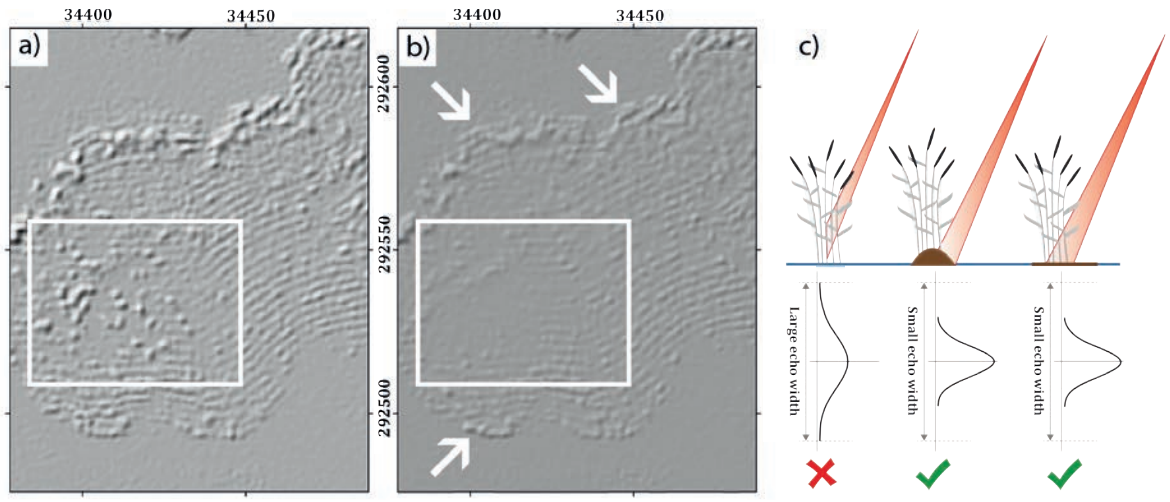

Figure 7.10: (a) Shading of the DTM generated without using echo widths as a pre-classifier for the point cloud, (b) shading of the DTM generated incorporating the echo widths into the filtering process, (c) illustration of different echo width situations for last echoes in the reed areas. Grid size of all DTMs = 0.5 x 0.5 m^2.

to represent the terrain or water surface (cases 2 and 3 in Fig. 7.10c), were kept accordingly. This pre-filtered point cloud served as input for DTM generation. Fig. 7.10 shows the resulting DTM. Compared to the initial DTM, created using the robust filtering approach without the incorporation of the echo widths, the DTM in Fig. 7.10b is much smoother in areas where echoes close to the water level with larger echo widths dominate (area inside the white rectangle). The bumps inside the reed were eliminated because of the fact that the points creating them had large echo widths. On the reed-water edge some smoothing could be observed, but still the edge was quite clearly visible due to some remaining bumps (white arrows in Fig. 7.10b). These bumps were not eliminated because they resulted from points with small echo widths, so consequently it can be reasoned that those elevations are truly present. As already mentioned, they might be the result of aggradation, although this assumption could not be evaluated due to the lack of proper ground truth data.

7.3.2 DSM generation

Three profiles located in the reed areas of the Zicklacke (see Fig. 7.1) were selected and the respective DSM elevations from both, the DSM_{mls} and the DSM_{max}, were plotted in Fig. 7.11. This figure shows the smoothing effect from the moving least squares interpolation of the DSM_{mls} (red lines). It features less abrupt height jumps when compared to the DSM_{max}. It also shows that the DSM_{mls} runs nearly always below the DSM_{max} with height differences of up to 1.5 m. Considering the average vegetation heights in the wetlands in this study (sea rush = 0.6 m, sawtooth sedge = 1.5 m and common reed 2.6 m), this is a significant influence. Estimations of plant heights are prone to errors of up to 100% if the DSM_{mls} is chosen as interpolation method. These errors directly contribute to consecutive models based on nDSMs, such as biomass estimations. Using the DTM created before, which is based on the echo width filtered points, and DSM_{max}, a nDSM (0.5 x 0.5 m^2 resolution) could be created. It corresponds to the height of the reed in and around the Zicklacke (Fig. 7.12) and shows plant heights of up to 2.9 m. The 0.5 x 0.5 m^2 raster map resolution also reveals mowing structures. Such a high level of detail makes investigations on reed bed fragmentation or reed-water-edge length possible and highly accurate. These two indicators for example were found to

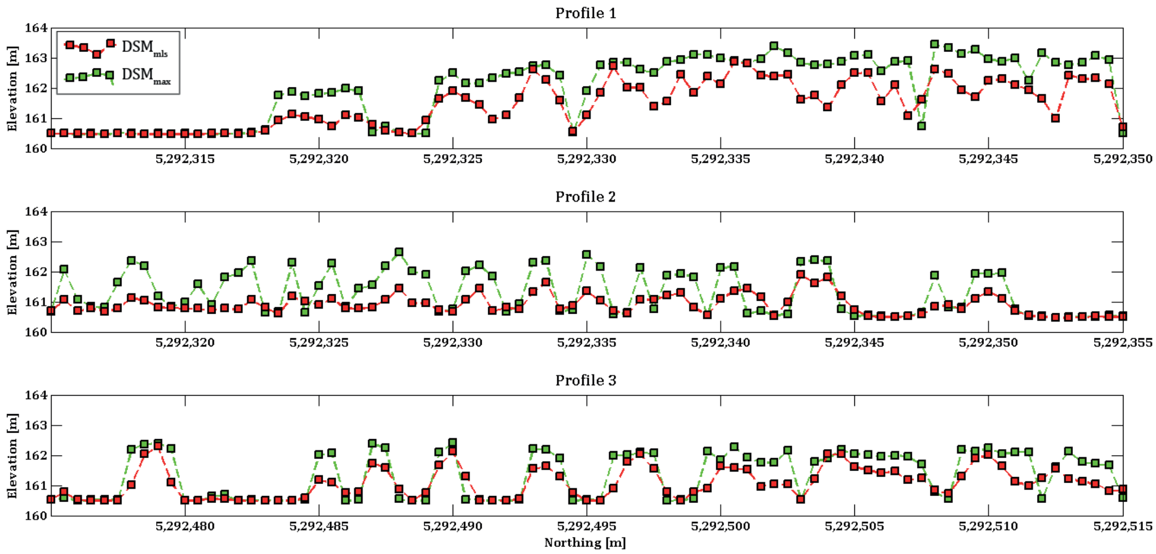

Figure 7.11: Three profiles through the reed areas of the Zicklacke showing the elevation differences between DSM_{mls} and DSM_{max}. The DSM_{mls} gives a smoother surface, but is often too low and thus underestimates the plant heights.

be important for reed habitat quality description [Baldi and Kisbedenek 1999] and reed height maps could also be used as evidence for reed health estimation [Zlinszky et al. 2012].

7.4 Conclusion

In this study the application of ALS in areas overgrown by short and tall wetland vegetation was investigated. Full-waveform ALS, especially the information on the width of the backscattered pulses, was found to provide additional valuable information. Firstly, using the echo width it was possible to parametrize height differences shorter than the width of the emitted laser pulse. Secondly, it could be applied as a filter to select only non-vegetation echoes as input for DTM generation, thus removing some of the unnatural surface undulations (bumps) in the DTM and consequently improve the quality of the DTM. Although in some patches of the test site these improvements were only minimal, the echo width can still be of use as an indicator for reliability of the DTM. Areas featuring large echo widths have a high potential for being vegetated, possible by very short plants, which tend to have an accuracy diminishing effect on DTMs. In other words: if all echoes of an area feature large echo widths, the quality of a DTM derived on the basis of these echoes is bound to be inferior.

The largest residuals of the 3D point cloud, as well as of the derived DTMs were found in patches that featured also large echo widths. The above described analyses strongly indicate that the echo width can be interpreted as a geometric parameter. Also it shows that it has a high potential of being used as a discriminative parameter for the two species sea rush and sawtooth sedge, a distinction that can hardly be achieved based on the 3D point cloud alone. However, this matter needs closer investigations and, moreover, a more extensive set of ground truth measurements in order to train the method and then evaluate the quality. The number of reference patches in this study was too small for that purpose.

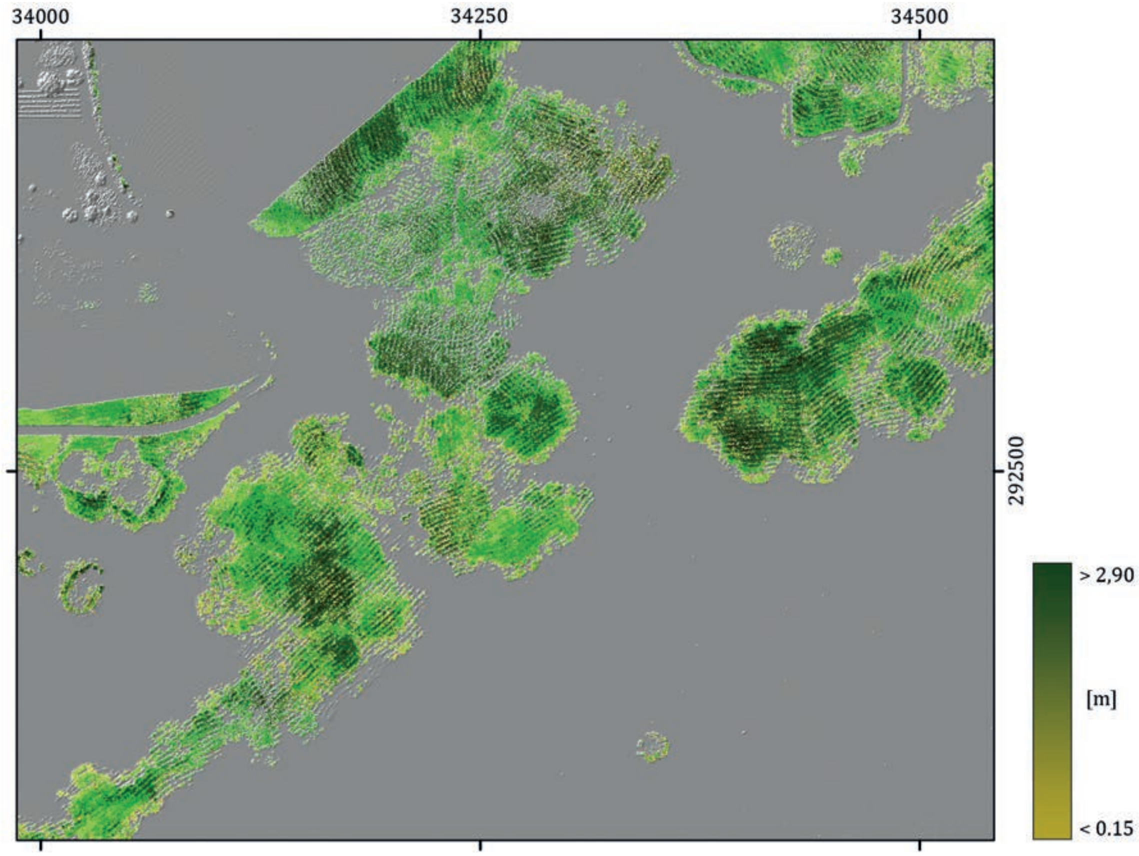

Figure 7.12: Reed height map, derived as the difference of DSM_{max} and DTM created from a pre-filtered point cloud based on echo width thresholds. The image background is the shading of the DSM. All models have a raster resolution of 0.5 x 0.5 m^2.

The amplitudes could not be used in both study sites because of unexpected and to a certain degree inexplicable behaviour. As stated in section 7.3.1, based on the findings in other studies it can be assumed that the amplitude can indeed be used as a valuable indicator for classification purposes in natural areas. It has to be noted that a pre-requisite in this context for both, full-waveform and discrete ALS data is the radiometric calibration of the used amplitude values. The hypothesis is that the calibrated measures become independent from the effects of overlapping ALS acquisition swaths, sensor characteristics, flying height and acquisition time [e.g. Briese et al. 2008; Kaasalainen et al. 2009; Korpela 2008]. All these afore mentioned properties are paramount in vegetation studies, when phenology plays a central role and multi-temporal data acquisitions are often at hand.

For DTM creation three different grid sizes (resp. neighbourhood distances) were investigated. Larger grid sizes increased the possibility of selecting echoes which are closer to the ground. For the study area presented here, this is especially true for densely vegetated patches. Increasing the grid size also goes along with a loss of detail, a fact that is crucial for wetlands, as some of the typical plant communities are highly sensitive to small elevation differences. Judging from the results of this study, for areas of similar topographic characteristics and plant compositions, there has to be a trade-off between DTM accuracy (meaning how well does it represent the actual elevations) and DTM adequacy (meaning to which degree does it still represent significant surface undulations).

The comparison of two common methods of DSM generation illustrates the necessity of choosing an adequate DSM creation method, also and especially in areas with low vegetation. As the examples have shown, differences of several decimetres and up to 1.5 m can occur. If not considered, they will result in loss of information, or even incorrect DSM-based estimations (e.g. plant heights, biomass, etc.). ALS data and derivatives may provide useful additional information for biologists and landscape ecologists interested in the vegetation structure of wetlands, especially for area wide analysis. The results can for example be included in adequate management strategies. At this point it shall be noted that textural and hyper spectral information gathered by modern airborne or space borne passive remote sensing techniques also holds significant information on the state of the wetland plants. A combination of both methods, passive and active, therefore shows the highest potential for ecological research in this area.

8
Concluding Remarks

Streamlining biodiversity indicators is one of the EU's top priorities in its policy on environment and sustainable development [SEBI2010 2004; SEBI2020 2014]. The consistent deterioration of biodiversity is considered a fact and without adequate counteractions it is bound to continue. Therefore a coherent set of indicators was released to be used for the complex task of quantifying biodiversity. These indicators are a key component for monitoring and reporting on the status of areas that were identified to be in need of special conservation and protection. Without dispute, this initiative, which predominantly addresses the assessment of threatening changes, is a big challenge and it can only be met through regular monitoring of the endangered sites.

This monitoring however is a major concern, as current practices are mostly ground-based, highly susceptible to inter-operator bias, non-standardized across country borders and often lack geographical coverage. In addition, the EU-prescribed assessment intervals of six years are barely manageable, while still being cost-effective.

The implementation of EO, in particular ALS, into the assessment process helps to overcome or, at least, lessen all of the above noted limitations. Airborne or spaceborne measurement techniques are able to cover large areas in short periods of time, even repetitively and with comparable quality and accuracy. Automated methods can be used to analyse one and the same data set with respect to various indicators, therefore achieving highly objective and reproducible results.
Some EO-based methods certainly require ground data for e.g. tuning or parameter estimation, but still then the amount of field mapping to be carried out and calculated is disproportionate to the area that can afterwards be mapped and analysed on the basis of adequately calibrated EO data.

The objectives of this thesis (c.f. Sec. 2.1) were to develop automatic and robust methods to support the monitoring process in a highly productive and also innovative way. For this purpose, three subjects of N 2000 importance were selected and the suitability of ALS point clouds as a data basis for the derivation of relevant quantities with respect to these three subjects was investigated. Each one of the proposed procedures and applications supports at least one of the declared biodiversity indicators, either directly or indirectly [SEBI2010 2004].

An approach to derive information about the abundance of sub-dominant vegetation layers in forests was developed and tested on selected CH2 study sites (Chap. 5). Presence of shrub layers could be estimated with high accuracy, while the identification of sub-dominant tree layers was possible, but not as successful as for the shrub layer.
As the vertical composition of the foliage is directly related to the requirements placed by different species on the respective part of the landscape to be used as a habitat or corridor, this application indirectly supports the SEBI indicators *Connectivity and Fragmentation*, as well as *Trends in extents of selected Biomes, Ecosystems and Habitats*, to name but a few.

A method to automatically detect deadwood in forests was presented (Chap. 6). A procedure to filter the ALS point cloud according to surface roughness estimates was implemented, which was able to remove echoes representing shrub vegetation effectively, thereby exposing objects underneath. It was shown that in this way fallen trees could be found very reliably, even if parts were covered by dense vegetation. Also, the derived roughness parameters were found to be a useful indication on the decay level of the detected tree stems. On the other hand, no reliable estimator could be found for the identification of standing dead trees.
This application directly serves as SEBI-compatible indicator on *Sustainable Use: Deadwood in Forests*.

Full-waveform ALS attributes were used to classify the point cloud from wetland study sites (Chap. 7). It was demonstrated that the applied procedures lead to the elimination of echoes from dense and short growing plants and consecutively to the computation of improved DTMs. The analysis also indicated that full-waveform attributes can be used as discriminative parameters for the classification of typical wetland plants.
Although this matter was not further examined, a strong connection to species was evident, which links to the SEBI indicator *Trends in the Abundance and Distribution of selected Species*, as one possibility, but the technique can also support the identification of wetland extents, thereby also supporting the indicators *Connectivity and Fragmentation* and *Trends in extents of selected Biomes, Ecosystems and Habitats*.

All of the proposed approaches are automated (or automatable) and therefore highly suitable for a rationalization of the assessment processes, a major goal of both, TEN and CH2 (c.f. Sec. 1.3), but also the EU.
Examination of their results has shown that none of them require extensive tuning of involved parameters, as all of them rely on geometrically interpretable features. These are assumed to be derivable and adaptable with a minimum of effort for other types of ALS data sets (e.g. different sensor, acquisition time, etc.) or study areas.
Provided comparable data sets as used for the presented studies and up-to-date computational power at hand, their runtime performance is not assumed to become a critical issue, even for wide area

applications. Although it shall be mentioned that computational performance was not an explicit focus of this work, nor was it investigated for every scenario.

Furthermore, all presented applications address topics which are related to vegetation structure. As outlined in chapters 1 and 3, there is strong evidence for a correlation between structure of habitats and the respective inhabitant. It is thus an accepted approach in the assessment of biodiversity relevant quantities with RS to focus on certain structural patterns. In this way, the adequacy of habitats can be estimated for a large number of species in a very time and cost-effective manner. Additionally, core areas, representing habitats for specific target groups of animals and plants can be located.
This forms the ideal basis for well coordinated ground assessment efforts in order to minimize, in particular, manual workload, to meet the ambitious framework requirements. One should however not get the impression that these requirements are circumstantial. After all, they benefit nature conservation, and ultimately, ourselves.

List of acronyms

(d)GNSS	(differential) Global navigation satellite system; includes GPS and GLONASS
CO_2	Carbon dioxide
CWD	Coarse woody debris
DBH	Diameter at breast height
DHM	Digital height model
DHM	Digital height model
EC	European Commission
EO	Earth Observation
ERDF	European regional development fund
EU	European Union
EW	Echowidth; full-waveform ALS parameter
Fig.	Figure
FWD	Fine woody debris
FWF	Full-waveform
GCP	Ground control point
GIS	Geographic Information Systems
GLONASS	*Globalnaya Navigatsionnaya Sputnikovaya Sistema* (rus. Global Navigation Satellite System
GPS	Global positioning system
GSD	Ground sampling distance
HQ	Habitat quality

IAPP	Industry-Academia-Partnership-Pathways
LP	Last pulse, i.e. last of many echoes
MTA	Multiple-time-around; A RIEGL LMS Q680i laser scanner feature.
N 2000	Natura 2000 network of protected sites in the EU
N 2000	The Natura 2000 network
NGO	Non-governmental organization
OBIA	Object based image analysis
RS	Remote Sensing
SAC	Special Area of Conservation
SME	small-and-medium-enterprises
SPA	Special Protection Areas
Tab.	Table
WD	Woody debris

Literature

Alexander, C., Tansey, K., Kaduk, J., Holland, D., and Tate, N. J. [Sept. 2010]. "Backscatter coefficient as an attribute for the classification of full-waveform airborne laser scanning data in urban areas". In: *ISPRS Journal of Photogrammetry and Remote Sensing* 65 (5), pp. 423–432. ISSN: 09242716. DOI: 10.1016/j.isprsjprs.2010.05.002.

Arroyo, L. A., Johansen, K., Armston, J., and Phinn, S. [Jan. 2010]. "Integration of LiDAR and QuickBird imagery for mapping riparian biophysical parameters and land cover types in Australian tropical savannas". In: *Forest Ecology and Management* 259 (3), pp. 598–606. ISSN: 0378-1127. DOI: 10.1016/j.foreco.2009.11.018.

Axelsson, P. [2000]. "DEM generation from laser scanner data using adaptive TIN models". In: *Proceedings of the XIX ISPRS Congress, International Archives of the Photogrammetry, Remote Sensing and Spatial Information Sciences, Vol. XXXIII, B4/1-3*. Ed. by D. Fritsch and M. Molenaar, pp. 111–118. URL: http://www.isprs.org/proceedings/XXXIII/congress/part4/111_XXXIII-part4.pdf.

Baldi, A. and Kisbedenek, T. [1999]. "Species-specific distribution of reed-nesting passerine birds across reed-bed edges: effects of spatial scale and edge type". In: *Acta Zoologica Academiae Scientiarum Hungaricae* 45(2), pp. 97–114. URL: http://www.nhmus.hu/~baldi/baldi_kisb_azh_reed_edge.pdf.

Baltsavias, E. P. [1999]. "Airborne laser scanning: basic relations and formulas". In: *ISPRS Journal of Photogrammetry and Remote Sensing* 54 (2), pp. 199–214. DOI: 10.1016/s0924-2716(99)00015-5.

Bater, C. W, Coops, N. C., Gergel, S. E., LeMay, V., and Collins, D. [2009]. "Estimation of standing dead tree class distributions in northwest coastal forests using lidar remote sensing". In: *Canadian Journal of Forest Research* 39 (6), 1080–1091. DOI: 10.1139/x09-030.

Benassi, G., Battisti, C., Luiselli, L., and Boitani, L. [Oct. 2009]. "Area-sensitivity of three reed bed bird species breeding in Mediterranean marshland fragments". en. In: *Wetlands Ecology and Management* 17 (5), pp. 555–564. ISSN: 0923-4861, 1572-9834. DOI: 10.1007/s11273-009-9135-9.

Bianchin, S., Hermann, A., Hainz-Renetzeder, C., Konkoly-Gyuró, É., Hollaus, M., Kuttner, M., Mücke, W., Neubert, M., Pfeifer, N., Skokanová, H., Tirászi, Á., Völler, S., Wrbka, T., Zhuber, T., and Zmelik, K. [2012]. *TransEcoNet CoreOutput XV - Ecosystem Services*. TransEcoNet Geoportal. URL: http://141.30.37.141/phpbb/.

Bissonette, J. and Storch, I. [2007]. *Temporal Dimensions of Landscape Ecology: Wildlife Responses to Variable Resources*. Springer. ISBN: 9780387454443. DOI: 10.1007/978-0-387-45447-4.

Blanchard, S. D., Jakubowski, M. K., and Kelly, M. [2011]. "Object-based image analysis of downed logs in disturbed forested landscapes using lidar". In: *Remote Sensing* 3 (11), pp. 2420–2439. DOI: 10.3390/rs3112420.

Blaschke, T., Tiede, D., and Heurich, M. [2004]. "3D-landscape metrics to modelling forest structure and diversity based on laser-scanning data". In: *Laser-Scanners for Forest and Landscape Assessment*. Ed. by M. Thies, B. Koch, H. Spiecker, and H. Weinacker. Vol. XXXVI, Part 8/W2. ISPRS Archives. Freiburg: Albert Ludwigs University, pp. 129–132. URL: http://www.isprs.org/proceedings/XXXVI/8-W2/BLASCHKE.pdf.

Bretar, F., Chauve, A., Bailly, J.-S., Mallet, C., and Jacome, A. [2009]. "Terrain surfaces and 3-D landcover classification from small footprint full-waveform lidar data: Application to badlands". In: *Hydrology and Earth System Sciences* 13 (8), pp. 1531–1545. DOI: 10.5194/hess-13-1531-2009.

Briese, C., Höfle, B., Lehner, H., Wagner, W., Pfennigbauer, M., and Ullrich, A. [2008]. "Calibration of full-waveform airborne laser scanning data for object classification". In: *SPIE Defense and Security Symposium*. International Society for Optics and Photonics. DOI: 10.1117/12.781086.

Burel, F. [1992]. "Effect of landscape structure and dynamics on species diversity in hedgerow networks". In: *Landscape Ecology* 6 (3), pp. 161–174. DOI: 10.1007/BF00130028.

Butts, S. R. and McComb, W. C. [2000]. "Associations of forest-floor vertebrates with coarse woody debris in managed forests of western Oregon". In: *The Journal of wildlife management*, pp. 95–104. DOI: 10.2307/3802978.

Central Europe [2013]. *Central Europe Programme*. http://www.central2013.eu/. (Visited on 02/12/2014).

ChangeHabitats2 [2013]. *The ChangeHabitats2 Project - For a better tomorrow*. URL: http://www.changehabitats.eu/ (visited on 11/28/2012).

Christensen, M., Hahn, K., Mountford, E. P., Odor, P., Standovar, T., Rozenbergar, D., Diaci, J., Wijdeven, S., Meyer, P., and Winter, S. [2005]. "Dead wood in European beech (Fagus sylvatica) forest reserves". In: *Forest Ecology and Management* 210 (1), pp. 267–282. DOI: 10.1016/j.foreco.2005.02.032.

Chust, G., Galparsoro, I., Borja, n., Franco, J., and Uriarte, A. [2008]. "Coastal and estuarine habitat mapping, using LIDAR height and intensity and multi-spectral imagery". In: *Estuarine, Coastal and Shelf Science* 78 (4), pp. 633–643. DOI: 10.1016/j.ecss.2008.02.003.

Clark, W. R. [2010]. "Principles of landscape ecology". In: *Nature Education Knowledge* 3(10):34. URL: http://www.nature.com/scitable/knowledge/library/principles-of-landscape-ecology-13260702 (visited on 02/12/2014).

Cobby, D. M., Mason, D. C., Horritt, M. S., and Bates, P. D. [2003]. "Two-dimensional hydraulic flood modelling using a finite-element mesh decomposed according to vegetation and topographic features derived from airborne scanning laser altimetry". In: *Hydrological Processes* 17 (10), pp. 1979–2000. ISSN: 1099-1085. DOI: 10.1002/hyp.1201.

Coops, N. C. and Wulder, M., eds. [2012]. *Proceedings SilviLaser 2012 - The 12th International Conference on LiDAR Applications for Assessing Forest Ecosystems*. Vancouver, British Columbia, Canada.

Coops, N. C., Hilker, T., Wulder, M. A., St-Onge, B., Newnham, G., Siggins, A., and Trofymow, J. T. [2007]. "Estimating canopy structure of Douglas-fir forest stands from discrete-return LiDAR". In: *Trees* 21 (3), pp. 295–310. DOI: 10.1007/s00468-006-0119-6.

Doneus, M., Briese, C., Fera, M., and Janner, M. [2008]. "Archaeological prospection of forested areas using full-waveform airborne laser scanning". In: *Journal of Archaeological Science* 35 (4), pp. 882–893. DOI: 10.1016/j.jas.2007.06.013.

Ellis, L. R., Mahler, W. D., and Richardson, T. C. [2012]. "LiDAR Based Delineation of Depressional Wetlands". In: *Trends in Soil Science and Plant Nutrition* 3 (1). ISSN: 2146-0841. URL: http://www.asciencejournal.net/asj/index.php/TSPN/article/view/255/pdf_43.

Elmqvist, M, Jungert, E, Lantz, F, Persson, A, and Soderman, U [2001]. "Terrain modelling and analysis using laser scanner data". In: *International Archives of Photogrammetry Remote Sensing and Spatial Information Sciences* 34 (3/W4), pp. 219–226.

EOL [2013]. *Encyclopedia of Life*. http://eol.org/. (Visited on 02/12/2014).

ERDF [2013]. *European regional development fund*. http://ec.europa.eu/regional_policy/index_en.cfm. (Visited on 02/12/2014).

ESRI [2013]. *ArcGIS - Mapping and Spatial Analysis for Understanding Our World*. URL: http://www.esri.com/software/arcgis (visited on 11/29/2012).

Esseen, P.-A., Ehnström, B., Ericson, L., and Sjöberg, K. [1992]. "Boreal forests - the focal habitats of Fennoscandia". In: *Ecological principles of nature conservation. Applied in temperate and boreal environments*, pp. 252–325. DOI: 10.1007/978-1-4615-3524-9_7.

European Commission [1979]. *The Birds Directive*. URL: http://ec.europa.eu/environment/nature/legislation/birdsdirective/ (visited on 02/12/2014).

— [1992a]. *The Habitats Directive*. URL: http://ec.europa.eu/environment/nature/legislation/habitatsdirective/ (visited on 02/12/2014).

— [1992b]. *The Natura 2000 network*. URL: http://ec.europa.eu/environment/nature/natura2000/ (visited on 02/12/2014).

— [2013a]. *European Environment Agency's home page - European Environment Agency (EEA)*. URL: http://www.eea.europa.eu/ (visited on 11/29/2012).

— [2013b]. *Research and Innovation - Marie Curie Actions*. URL: http://ec.europa.eu/research/mariecurieactions/ (visited on 02/12/2014).

European Environment Agency [2014a]. *Debrecen - Nagerdö - NATURA 2000 - Standard data form*. URL: http://natura2000.eea.europa.eu/Natura2000/SDF.aspx?site=HUHN20033&release=4&form=Clean (visited on 02/13/2014).

— [2014b]. *Debrecen-hajdúböszörményi tölgyesek - Factsheet*. URL: http://eunis.eea.europa.eu/sites/HUHN20033 (visited on 02/13/2014).

— [2014c]. *Hardenbeck-Küstrinchen - Factsheet*. URL: http://eunis.eea.europa.eu/sites/DE2746301 (visited on 02/13/2014).

Ferraz, A., Bretar, F., Jacquemoud, S., Gonçalves, G., Pereira, L., Tomé, M., and Soares, P. [2012]. "3-D mapping of a multi-layered Mediterranean forest using ALS data". In: *Remote Sensing of Environment* 121, pp. 210–223. DOI: 10.1016/j.rse.2012.01.020.

Fleury, A. M. and Brown, R. D. [1997]. "A framework for the design of wildlife conservation corridors With specific application to southwestern Ontario". In: *Landscape and Urban Planning* 37 (3–4), pp. 163 –186. ISSN: 0169-2046. DOI: 10.1016/S0169-2046(97)80002-3.

Foody, G. M. [2010]. "Assessing the accuracy of land cover change with imperfect ground reference data". In: *Remote Sensing of Environment* 114 (10), pp. 2271–2285. DOI: 10.1016/j.rse.2010.05.003.

Forman, R. T. [1995]. "Some general principles of landscape and regional ecology". In: *landscape ecology* 10 (3), pp. 133–142. DOI: 10.1007/bf00133027.

Forman, R. and Godron, M. [1986]. *Landscape Ecology*. Wiley. ISBN: 978-0471870371.

FugroViewer [2014]. *A free 3D geodata viewer*. http://www.fugroviewer.com/. Vienna, Austria. (Visited on 02/13/2014).

Gaveau, D. L. and Hill, R. A. [2003]. "Quantifying canopy height underestimation by laser pulse penetration in small-footprint airborne laser scanning data". In: *Canadian Journal of Remote Sensing* 29 (5), pp. 650–657. DOI: 10.5589/m03-023.

Gilvear, D., Tyler, A., and Davids, C. [2004]. "Detection of estuarine and tidal river hydromorphology using hyper-spectral and LiDAR data: Forth estuary, Scotland". In: *Estuarine, Coastal and Shelf Science* 61 (3), pp. 379–392. DOI: 10.1016/j.ecss.2004.06.007.

Gobakken, T. and Næsset, E. [2005]. "Weibull and percentile models for lidar-based estimation of basal area distribution". In: *Scandinavian Journal of Forest Research* 20 (6), pp. 490–502. DOI: 10.1080/02827580500373186.

Goetz, S. J., Steinberg, D., Betts, M. G., Holmes, R. T., Doran, P. J., Dubayah, R., and Hofton, M. [2010]. "Lidar remote sensing variables predict breeding habitat of a Neotropical migrant bird". In: *Ecology* 91 (6), pp. 1569–1576. DOI: 10.1890/09-1670.1.

Grillmayer, R. [2002]. "Landscape structure model". In: *Contribution to Enviro Info*. September 27-29, Vienna. URL: http://ivfl.boku.ac.at/Projekte/Woek_Austria/pdf/Grillmayer_Lc_Model.pdf.

Hancock, S., Lewis, P., Foster, M., Disney, M., and Muller, J.-P. [2012]. "Measuring forests with dual wavelength lidar: A simulation study over topography". In: *Agricultural and Forest Meteorology* 161 (0), pp. 123 –133. ISSN: 0168-1923. DOI: 10.1016/j.agrformet.2012.03.014.

Heilmeier, H., Burai, P., Lénárt, C., Mücke, W., and Schroiff, A. [2011]. "ChangeHabitats2 - Habitat monitoring by airborne laser scanning and hyperspectral imaging supported field work". In: *Abstract Book 12th European Ecological Federation Congress "Responding to Rapid Environmental Change"*. Ed. by EEF. Avila, Spain: Asociación Española de Ecologia Terrestre, p. 69. URL: http://publik.tuwien.ac.at/files/PubDat_204939.pdf.

Heipke, C., Mayer, H., Wiedemann, C., and Jamet, O. [1997]. "Evaluation of automatic road extraction". In: *International Archives of Photogrammetry and Remote Sensing* 32 (3 SECT 4W2), 151–160. URL: http://www.ifp.uni-stuttgart.de/publications/wg34/wg34_heipke.pdf.

Hermann, A., Kuttner, M., Prinz, M., Hainz-Renetzeder, C., Schindler, S., Wagner, I., Skokanová, H., Wrbka, T., and Zmelik, K. [2010]. *TransEcoNet - Output I: Assessment of landscape functionality*. TransEcoNet Geoportal. URL: http://141.30.37.141/phpbb/ (visited on 02/12/2014).

Hill, R. [2003]. "Quantifying Canopy Height Underestimation by Laser Pulse Penetration in Small-Footprint Airborne Laser Scanning Data". In: *Canadian Journal of Remote Sensing* 29 (5), pp. 650–657. DOI: 10.5589/m03-023.

Hill, R. A., Hinsley, S. A., and Bellamy, P. E. [2004]. "Integrating multiple datasets for the remote quantification of woodland bird habitat quality". In: *Proceedings of ISPRS Working Group VIII/2: Laser Scanners for Forest and Landscape Assessment*. Vol. 36. Part 8, W2. URL: http://www.isprs.org/proceedings/XXXVI/8-W2/HILL.pdf.

Hladik, C. and Alber, M. [2012]. "Accuracy assessment and correction of a LIDAR-derived salt marsh digital elevation model". In: *Remote Sensing of Environment* 121, pp. 224–235. DOI: 10.1016/j.rse.2012.01.018.

Hoechstetter, S. [2009]. "Enhanced methods for analysing landscape structure: Landscape metrics for characterising three-dimensional patterns and ecological gradients". PhD thesis. TU Dresden. ISBN: 978-3941216136.

Höfle, B., Vetter, M., Pfeifer, N., Mandlburger, G., and Stötter, J. [2009]. "Water surface mapping from airborne laser scanning using signal intensity and elevation data". In: *Earth Surface Processes and Landforms* 34 (12), pp. 1635–1649. DOI: 10.1002/esp.1853.

Hollaus, M., Mücke, W., Roncat, A., Pfeifer, N., and Briese, C. [2014]. "Full-waveform recording systems and their possibilities in forest applications". In: *Forestry applications of airborne laser scanning – Concepts and Case Studies*. Ed. by M. Maltamo, E. Næsset, and J. Vauhkonen. Managing Forest Ecosystems. Heidelberg London New York: Springer Science+Business Media B.V. Chap. 3. ISBN: 978-94-017-8662-1. DOI: 10.1007/978-94-017-8663-8__3.

Hollaus, M., Mandlburger, G., Pfeifer, N., and Mücke, W. [2010]. "Land cover dependent derivation of digital surface models from Airborne laser Scanning data". In: *Proceedings of the ISPRS WG III/2, I/2, V/3, V International Archives of the Photogrammetry, Remote Sensing and Spatial*

Information Sciences. Vol. XXXVIII Part 3A. Ed. by G. V. F. Bretar M. Pierrot-Deseiligny. Paris, France, pp. 221–226. URL: http://publik.tuwien.ac.at/files/PubDat_187839.pdf.

Hollaus, M., Eysn, L., Mücke, W., Pfeifer, N., and Mandlburger, G. [2011a]. "Forest Delineation and Structure Assessment Based on Airborne Laserscanning Data". In: *Proceedings European LiDAR Mapping Forum (ELMF) 2011 Conference*. Ed. by ELMF. Salzburg, Austria. URL: http://publik.tuwien.ac.at/files/PubDat_204692.pdf.

Hollaus, M., Aubrecht, C., H"ofle, B., Steinnocher, K., and Wagner, W. [Mar. 2011b]. "Roughness Mapping on Various Vertical Scales Based on Full-Waveform Airborne Laser Scanning Data". In: *Remote Sensing* 3 (3), pp. 503–523. ISSN: 2072-4292. DOI: 10.3390/rs3030503.

Hollaus, M., Mücke, W., and Eysn, L. [2012]. "Forest structure and stem volume assessment based on airborne laser scanning". In: *Ambiência* 8, pp. 471–482. DOI: 10.5777/ambiencia.2012.04.03.

Hopkinson, C., Chasmer, L. E., Sass, G., Creed, I. F., Sitar, M., Kalbfleisch, W., and Treitz, P. [2005]. "Vegetation class dependent errors in lidar ground elevation and canopy height estimates in a boreal wetland environment". In: *Canadian Journal of Remote Sensing* 31 (2), pp. 191–206. DOI: 10.5589/m05-007.

Hutton, C. and Brazier, R. [2012]. "Quantifying riparian zone structure from airborne LiDAR: Vegetation filtering, anisotropic interpolation, and uncertainty propagation". In: *Journal of Hydrology* 442–443 (0), pp. 36 –45. ISSN: 0022-1694. DOI: 10.1016/j.jhydrol.2012.03.043.

Hyyppä, J., Hyyppä J., H., Litkey, P., Yu, X., Haggrén, H., Rännholm, P., Pyysalo, U., Pitkänen, J., and Maltamo, M. [2004]. "Algorithms and Methods of Airborne Laser Scanning for Forest Measurements". In: *International Archives of Photogrammetry, Remote Sensing and Spatial Information Sciences* XXXVI (Part 8/W2), pp. 82–89. ISSN: ISSN 1682-1750. URL: http://tinyurl.com/nk96c6w.

Jaskierniak, D., Lane, P. N., Robinson, A., and Lucieer, A. [2011]. "Extracting LiDAR indices to characterise multilayered forest structure using mixture distribution functions". In: *Remote Sensing of Environment* 115 (2), pp. 573–585. DOI: 10.1016/j.rse.2010.10.003.

Jenkins, R. B. and Frazier, P. S. [2010]. "High-resolution remote sensing of upland swamp boundaries and vegetation for baseline mapping and monitoring". In: *Wetlands* 30 (3), pp. 531–540. DOI: 10.1007/s13157-010-0059-1.

Jenness, J. S. [2004]. "Calculating landscape surface area from digital elevation models". In: *Wildlife Society Bulletin* 32 (3), pp. 829–839. URL: http://www.jennessent.com/downloads/WSB_32_3_Jenness.pdf.

Johansen, K., Arroyo, L. A., Armston, J., Phinn, S., and Witte, C. [July 2010]. "Mapping riparian condition indicators in a sub-tropical savanna environment from discrete return LiDAR data using object-based image analysis". In: *Ecological Indicators* 10 (4), pp. 796–807. ISSN: 1470-160X. DOI: 10.1016/j.ecolind.2010.01.001.

Joosten, H. et al. [2009]. "The Global Peatland CO2 Picture: peatland status and drainage related emissions in all countries of the world." In: *The Global Peatland CO2 Picture: peatland status* *and drainage related emissions in all countries of the world*. URL: http://www.wetlands.org/Portals/0/publications/Report/The%20Global%20Peatland%20CO2%20Picture_web.pdf.

Juutilainen, K., Halme, P., Kotiranta, H., and Mänkkänen, M. [Oct. 2011]. "Size matters in studies of dead wood and wood-inhabiting fungi". In: *Fungal Ecology* 4 (5), pp. 342–349. ISSN: 1754-5048. DOI: 10.1016/j.funeco.2011.05.004.

Kaasalainen, S., Hyyppa, H., Kukko, A., Litkey, P., Ahokas, E., Hyyppa, J., Lehner, H., Jaakkola, A., Suomalainen, J., Akujarvi, A., et al. [2009]. "Radiometric calibration of LIDAR intensity with commercially available reference targets". In: *Geoscience and Remote Sensing, IEEE Transactions on* 47 (2), pp. 588–598. DOI: 10.1109/tgrs.2008.2003351.

Kager, H. [2004]. "Discrepancies Between Overlapping Laser Scanning Strips - Simultaneous Fitting of Aerial Laser Scanner Strips". In: *International Archives of the Photogrammetry, Remote Sensing and Spatial Information Sciences 35 (Part B1)*. Istanbul, Turkey, pp. 555–560. URL: http://www.isprs.org/proceedings/XXXV/congress/comm1/papers/99.pdf.

Kati, V., Dimopoulos, P., Papaioannou, H., and Poirazidis, K. [2009]. "Ecological management of a Mediterranean mountainous reserve (Pindos National Park, Greece) using the bird community as an indicator". In: *Journal for Nature Conservation* 17 (1), pp. 47–59. DOI: 10.1016/j.jnc.2008.12.002.

Keddy, P. A. [2010]. *Wetland ecology: principles and conservation*. Cambridge University Press. DOI: 10.1017/cbo9780511778179.

Keddy, P. A. and Drummond, C. G. [1996]. "Ecological properties for the evaluation, management, and restoration of temperate deciduous forest ecosystems". In: *Ecological Applications*, pp. 748–762. DOI: 10.2307/2269480.

Kim, Y., Yang, Z., Cohen, W. B., Pflugmacher, D., Lauver, C. L., and Vankat, J. L. [2009]. "Distinguishing between live and dead standing tree biomass on the North Rim of Grand Canyon National Park, USA using small-footprint lidar data". In: *Remote sensing of environment* 113 (11), pp. 2499–2510. URL: 10.1016/j.rse.2009.07.010.

Kimberly, A. [2002]. "The landscape ecology of invasive spread". In: *Conservation Biology* 16 (5), pp. 1192–1203. DOI: 10.1046/j.1523-1739.2002.01064.x.

Korpela, I., Hovi, A., and Morsdorf, F. [2012]. "Understory trees in airborne LiDAR data - Selective mapping due to transmission losses and echo-triggering mechanisms". In: *Remote Sensing of Environment* 119, pp. 92–104. DOI: 10.1016/j.rse.2011.12.011.

Korpela, I. S. [2008]. "Mapping of understory lichens with airborne discrete-return LiDAR data". In: *Remote Sensing of Environment* 112 (10), pp. 3891–3897. DOI: 10.1016/j.rse.2008.06.007.

Kraus, K. [2000]. *Photogrammetrie, Band 3, Topographische Informationssysteme*. An english edition by Taylor and Francis (translator: H. Rüther) is in preparation. Dümmler. DOI: 10.1515/9783110906165.

Kraus, K. [2007]. *Photogrammetry – Geometry from Images and Laser Scans*. 2nd ed. de Gruyter, p. 459. ISBN: 978-3110190076.

Kraus, K. and Pfeifer, N. [1998]. "Determination of terrain models in wooded areas with airborne laser scanner data". In: *ISPRS Journal of Photogrammetry & Remote Sensing* 53 (4), pp. 193–203. DOI: 10.1016/s0924-2716(98)00009-4.

Lapin, M. and Barnes, B. [1995]. "Using the landscape ecosystem approach to assess species and ecosystem diversity". In: *Conservation Biology* 9 (5), pp. 1148–1158. DOI: 10.1046/j.1523-1739.1995.9051134.x-i1.

Lassauce, A., Paillet, Y., Jactel, H., and Bouget, C. [2011]. "Deadwood as a surrogate for forest biodiversity: meta-analysis of correlations between deadwood volume and species richness of saproxylic organisms". In: *Ecological Indicators* 11 (5), pp. 1027–1039. DOI: 10.1016/j.ecolind.2011.02.004.

Lefsky, M. A., Cohen, W., Acker, S., Parker, G. G., Spies, T., and Harding, D [1999]. "Lidar remote sensing of the canopy structure and biophysical properties of Douglas-fir western hemlock forests". In: *Remote sensing of environment* 70 (3), pp. 339–361. DOI: 10.1016/S0034-4257(99)00052-8.

Leiterer, R., Morsdorf, F., Schaepman, M., Mücke, W., Pfeifer, N., and Hollaus, M. [2012]. "3D Vegetationskartierung: flugzeuggestütztes Laserscanning für ein operationelles Waldstrukturmonitoring". In: *Proceedings AK Fernerkundung 2012 Bochum*. Ed. by AK Fernerkundung. Bochum, Germany. URL: http://publik.tuwien.ac.at/files/PubDat_211134.pdf.

Lenart, M. [Dec. 2009]. "An unseen carbon sink". In: (0912), pp. 137–138. DOI: 10.1038/climate.2009.125.

Lin, Y. C. and Mills, J. P. [2009]. "Integration of full-waveform information into the airborne laser scanning filtering process". In: *International Archives of Photogrammetry, Remote Sensing and Spatial Information Sciences* 38. URL: http://www.isprs.org/proceedings/XXXVIII/3-W8/papers/p39.pdf.

Lindberg, E., Olofsson, K., Holmgren, J., and Olsson, H. [2012]. "Estimation of 3D vegetation structure from waveform and discrete return airborne laser scanning data". In: *Remote Sensing of Environment* 118, pp. 151–161. DOI: 10.1016/j.rse.2011.11.015.

Lindberg, E., Hollaus, M., Mücke, W., Fransson, J. E. S., and Pfeifer, N. [2013]. "Detection of lying tree stems from airborne laser scanning data using a line template matching algorithm". In: *ISPRS Annals of the Photogrammetry, Remote Sensing and Spatial Information Sciences*. Vol. II-5/W2. talk: ISPRS Workshop Laser Scanning 2013, Antalya, Turkey; 2013-11-11 – 2013-11-13, pp. 169–174. DOI: 10.5194/isprsannals-II-5-W2-169-2013. URL: http://publik.tuwien.ac.at/files/PubDat_221148.pdf.

Lohr, S. M., Gauthreaux, S. A., and Kilgo, J. C. [2002]. "Importance of coarse woody debris to avian communities in loblolly pine forests". In: *Conservation Biology* 16 (3), pp. 767–777. DOI: 10.1046/j.1523-1739.2002.01019.x.

MacArthur, R. H. and MacArthur, J. W. [1961]. "On bird species diversity". In: *Ecology* 42 (3), pp. 594–598. DOI: 10.2307/1932254.

MacArthur, R. H. [1967]. *The theory of island biogeography*. Vol. 1. Princeton University Press. ISBN: 0-691-08836-5.

Maltamo, M, Packalén, P, Yu, X, Eerikäinen, K, Hyyppä, J, and Pitkänen, J [2005]. "Identifying and quantifying structural characteristics of heterogeneous boreal forests using laser scanner data". In: *Forest ecology and management* 216 (1), pp. 41–50. DOI: 10.1016/j.foreco.2005.05.034.

Mandlburger, G., Briese, C., and Pfeifer, N. [2007]. "Progress in LiDAR sensor technology - chance and challenge for DTM generation and data administration". In: *Proceedings of the 51th Photogrammetric Week, D. Fritsch (ed.)* Heidelberg, Germany: Herbert Wichmann Verlag, pp. 159–169. URL: http://www.ifp.uni-stuttgart.de/publications/phowo07/200Mandlburger.pdf.

Martinuzzi, S., Vierling, L. A., Gould, W. A., Falkowski, M. J., Evans, J. S., Hudak, A. T., and Vierling, K. T. [2009]. "Mapping snags and understory shrubs for a LiDAR-based assessment of wildlife habitat suitability". In: *Remote Sensing of Environment* 113 (12), pp. 2533–2546. DOI: 10.1016/j.rse.2009.07.002.

Mathworks [2013]. *MathWorks Germany - MATLAB and Simulink for Technical Computing*. URL: http://www.mathworks.com/products/matlab/ (visited on 02/12/2014).

McGarigal, K. [2013]. "Introduction to landscape ecology". In: Landscape Ecology course notes. URL: http://www.umass.edu/landeco/about/landeco.pdf.

McGarigal, K., Cushman, S., Neel, M., and Ene, E [2002]. "FRAGSTATS: spatial pattern analysis program for categorical maps". In: URL: http://www.umass.edu/landeco/research/fragstats/fragstats.html (visited on 02/12/2014).

Miura, N. and Jones, S. D. [2010]. "Characterizing forest ecological structure using pulse types and heights of airborne laser scanning". In: *Remote Sensing of Environment* 114 (5), pp. 1069–1076. DOI: 10.1016/j.rse.2009.12.017.

Montane, J. M. and Torres, R. [2006]. "Accuracy assessment of LIDAR saltmarsh topographic data using RTK GPS". In: *Photogrammetric Engineering and Remote Sensing* 72 (8), pp. 961–967. DOI: 10.14358/pers.72.8.961.

Morris, J. T., Porter, D., Neet, M., Noble, P. A., Schmidt, L., Lapine, L. A., and Jensen, J. R. [2005]. "Integrating LIDAR elevation data, multi-spectral imagery and neural network modelling for marsh characterization". In: *International Journal of Remote Sensing* 26 (23), pp. 5221–5234. DOI: 10.1080/01431160500219018.

Morsdorf, F., Nichol, C., Malthus, T., and Woodhouse, I. H. [2009]. "Assessing forest structural and physiological information content of multi-spectral LiDAR waveforms by radiative transfer modelling". In: *Remote Sensing of Environment* 113 (10), pp. 2152 –2163. ISSN: 0034-4257. DOI: 10.1016/j.rse.2009.05.019.

Morsdorf, F., Mårell, A., Koetz, B., Cassagne, N., Pimont, F., Rigolot, E., and Allgöwer, B. [2010]. "Discrimination of vegetation strata in a multi-layered Mediterranean forest ecosystem using height and intensity information derived from airborne laser scanning". In: *Remote Sensing of Environment* 114 (7), pp. 1403–1415. DOI: 10.1016/j.rse.2010.01.023.

Moser, D., Zechmeister, H. G., Plutzar, C., Sauberer, N., Wrbka, T., and Grabherr, G. [2002]. "Landscape patch shape complexity as an effective measure for plant species richness in rural landscapes". In: *Landscape Ecology* 17 (7), pp. 657–669. URL: http://tinyurl.com/p7pa5dn.

Mücke, W. and Hermann, A. [2010]. "Estimation of biodiversity relevant quantities from airborne laser scanning data". In: *Österreichische Zeitschrift für Vermessung und Geoinformation (VGI)* 4, pp. 201–210. URL: http://www.ovg.at/index.php?id=2042 (visited on 02/12/2014).

Mücke, W. and Hollaus, M. [2012]. "Estimation of forest layer structure and canopy density using airborne laser scanning data". In: *Proceedings SilviLaser 2012 - The 12th International Conference on LiDAR Applications for Assessing Forest Ecosystems*. Ed. by N. C. Coops and M. Wulder. Vancouver, British Columbia, Canada.

Mücke, W, Hollaus, M., and Prinz, M. [2010a]. "Derivation of 3D landscape metrics from airborne laser scanning data". In: *Proceedings SilviLaser 2010 - The 10th International Conference on LiDAR Applications for Assessing Forest Ecosystems*. Ed. by B. Koch, G. Kändler, and C. Teguem. Freiburg im Breisgau, Germany.

Mücke, W., Hollaus, M., and Briese, C. [2010b]. "Reed structure mapping in airborne laser scanning data". In: *Proceedings ForestSat 2010 - Operational tools in forestry remote sensing techniques*. Ed. by D. Miranda, J. Suárez, and R. Crescente. Lugo, Spain.

— [2011]. "Applications and analysis of airborne laser scanning data on reed beds". In: *International Symposium on Advanced Methods of Monitoring Reed Habitats in Europe*. Fernerkundung und angewandte Geoinformatik. Rhombos-Verlag, pp. 109–121. ISBN: 978-3941216785.

Mücke, W., Hollaus, M., and Pfeifer, N. [2012a]. "Identification of dead trees using small footprint full-waveform airborne laser scanning data". In: *Proceedings SilviLaser 2012 - The 12th International Conference on LiDAR Applications for Assessing Forest Ecosystems*. Ed. by N. C. Coops and M. Wulder. Vancouver, British Columbia, Canada.

Mücke, W., Zlinszky, A., Rieger, P., Hollaus, M., and Pfeifer, N. [2012b]. "Towards operative habitat mapping using airborne laser scanning - Applications in the ChangeHabitats2 project". In: *European Journal of Remote Sensing*. (Manuscript in preparation).

Mücke, W., Zlinszky, A., Hollaus, M., and Pfeifer, N. [2012c]. "Towards operative habitat mapping using airborne laser scanning - The ChangeHabitats2 project". In: *Proceedings ForestSat 2012 - Promoting science based application of remote sensing and other spatial data in forested systems*. Ed. by W. B. Cohen, M. V. Duane, and M. G. Wing. Corvallis, Oregon, USA.

Mücke, W., Deák, B., Schroiff, A., Hollaus, M., and Pfeifer, N. [2013a]. "Detection of fallen trees in forested areas using small footprint airborne laser scanning data". In: *Canadian Journal of Remote Sensing* 39(s1), pp. 32–40. DOI: 10.5589/m13-013.

Mücke, W. [2008]. “Analysis of full-waveform airborne laser scanning data for the improvement of DTM generation”. MA thesis. Institute of Photogrammetry and Remote Sensing, Vienna University of Technology. URL: http://publik.tuwien.ac.at/files/PubDat_170289.pdf.

Mücke, W., Briese, C., and Hollaus, M. [2010c]. “Terrain Echo Probability Assignment Based On Full-Waveform Airborne Laser Scanning Observables”. In: *ISPRS Technical Commission VII Symposium 2010: 100 Years ISPRS - Advancing Remote Sensing Science, Vol. 38 (Part 7A)*. Ed. by W. Wagner and B. Szekely. Vienna, Austria. URL: http://www.isprs.org/proceedings/XXXVIII/part7/a/pdf/157_XXXVIII-part7A.pdf.

Mücke, W., Hollaus, M., Pfeifer, N., Schroiff, A., and Deák, B. [2013b]. “Comparison of discrete and full-waveform ALS for dead wood detection”. In: *ISPRS Annals of the Photogrammetry, Remote Sensing and Spatial Information Sciences*. Vol. II-5/W2. talk: ISPRS Workshop Laser Scanning 2013, Antalya, Turkey; 2013-11-11 – 2013-11-13, pp. 199–204. DOI: 10.5194/isprsannals-II-5-W2-199-2013.

Næsset, E., Gobakken, T., Holmgren, J., Hyyppä H., H., Hyyppä H., J., Maltamo, M., Nilsson, M., and Söderman, U. [2004]. “Laser scanning of forest resources: The nordic experience”. In: *Scandinavian Journal of Forest Research* 19 (6), pp. 482–499. DOI: 10.1080/02827580410019553.

NASA [2014]. *SLICER - Scanning LiDAR Imager of Canopies by Echo Recovery*. http://denali.gsfc.nasa.gov/research/laser/slicer/slicer.html. (Visited on 02/12/2014).

Nichols, W., Killingbeck, K., and August, P. [1998]. “The Influence of Geomorphological Heterogeneity on Biodiversity. II. A Landscape Perspective”. In: *Conservation Biology* 12 (2), pp. 371–379. DOI: 10.1046/j.1523-1739.1998.96237.x.

Nyström, M., Holmgren, J., Fransson, J. E., and Olsson, H. [2014]. “Detection of windthrown trees using airborne laser scanning”. In: *International Journal of Applied Earth Observation and Geoinformation* 30, pp. 21 –29. ISSN: 0303-2434. DOI: http://dx.doi.org/10.1016/j.jag.2014.01.012.

Odum, E. P. and Barrett, G. W. [1971]. “Fundamentals of ecology”. In: URL: http://tinyurl.com/ohzpb49.

Ohlson, M., Söderström, L., Hörnberg, G., Zackrisson, O., and Hermansson, J. [1997]. “Habitat qualities versus long-term continuity as determinants of biodiversity in boreal old-growth swamp forests”. In: *Biological conservation* 81 (3), 221–231. DOI: 10.1016/s0006-3207(97)00001-3.

OPALS [2013]. *OPALS - Orientation and Processing of Airborne Laser Scanning data*. URL: http://geo.tuwien.ac.at/opals (visited on 02/12/2014).

Ostendorp, W. [1993]. “Reed bed characteristics and significance of reeds in landscape ecology”. In: *Limnologie aktuell* 5, pp. 149–161. URL: http://tinyurl.com/qgjuytj.

Paillet, Y., Bergés, L., Hjälten, J., Ódor, P., Avon, C., Bernhardt-Römermann, M., Bijlsma, R. J. A. N., De Bruyn, L. U. C., Fuhr, M., and Grandin, U. L. F. [2010]. “Biodiversity Differences between Managed and Unmanaged Forests: Meta-Analysis of Species Richness in Europe”. In: *Conservation Biology* 24 (1), 101–112. DOI: 10.1111/j.1523-1739.2009.01399.x.

Parker, G. G., Lowman, M., and Nadkarni, N. [1995]. "Forest canopies". In: *Forest canopies*.

Pesonen, A., Maltamo, M., Eerikäinen, K., and Packalén, P. [2008]. "Airborne laser scanning-based prediction of coarse woody debris volumes in a conservation area". In: *Forest Ecology and Management* 255 (8), 3288–3296. DOI: 10.1016/j.foreco.2008.02.017.

Pfeifer, N., Stadler, P., and Briese, C. [2001]. "Derivation of Digital Terrain Models in the SCOP++ Environment". In: *Proceedings of OEEPE Workshop on Airborne Laserscanning and Interferometric SAR for Detailed Digital Terrain Models*. Ed. by K. Torlegård and J. Nelson. Stockholm, Sweden. URL: http://bono.hostireland.com/~eurosdr/publications/40.pdf.

Pfeifer, N., Mandlburger, G., Otepka, J., and Karel, W. [2013]. "OPALS - A framework for Airborne Laser Scanning data analysis". In: *Computers, Environment and Urban Systems*. accepted for publication. DOI: 10.1016/j.compenvurbsys.2013.11.002.

Reitberger, J, Schnörr, C., Krzystek, P, and Stilla, U [2009]. "3D segmentation of single trees exploiting full waveform LIDAR data". In: *ISPRS Journal of Photogrammetry and Remote Sensing* 64 (6), pp. 561–574. DOI: 10.1016/j.isprsjprs.2009.04.002.

Ricotta, C., Corona, P., Marchetti, M., Chirici, G., and Innamorati, S. [2003]. "LaDy: software for assessing local landscape diversity profiles of raster land cover maps using geographic windows". In: *Environmental Modelling & Software* 18 (4), pp. 373–378. DOI: 10.1016/S1364-8152(02)00104-4.

Rieger, P. and Ullrich, A. [2011]. "Resolving range ambiguities in high-repetition rate airborne lidar applications". In: *Proceedings of SPIE*. Vol. 8186. 1. DOI: 10.1117/1.jrs.6.063552.

RIEGL Laser Measurment Systems GmbH [2013a]. *RIEGL LMS Q680i*. URL: http://www.riegl.com/nc/products/airborne-scanning/produktdetail/product/scanner/23/ (visited on 04/25/2012).

— [2013b]. *RIEGL RiPROCESS*. URL: http://www.riegl.com/products/software-packages/riprocess/ (visited on 04/25/2012).

Riffell, S., Verschuyl, J., Miller, D., and Wigley, T. B. [2011]. "Biofuel harvests, coarse woody debris, and biodiversity–A meta-analysis". In: *Forest Ecology and Management* 261 (4), 878–887. DOI: 10.1016/j.foreco.2010.12.021.

Rose, L. S., Seong, J. C., Ogle, J., Beute, E., Indridason, J., Hall, J. D., Nelson, S., Jones, T., and Humphrey, J. [2012]. "Challenges and lessons from a wetland LiDAR project: a case study of the Okefenokee Swamp, Georgia, USA". In: *Geocarto International* 0, pp. 1–17. DOI: 10.1080/10106049.2012.681707.

Rutzinger, M., Höfle, B., Hollaus, M., and Pfeifer, N. [2008]. "Object-Based Point Cloud Analysis of Full-Waveform Airborne Laser Scanning Data for Urban Vegetation Classification". In: *Sensors* 8, pp. 4505–4528. DOI: 10.3390/s8084505.

Sallabanks, R., Arnett, E. B., Wigley, T. B., and Irwin, L. [2001]. *Accomodating Birds in Managed Forests of North America: A Review of Bird-forestry Relationships*. National Council for Air and

Stream Improvement. URL: http://gis.fs.fed.us/psw/publications/documents/psw_gtr191/Asilomar/pdfs/345-372.pdf.

Schindler, S., Poirazidis, K., and Wrbka, T. [2008a]. “Towards a core set of landscape metrics for biodiversity assessments: A case study from Dadia National Park, Greece”. In: *Ecological Indicators* 8 (5), pp. 502–514. DOI: 10.1016/j.ecolind.2007.06.001.

Schindler, S., Poirazidis, K., Kati, V., Kalivas, D., Papageorgiou, A., and Wrbka, T. [2008b]. “Earth observation as a prerequisite for biodiversity management in a Mediterranean forest landscape (accepted)”. In: *Impact Assessment of Land Use Change, International Conference, 6-9 April, Berlin, Germany, Book of Abstracts*, p. 60. URL: http://tran.zalf.de/home_ip-sensor/conference/12_pdf/Audimax_04_Schindler_IALUC_Berlin_Apr08.pdf.

SCOP++ [2008]. *Department of Geodesy and Geoinformation, Research Groups Photogrammetry and Remote Sensing*. http://photo.geo.tuwien.ac.at/software/scop/. Vienna, Austria. (Visited on 02/13/2014).

SEBI2010 [2004]. *Streamlining European 2010 Biodiversity Indicators*. URL: http://biodiversity.europa.eu/topics/sebi-indicators (visited on 02/12/2014).

SEBI2020 [2014]. *Streamlining European Biodiversity Indicators 2020*. URL: http://www.eea.europa.eu/publications/streamlining-european-biodiversity-indicators-2020 (visited on 02/12/2014).

Sithole, G. and Vosselman, G [2003]. “Comparison of filtering algorithms”. In: *Proceedings of the ISPRS working group III/3 workshop 3-D reconstruction from airborne laserscanner and InSAR data, International Archives of the Photogrammetry, Remote Sensing and Spatial Information Sciences, Vol. XXXIV, 3/W13*. Ed. by H.-G. Maas, G. Vosselman, and A. Streilein. Dresden: Institute of Photogrammetry and Remote Sensing, Dresden University of Technology, Germany. ISBN: 1682-1750. URL: http://www.isprs.org/proceedings/XXXIV/3-W13/papers/Sithole_ALSDD2003.pdf.

Solomon, E. P., Berg, L. R., and Martin, D. W. [2011]. *Biology*. Ed. by B. . Cole. Belmont, CA. ISBN: 978-0538741255.

Straatsma, M. W. and Baptist, M. J. [2008]. “Floodplain roughness parameterization using airborne laser scanning and spectral remote sensing”. In: *Remote Sensing of Environment* 112 (3), pp. 1062–1080. DOI: 10.1016/j.rse.2007.07.012.

Strand, G.-H., Dramstad, W., and Engan, G. [2002]. “The effect of field experience on the accuracy of identifying land cover types in aerial photographs”. In: *International Journal of Applied Earth Observation and Geoinformation* 4 (2), pp. 137 –146. ISSN: 0303-2434. DOI: http://dx.doi.org/10.1016/S0303-2434(02)00011-9.

TerraScan [2013]. *Terrasolid - Processing laser and images*. Vienna, Austria. URL: http://www.terrasolid.com/products.html (visited on 02/12/2014).

Tews, J, Brose, U, Grimm, V, Tielbörger, K, Wichmann, M., Schwager, M, and Jeltsch, F [2004]. “Animal species diversity driven by habitat heterogeneity/diversity: the importance of keystone structures”. In: *Journal of Biogeography* 31 (1), pp. 79–92. DOI: 10.1046/j.0305-0270.2003.00994.x.

Thomas, V, Oliver, R., Lim, K, and Woods, M [2008]. “LiDAR and Weibull modeling of diameter and basal area”. In: *The Forestry Chronicle* 84 (6), pp. 866–875. DOI: 10.5558/tfc84866-6.

Tóvari, D. and Pfeifer, N. [2005]. “Segmentation based robust interpolation – a new approach to laser data filtering”. In: *Proceedings of the ISPRS working group III/3, III/4, V/3 workshop Laserscanning 2005, International Archives of the Photogrammetry, Remote Sensing and Spatial Information Sciences*. Ed. by G. Vosselman and C. Brenner. International Archives of Photogrammetry, Remote Sensing and Spatial Information Science. Enschede, The Netherlands, pp. 79–84. URL: http://www.isprs.org/proceedings/XXXVI/3-W19/papers/079.pdf.

TransEcoNet [2013]. *Transnational ecological networks*. URL: http://www.transeconet.eu/ (visited on 02/13/2014).

Trnka, A. and Prokop, P. [2006]. “Reedbed structure and habitat preference of reed passerines during the post-breeding period”. In: *Biologia* 61 (2), pp. 225–230. DOI: 10.2478/s11756-006-0034-8.

Troll, C. [1939]. *Luftbildplan und ökologische Bodenforschung: ihr zweckmässiger Einsatz für die wissenschaftliche Erforschung und praktische Erschliessung wenig bekannter Länder*. Ges. für Erdkunde. URL: http://books.google.at/books?id=HEXiYgEACAAJ.

Turner, M. G. [1990]. “Spatial and temporal analysis of landscape patterns”. English. In: *Landscape Ecology* 4 (1), pp. 21–30. ISSN: 0921-2973. DOI: 10.1007/BF02573948.

Turner, M. G., Gardner, R. H., and O’neill, R. V. [2001]. *Landscape ecology in theory and practice: pattern and process*. Springer. ISBN: 978-0-387-95122-5. DOI: 10.1007/b97434.

Uckermark [2014]. *Uckermark / Wikipedia*. URL: http://de.wikipedia.org/wiki/Uckermark (visited on 02/13/2014).

United Nations [1992]. “Multilateral Convention on biological diversity (with annexes)”. In: *United Nations Treaty Series* 1760. Concluded in Rio de Janeiro on 5 June 1992, 146 ff. URL: https://treaties.un.org/doc/Publication/UNTS/Volume%201760/v1760.pdf.

Vehmas, M., Packalén, P., Maltamo, M., and Eerikäinen, K. [June 2011]. “Using airborne laser scanning data for detecting canopy gaps and their understory type in mature boreal forest”. In: *Annals of Forest Science* 68 (4), pp. 825–835. ISSN: 1286-4560, 1297-966X. DOI: 10.1007/s13595-011-0079-x.

Verein Welterbe Neusiedler See [2013]. *UNESCO World Heritage Neusiedler See-Seewinkel*. URL: http://www.welterbe.org/ (visited on 02/12/2014).

Verkerk, P. J., Lindner, M., Zanchi, G., and Zudin, S. [2011]. “Assessing impacts of intensified biomass removal on deadwood in European forests”. In: *Ecological Indicators* 11 (1), 27–35. DOI: 10.1016/j.ecolind.2009.04.004.

Vetter, M, Höfle, B, Hollaus, M, Gschöpf, C, Mandlburger, G, Pfeifer, N, and Wagner, W [2011]. “Vertical vegetation structure analysis and hydraulic roughness determination using dense ALS point cloud data–a voxel based approach”. In: *International Archives of Photogrammetry, Remote*

Sensing and Spatial Information Sciences 38, p. 5. URL: http://www.waterresources.at/fileadmin/user_uploads/Publications/Vetter_ISPRS_Workshop_2011.pdf.

Vosselman, G. [2000]. "Slope based Filtering of Laser Altimetry Data". In: *Proceedings of the XIX ISPRS Congress, International Archives of the Photogrammetry, Remote Sensing and Spatial Information Sciences, Vol. XXXIII, B3/1+2*. Ed. by G. V. Toni Schenk. International Archives of Photogrammetry, Remote Sensing and Spatial Information Science. Amsterdam, Netherlands, pp. 935–942. URL: http://www.isprs.org/proceedings/XXXIII/congress/part3/935_XXXIII-part3.pdf.

Wagner, W., Ullrich, A., Ducic, V., Melzer, T., and Studnicka, N. [2006]. "Gaussian decomposition and calibration of a novel small-footprint full-waveform digitising airborne laser scanner". In: *ISPRS Journal of Photogrammetry & Remote Sensing* 60 (2), pp. 100–112. DOI: 10.1016/j.isprsjprs.2005.12.001.

Wagner, W., Hollaus, M., Briese, C., and Ducic, V. [2008]. "3D vegetation mapping using small-footprint full-waveform airborne laser scanners". In: *International Journal of Remote Sensing* 29 (5), pp. 1433–1452. DOI: 10.1080/01431160701736398.

Wang, C., Menenti, M., Stoll, M.-P., Feola, A., Belluco, E., and Marani, M. [2009]. "Separation of ground and low vegetation signatures in LiDAR measurements of salt-marsh environments". In: *Geoscience and Remote Sensing, IEEE Transactions on* 47 (7), pp. 2014–2023. DOI: 10.1109/tgrs.2008.2010490.

Wang, C.-K., Tseng, Y.-H., and Chu, H.-J. [2014]. "Airborne Dual-Wavelength LiDAR Data for Classifying Land Cover". In: *Remote Sensing* 6 (1), pp. 700–715. DOI: 10.3390/rs6010700.

Wei, G., Shalei, S., Bo, Z., Shuo, S., Faquan, L., and Xuewu, C. [2012]. "Multi-wavelength canopy LiDAR for remote sensing of vegetation: Design and system performance". In: *ISPRS Journal of Photogrammetry and Remote Sensing* 69. cited By (since 1996)1, pp. 1–9. DOI: 10.1016/j.isprsjprs.2012.02.001.

Woodhouse, I., Nichol, C., Sinclair, P., Jack, J., Morsdorf, F., Malthus, T., and Patenaude, G. [2011]. "A multispectral canopy LiDAR demonstrator project". In: *IEEE Geoscience and Remote Sensing Letters* 8 (5). cited By (since 1996)2, pp. 839–843. DOI: 10.1109/LGRS.2011.2113312.

Wulder, M. A., White, J. C., Nelson, R. F., Næsset, E., Ørka, H. O., Coops, N. C., Hilker, T., Bater, C. W., and Gobakken, T. [2012]. "Lidar sampling for large-area forest characterization: A review". In: *Remote Sensing of Environment* 121, pp. 196–209. DOI: 10.1016/j.rse.2012.02.001. (Visited on 11/28/2012).

Yao, W., Krzystek, P., and Heurich, M. [2012]. "Identifying standing dead trees in forest areas based on 3D single tree detection from full waveform lidar data". In: *ISPRS Annals of the Photogrammetry, Remote Sensing and Spatial Information Sciences* I-7. XXII ISPRS Congress, 25 August - 01 September 2012, Melbourne, Australia, pp. 359–364. DOI: 10.5194/isprsannals-i-7-359-2012.

Zlinszky, A., Mücke, W., Lehner, H., Briese, C., and Pfeifer, N. [June 2012]. “Categorizing wetland vegetation by airborne laser scanning on Lake Balaton and Kis-Balaton, Hungary”. en. In: *Remote Sensing* 4 (6), pp. 1617–1650. DOI: 10.3390/rs4061617.

Curriculum Vitae

Werner Mücke studied Surveying and Geoinformation with a focus on geoinformation, photogrammetry and remote sensing at the Vienna University of Technology. During his master studies he worked as a part time project assistant at the Research Groups Photogrammetry and Remote Sensing, Department of Geodesy and Geoinformation (former Institute of Photogrammetry and Remote Sensing), where he was mainly involved in the processing of ALS data and gained experience in the handling of wide-area projects. He finished his master studies and earned his master's degree in November 2008 with his diploma thesis on the improvement of digital terrain modelling using full-waveform ALS attributes.

Since then he has been a full time employee and project assistant at the Research Groups of Photogrammetry and Remote Sensing, being engaged in various research topics and applications of ALS. He predominantly focuses on feature extraction from ALS point clouds for the derivation of vegetation parameters, digital terrain and surface modelling, as well as building footprint estimation and the management of topographic data.

Werner Mücke is married with one child and lives in Wels, Upper Austria.